Individual and competitive adsorption of phosphate and arsenate onto manganese oxide in seawater

By

Maryon Paulsen Strugstad

Department of Earth and Planetary Sciences

McGill University

Montréal, QC, Canada

August 2013

A thesis submitted to McGill University in partial fulfillment of the requirements of the degree of Master of Science

Abstract

The individual and competitive adsorption and desorption of arsenate and phosphate on amorphous hydrous manganese oxide (HMO) from seawater suspensions were investigated over 48 hours at 23 ± 3°C. The specific surface area of the HMO was 270 m^2/g and the solid:solution ratio was 0.15 g/L in all experiments. The oxyanion concentrations ranged from 2-46 μM (phosphate) and 0.6-6 μM (arsenate). In competitive adsorption experiments, the oxyanions were added simultaneously or sequentially to the suspensions [As(V)]:[SRP] (molar ratio)= 1:2.5, 1:10, 1:100. The adsorption data from individual experiments were fitted to Langmuir and Freundlich adsorption isotherms and the adsorption capacity (Γ_{max}) and the adsorption constants (K_{ads} and K_f) were determined. Arsenate displayed a stronger affinity (70-79 % adsorbed) than phosphate (21-44 % adsorbed) for HMO in individual adsorption experiments. The adsorption kinetics were similar for both oxyanions with rapid initial adsorption followed by a slower adsorption, and the kinetics fit well to pseudo-first- and pseudo-second-order models. The individual desorption experiments revealed that both phosphate- and arsenate-laden HMO rapidly release phosphate and arsenate back into solution when exposed to natural seawater containing ~ 2.1 μM SRP and 14 nM As(V). They also demonstrate that arsenate adsorption onto HMO in seawater is reversible, whereas a fraction of the phosphate is irreversibly bound to the HMO. When the two oxyanions were added simultaneously, effective competition was only observed at [As(V)]:[SRP] = 1:100, resulting in reduced adsorption of both oxyanions, whereas a synergistic effect (increased adsorption of ~4 % [As(V)] and 6-10 % [SRP]) was noted at [As(V)]:[SRP] = 1:2.5 and 1:10. When phosphate was added first, subsequent addition of arsenate had little effect on phosphate adsorption, but when arsenate was added first, subsequent phosphate addition caused a 5 % desorption of arsenate when [As(V)]:[SRP] = 1:10 in both sequential experiments.

Résumé

L'adsorption et la désorption individuelle et compétitive des ions arséniate et phosphate sur un oxyde de manganèse amorphe hydraté(OMH) en suspension dans une solution d'eau de mer ont été étudiées pendant 48 heures à 23 ± 3°C. L'aire de surface spécifique de l'OMH était 270 m^2/g tandis que le rapport solide:solution était constant à 0.15 g/L dans toutes les expériences. Les concentrations en oxoanions étaient comprises entre 2 et 46 μM pour le phosphate, et de 0.6 à 6 μM pour l'arséniate. Dans les expériences d'adsorption compétitive, les oxoanions furent ajoutés aux suspensions simultanément ou séquentiellement à [As(V)]:[SRP] (rapport molaire)= 1:2.5, 1:10, 1:100. Les résultats expérimentaux d'adsorption individuelle ont été projetés sur des isothermes d'adsorption de Langmuir et Freundlich pour déterminer la capacité d'adsorption (Γ_{max}) et ses constantes (K_{ads} et K_f). L'arsénate possède une plus forte affinité (70-79 % adsorbé) que le phosphate (21-44 % adsorbé) pour l'OMH dans les expériences d'adsorption individuelle. Les cinétiques d'adsorption sont similaires pour les deux oxoanions, soit une rapide adsorption initiale, suivie d'une période plus lente et s'accordent bien avec les modèles de pseudo-premier ordre et pseudo-second ordre. Les expériences de désorption individuelle révèlent que les OMH chargés en phosphates et arsénates libèrent rapidement les deux oxoanions à la solution quand ils sont exposés à de l'eau de mer naturelle contenant ~ 2.1 μM de phosphate et 14 nM d'arséniate. Elles démontrent également que l'adsorption d'arséniate à la surface de l'OMH dans l'eau de mer est réversible, tandis qu'une partie du phosphate est irréversiblement liée aux OMH. Quand les deux oxoanions sont ajoutés simultanément à la suspension, une véritable compétition est seulement observée à [As(V)]:[SRP] = 1:100 ce qui provoque une réduction de l'adsorption des deux oxoanions. Cependant, un effet synergique (augmentation d'adsorption d'arséniate et de phosphate de ~4 % et 6-10 %, respectivement) est noté à [As(V)]:[SRP] = 1:2.5 et

1:10. Lorsque le phosphate est ajouté en premier, l'addition subséquente d'arséniate a peu d'effet sur l'adsorption du phosphate. En revanche, quand l'arséniate est ajouté en premier, l'addition subséquente de phosphate provoque une désorption de 5 % d'arséniate lorsque [As(V)]:[SRP] = 1:10 pour les deux experiences séquentelles.

Acknowledgments

I would like to thank my supervisors, Dr. Alfonso Mucci and Dr. Bjorn Sundby, for making the writing of this thesis possible and for giving me an opportunity and the resources to complete the research that underlies it. Their invaluable guidance, selfless teachings and insightful dialogue has shaped the discussions and made this learning experience a truly wonderful and unique one. I can't think of them as only my teachers, but also as mentors, and a part of an extend family that I look forward to revisiting in the years to come. The learning will never stop.

Further, I would like to express gratitude to my peers, starting with officemates Stelly Lefort, Qiang Chen, Claire Lix and Chloé Martias for their contribution to academic discussions; Isabelle Richer and Constance Guignard for technical help in the laboratory; Michel Preda, who performed the XRD analyses at Geotop.

A note of mention for the Department of Earth and Planetary Sciences at McGill University for the opportunity to pursue a Master's degree. The thesis was funded by the Norwegian State Educational Fund and NSERC Discovery Research grants to Drs. Alfonso Mucci and Bjorn Sundby, and supported by Alexander McGregor, J.B. Lynch, and Reinhart C. Fellowships, as well as teaching assistantships from the Department of Earth and Planetary Sciences at McGill University.

Finally, my sincere appreciation and mention to my father, John Eirik Paulsen, who peaked my interests in science and was the first to encourage me to pursue geology; all of the family for their continuous support, and special thanks to my partner who continuously encourages my academic pursuits.

Thank you all.

Table of contents

List of tables

List of Figures

1. INTRODUCTION

Adsorption is the attraction of molecules (adsorbates) to the surface of a solid substance (adsorbent). It occurs as a result of physical (van der Waals or electrostatic) or chemical interactions (covalent bonding) depending on the species involved, and is strictly a surface phenomenon (2D) as opposed to absorption or co-precipitation where molecules are incorporated into the substrate (a 3D phenomenon). When the two processes cannot be distinguished, the term "sorption" is often substituted. The reverse of adsorption is desorption, and the adsorption equilibrium is defined as a state where the rates of adsorption and desorption are equal. The adsorption equilibrium is often described through various models (e.g. Langmuir and Freundlich adsorption isotherms) that express the amount of adsorbate on the adsorbent as a function of the adsorbate equilibrium concentration in solution at a constant temperature and pH. The Langmuir and Freundlich isotherms are empirical models and the most commonly used. The Langmuir model assumes monolayer adsorption, that the solid has a specific number of adsorption sites that can only accommodate a single molecule of adsorbate, and that each adsorption site is energetically equivalent (energetically homogeneous surface) with no interaction between adsorbed molecules. Alternatively, the Freundlich model allows for multi-layer adsorption and accounts for the presence of sites of different affinity for the adsorbate (energetically heterogeneous surface). Most adsorption data will fit one of these models, but the system may not comply with all the model assumptions in which case the constants that can be extracted are only valid under specified environmental conditions (e.g. temperature, pH, specific surface area, ionic strength, the presence of ligands and competing adsorbates). These adsorption models serve to determine the adsorption capacity or maximum adsorption density of a given mass of adsorbent for a specific adsorbate at various adsorbate

concentrations under a set of environmental conditions. In this way the adsorbed quantity can be normalized and compared with different materials, although comparison is not trivial unless the interactions are identical (physical or chemical) and the substrates are the same.

In natural aqueous environments, there are numerous candidate adsorbents. Hydrous oxides of iron and manganese are solid mineral phases common in the top layers of marine sediments, and they are well known for their strong affinity for various cationic and anionic substances (e.g. Krauskopf, 1956; Jenne, 1968; Posselt and Anderson, 1968; Hingston, 1970; Murray, 1975; Pierce and Moore, 1982; Gao and Mucci 2001, 2003). These metal oxide-rich layers accumulate above the redox boundary in sediment and are recycled through diagenesis (burial, reduction, dissolution, upward transport, reoxidation, reprecipitation). Diagenesis is driven by microbial degradation of organic matter, which gives rise to a vertical redox zonation in the sediment column (Fig. 1). As oxygen, supplied by diffusion from the overlying water column, becomes depleted (aerobic respiration), alternate electron-acceptors such as nitrate and metal oxides (Fe(III) and Mn(III,IV)) are respired in the suboxic layer (Froelich et al., 1979; Canfield, 1989; Canfield et al., 1993). Diagenetic processes, such as redox reactions, result in the recycling of these metal oxide-rich layers as they are buried below the oxic layer as sediment accumulate at the sediment-water interface. Thus, the metal oxide rich layers are not permanent, but constantly renewed (Fig. 2). They nevertheless act as a boundary between the overlying water and the sediments; porewater solutes must pass through metal oxide enriched sediment to enter the overlying waters and vice versa. Reactions between metal oxides and porewater solutes buffer the concentration of the solutes and mediate solute exchange between the porewater and the overlying water column (e.g., Froelich, 1988; Sundby et al., 1992).

Dissolution of metal oxides in the reducing subsurface sediments liberates the species that are adsorbed to the oxides and releases them to the porewater (Fig. 3). Consequently, the porewater concentrations of dissolved iron and manganese, as well as desorbed species will increase, resulting in concentration gradients. Depending on the gradients, the solutes can diffuse downward, where they may be trapped by mineral precipitation or co-precipitation, or upward towards the sediment-water interface. Reduced iron and manganese diffusing up will typically be re-oxidized and precipitated once they encounter porewater oxygen and accumulate as iron- and manganese oxide-rich layers near the oxic-suboxic redox boundary. The species that were previously adsorbed onto the oxides can be re-adsorbed onto the newly-precipitated (authigenic) and recently deposited solid oxides or diffuse out of the sediment into the overlying waters. Consequently, the amount of metal oxides present and their adsorption capacities for individual species can greatly influence the migration of solutes at the sediment-water interface.

Arsenic and phosphorus are group V elements and occur as oxyanions in aqueous solutions. Otherwise, their speciation is controlled by the solution composition, including pH and, in the case of arsenic, the redox potential. Arsenic has two prevalent oxidation states in the marine environment, the + III (arsenite; reducing conditions) and the + V (arsenate; oxidizing conditions) (Ferguson and Gavis, 1972; Riedel, 1993), whereas phosphorus only occurs in the +V state. Eh-pH diagrams of aqueous arsenic and phosphorus are presented in Fig. 4 and 5. At the pH of seawater (pHt = 7.9), the dominant arsenite, arsenate and phosphate species are $H_3AsO_3/H_2AsO_3^-$, $HAsO_4^{-2}$, and HPO_4^{2-}, respectively. Arsenate and phosphate display comparable adsorptive behaviours and compete for adsorption on the same adsorbents in aquatic environments (Hingston, 1971; Manning and Goldberg, 1996; Gao and Mucci, 2003). Which oxyanion will adsorb preferentially and stay adsorbed

depends on many factors including the concentrations and speciation of the adsorbate and adsorbent, the energetic threshold required for adsorption, and the bond strength between the adsorbate and adsorbent. In seawater, ion pairing of phosphate and arsenate with Mg^{2+} and Ca^{2+} in the seawater has been reported and may increase adsorption (Millero and Schreiber, 1982; Whiting, 1992; Yao and Millero, 1996).

Although chemically similar, these oxyanions have different functions in biological systems depending on their concentrations (e.g. essential nutrient (phosphate), eutrophication (phosphate), and toxic (arsenic)). Since arsenate and phosphate compete for adsorption sites, and taking into consideration their significant biological differences, it is important to know the capacity of various metal oxides to adsorb these species. Few studies have investigated the competitive adsorption-desorption reactions of arsenate and phosphate on metal oxides (Feely et al., 1991; Manning and Goldberg, 1996; Mucci et al., 2000; Hongshao and Stanforth, 2001; Ouvrard, 2002a; Gao and Mucci, 2003; Luengo, 2007). Furthermore, nearly all competitive adsorption studies of arsenate and phosphate to date have focused on iron oxides, likely because they are typically more abundant in sedimentary environments and display a greater affinity for these oxyanions than manganese oxides (Gao and Mucci, 2003; Antelo et al., 2005; Ying et al., 2012). Nevertheless, several studies have demonstrated affinity of arsenate and phosphate for manganese oxides (Takamatsu, et al., 1985; Kawashima et al., 1986; Yao and Millero, 1996) and the role of the latter in oxidizing arsenite to arsenate (Oscarson et al., 1981a,b, 1983a; Driehaus et al., 1995; Scott and Morgan, 1995; Mucci et al., 2000; Tournassat et al., 2002; Lafferty et al., 2010a,b; Ying et al., 2012). For this reason, more research is needed to better understand their role in the diagenetic cycles of arsenate and phosphate.

The objective of this project is to evaluate the individual and competitive adsorption of arsenate and phosphate onto an amorphous hydrous manganese oxide in seawater. This includes the kinetics of adsorption and the amount of desorption. The experiments were carried out at environmentally relevant arsenate and phosphate concentrations, at a constant solid:solution ratio (0.15 g/L) and various molar concentration ratios of the oxyanions (As:P; 1:2.5, 1:10, and 1:100). The results will provide insight into the importance of manganese oxides as adsorbents for phosphate and arsenate in seawater and the relative affinities of arsenate and phosphate for the hydrous manganese oxide surface.

Figure 1: Vertical porewater profiles of oxygen, nitrate, manganese, iron, and sulfate, including processes and electron acceptors (Figure adapted from Froelich et al., 1979 and Burdige, 1993).

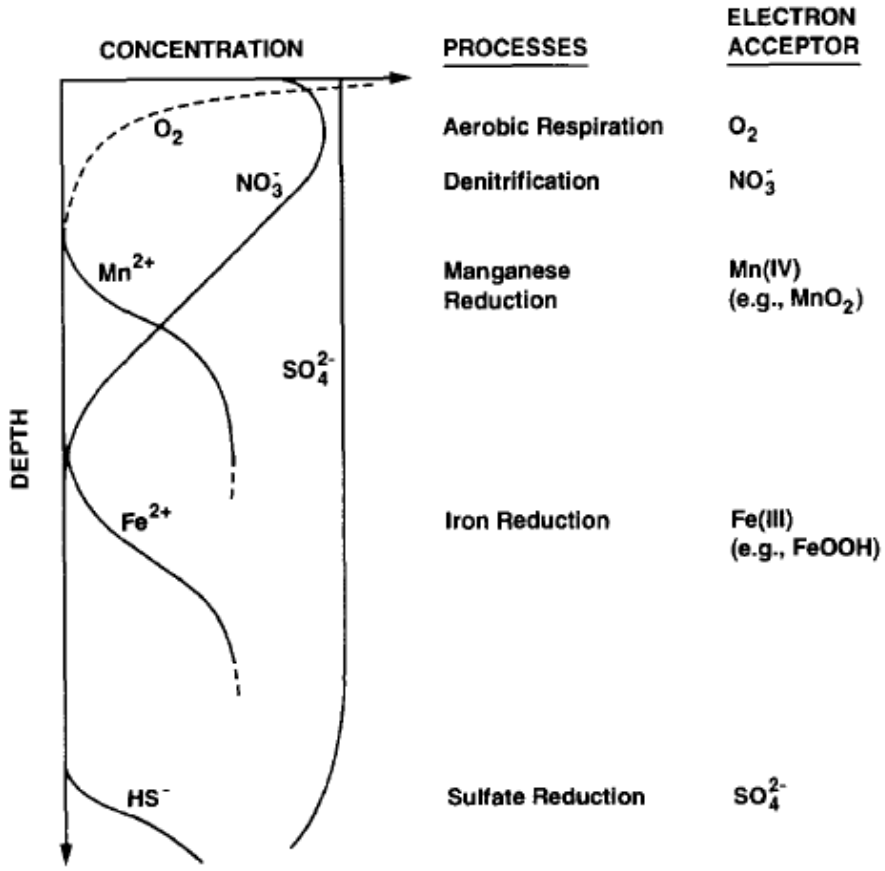

Figure 2: Cycling of manganese, iron, phosphate and arsenate in sediments (conceptual model) (Figure adapted from Burdige, 2006).

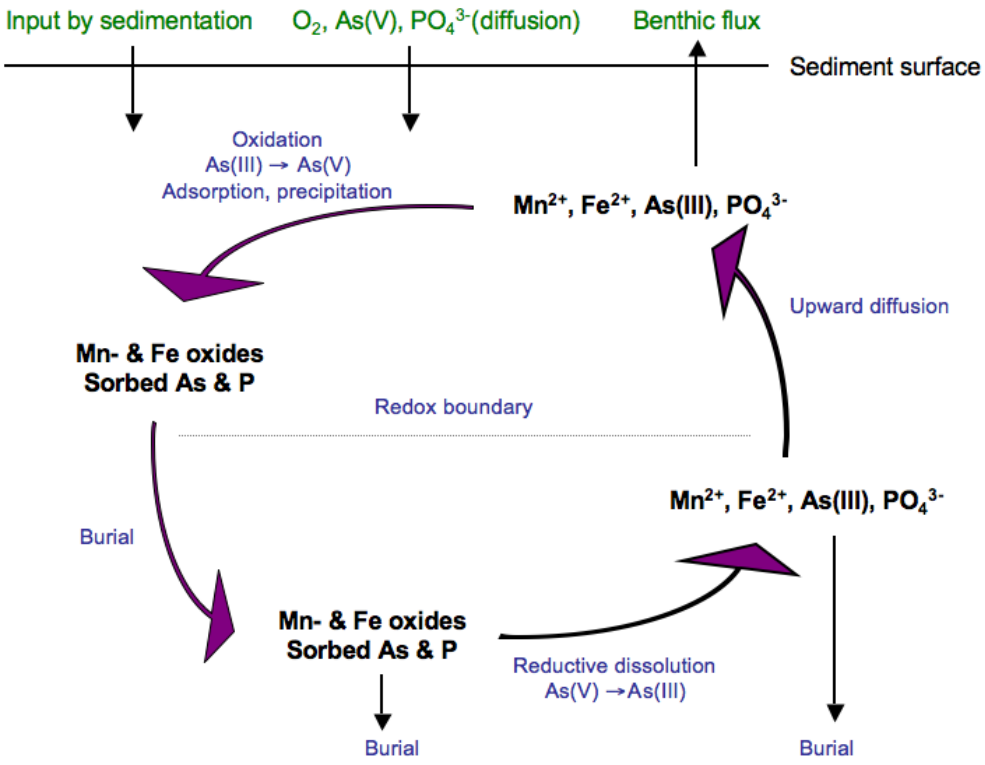

Figure 3: Typical porewater profiles for arsenic, phosphate and manganese, and solid sediment profile for manganese (Figure adapted from Edenborn et al., 1986; Mucci et al., 2000; Burdige, 2006).

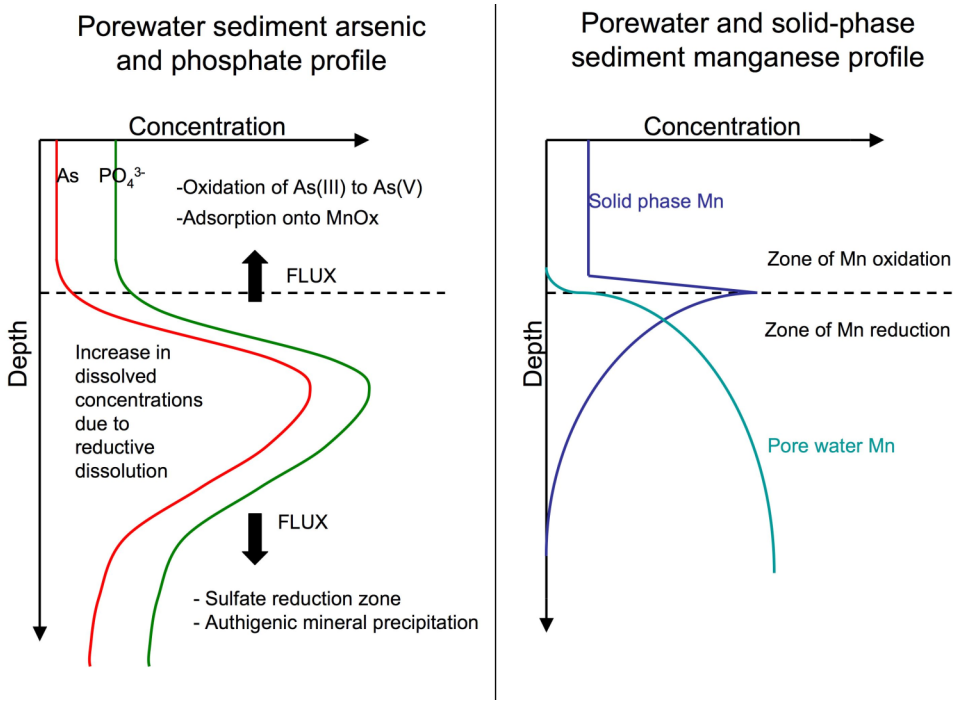

Figure 4: Eh-pH diagram of phosphorus species in the aqueous phase (Figure adapted from Brookins, 1988).

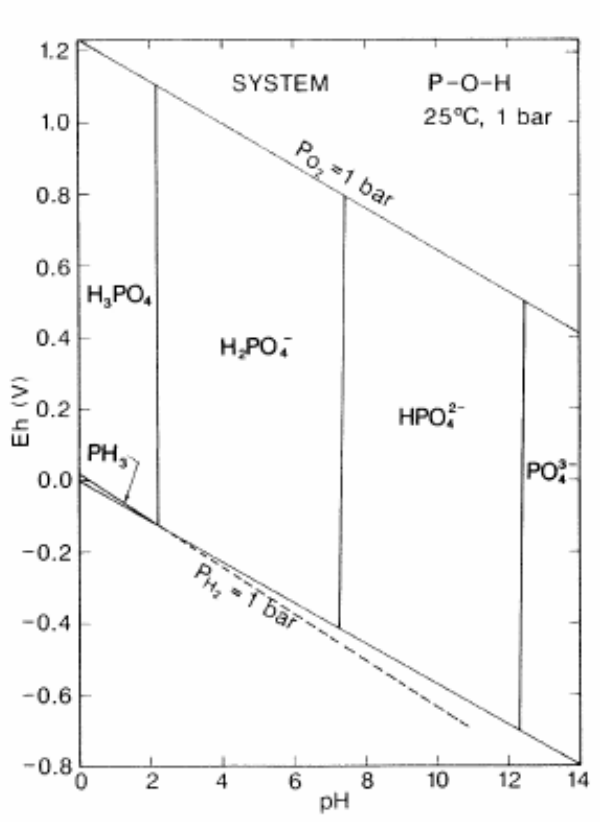

Figure 5: Eh-pH diagram for arsenic species in the aqueous phase (Figure adapted from Brookins, 1988).

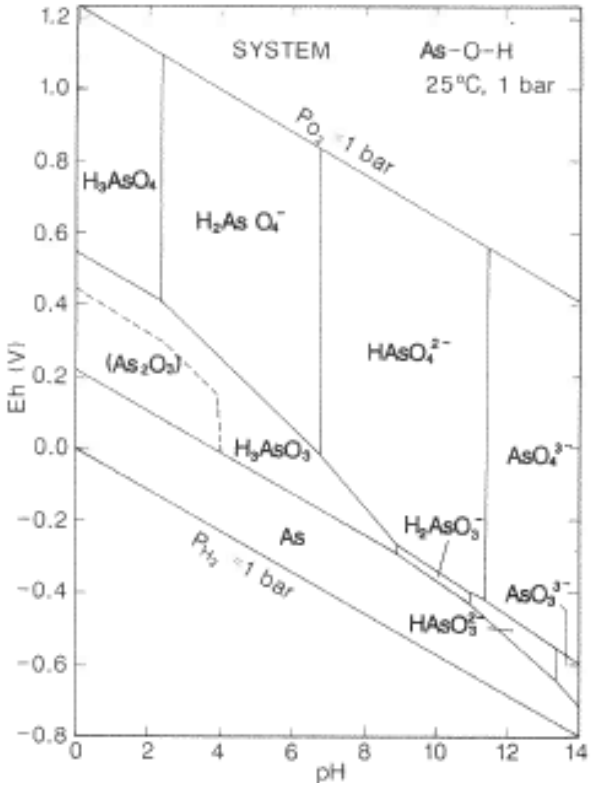

2. LITERATURE REVIEW

Interest in adsorption of phosphate on naturally occurring surfaces surged with the realization that elevated phosphate concentrations due to agricultural and urban effluents (used as fertilizer and a component of detergent formula) can cause eutrophication of lakes and rivers (e.g. Schindler et al., 1971; Schindler, 1974; Smil, 2000). Similarly, the interest in arsenic adsorption has grown rapidly because of the discovery that groundwater used for human consumption in areas such as Bangladesh contains elevated concentrations of this toxic element (e.g. Caldwell et al., 2003). Numerous studies have been carried out on the adsorption of arsenic (as arsenite and/or arsenate) and/or phosphate onto metal oxides, including iron hydroxide (e.g. goethite) (e.g Hongshao and Stanforth, 2001; Gao and Mucci, 2003; Luengo et al., 2007), aluminium oxide (e.g. gibbsite) (e.g Van Riemsdijk and Lyklema, 1980; Fitzpatrick, 1998), titanium dioxide (Dutta et al., 2004), manganese oxide (e.g. Yao and Millero, 1996; Manning et al., 2002) and single or mixed metal oxide coatings or nodules (e.g. Oscarson et al., 1983b; Maity et al., 2005; Boujelben et al., 2008).

2.1 Adsorption of arsenate and phosphate onto manganese oxide

Several studies have examined the adsorption of arsenic onto manganese oxides, known for their ability to adsorb ions, but only a few have investigated the adsorption of phosphate (Takamatsu et al., 1985; Yao and Millero, 1996; Mustafa et al., 2008) or their competitive adsorption on these oxides (Chiu and Hering, 2000; Ouvrard et al., 2001; Parikh et al., 2010; Lafferty et al., 2011). Furthermore, most of the studies of arsenic have focussed on the adsorption and subsequent oxidation of arsenite to arsenate rather than the adsorption of arsenate (e.g., Oscarson et al.,

1983a, Moore et al., 1990; Scott and Morgan, 1995; Tournassat et al., 2002, Lafferty et al., 2010a,b). This is because manganese oxides, besides being minor adsorbates relative to oxides of iron and aluminum, are considered to be active oxidants in the cycling of arsenic (e.g. Oscarson et al., 1980, 1983b; Parikh et al., 2010; Ying et al., 2012). Ying et al. (2012) examined the competitive retention of arsenic between iron- and manganese oxides and found that manganese oxides operate primarily as strong oxidants in the transformation of arsenite to arsenate, and that arsenate preferentially adsorbs onto iron oxides. Nevertheless, they suggest that manganese oxides can act as temporary sorbents for arsenic. Similar observations have also been reported by Tessier et al. (1996).

There are more than 30 known manganese (IV,III) oxide/hydroxide/oxyhydroxide minerals, hereafter referred to as manganese oxides. They display a variety of structures such as tunnel structures (e.g. pyrolusite), layered sheets (e.g. birnessite), and spinel-like structures (e.g. hausmannite) (Hem, 1978; Post, 1999; Tebo et al., 2004), and a more detailed description can be found in Table 1. Various manganese oxides have been used in adsorption studies of arsenate and/or phosphate: biogenic manganese oxide (Katsoyiannis et al., 2004), natural manganese oxide (Ouvrard et al., 2001; Ouvrard et al., 2002a,b), hydrous manganese oxide (Takamatsu et al., 1985; Parikh et al., 2010), synthetic β-MnO_2 (Mustafa et al., 2008), birnessite (Oscarson et al., 1983b; Manning et al., 2002; Ying et al., 2012), manganite (Chiu and Hering, 2000), and cryptomelane and pyrulosite (Oscarson et al., 1983a). Some of these are considered to be poorly crystalline (e.g. Oscarson et al., 1983a; Lafferty et al., 2010a,b; Parikh et al., 2010, Lafferty et al., 2011), which would be similar to the manganese oxides that precipitate in marine sediments (Post, 1999; Li and Schoonmaker, 2005).

Table 1: pH_{ZPC} of various manganese oxides and their occurrence in the environment.

Name and formula	pH_{ZPC}	Occurrence	References
Birnessite, δ-MnO_2 or $Na_4Mn_{14}O_{27}\cdot 9H_2O$ or $(Na,Ca)Mn_7O_{14}\cdot 2.8H_2O$ Structure: layered sheets	1.2-1.6	Widely distributed in marine sediments. Formed by precipitation and is a major component of manganese nodules.	McKenzie (1981), Balistrieri and Murray (1982), Post (1999), Tan et al. (2008)
Hydrous manganese oxide, $MnO_2\cdot nH_2O$ Structure: amorphous	2.3	(Same as birnessite)	Murray (1974), Hem (1978), Mok and Wai (1994), Hu and Tsou (2002)
Cryptomelane (Hollandite group), α-MnO_2 or $K_x(Mn^{4+},Mn^{3+})_8O_{16}$ Structure: tunnel	1.5-2.8	Common in oxidized manganese deposits	McKenzie (1981), Oscarson et al. (1983), Tan et al. (2008)
Todorokite, $(Ca,Na,K)_x(Mn^{4+},Mn^{3+})_6O_{12}\cdot 3.5H_2O$ Structure: tunnel	3.5-4.0	Deep ocean manganese nodules	Post (1999), Tan et al. (2008)
Manganite, γ-MnOOH Structure: tunnel	6.2	Hydrothermal vein deposits or alteration product of other manganese-bearing minerals	Post (1999), Chiu and Hering (2000)
Pyrolusite, β-MnO_2 Structure: tunnel	6.4 7.5	Low-temperature hydrothermal deposits or as replacement after other manganese oxide minerals	Oscarson et al. (1983), Post (1999) Mustafa et al. (2008)
Pyrochroite, $Mn(OH)_2$	7.0	Primary minerals in some volcanogenic massive sulfide deposits	Parks (1965), Hem (1978)

Electrostatic (outer-sphere) adsorption onto manganese oxides is likely related to their pH of zero-point-of-charge (pH_{ZPC}) (Murray, 1974; Oscarson et al, 1983b). The pH_{ZPC} of various manganese oxides ranges from 1.2-7.5 (Table 1). By comparison, the pH_{ZPC} of goethite is 7.9-8.3 (Tan et al., 2008) and gibbsite is 9.5-9.8 (Manning and Goldberg, 1996), and these metal oxides will have a net positive surface charge in most natural aquatic environments. Hydrous manganese oxide (HMO) has a pH_{ZPC} of about 2.3 (Murray, 1974; McKenzie, 1981) and will have a net negative surface charge at the pH of seawater. As a result, HMO is not expected to adsorb oxyanions such as arsenate or phosphate since the specific adsorption energy would not be sufficient to overcome the electrostatic repulsion with the surface (Balistrieri and Murray, 1982). However, adsorption of cations from seawater changes the pH_{ZPC} of the HMO surface and makes it favourable for anion adsorption. Takamatsu et al. (1985) reported that, in the absence of divalent cations, no significant arsenate adsorption was observed onto HMO over 2 hours, whereas the percent arsenate adsorption increased to 100 % at pH 6-8 in the presence of divalent cations ([HMO] = 36 mM, [phosphate] = 3.2 μM). Similarly, Kawashima et al. (1986) found that, in the absence of divalent cations, phosphate was not adsorbed onto HMO at near neutral to alkaline pH, but the percent adsorption increased to about 80 % at pH 6-8 in the presence of divalent cations and transition metals ([HMO] = 5 mg Mn, [arsenate] = 5 μg As). In both cases, the results were attributed to a change in the surface charge of the HMO due to the adsorption of cation(s). Yao and Millero (1996) also observed increased adsorption of phosphate when Ca^{2+} and Mg^{2+} were added to a 0.7 M NaCl solution ([δ-MnO_2] = 1 mM, [phosphate] = 10 μM). Conversely, the presence of sulfate and humic acids appeared to have no effect on phosphate adsorption at pH above 6, and adsorption of phosphate was independent of salinity between 5 and 35. Enhanced adsorption of phosphate to iron oxides has also been documented upon the addition of Ca^{2+} and

Mg^{2+} to a solution (Gao and Mucci, 2003). Bicarbonate ions can compete with arsenate and phosphate adsorption onto manganese oxides. Weak competition has been observed with arsenate and bicarbonate on goethite at pH 7-11 (Stachowics et al., 2007), arsenate and bicarbonate on hematite (Arai et al., 2004), and phosphate and bicarbonate onto kaolinite (Nagaraja et al., 1968). On the other hand, Radu et al. (2005) found that increasing concentrations of bicarbonate had little effect on arsenate adsorption onto iron oxide-coated sand at pH 7.

In the marine environment, the surfaces of hydrous manganese oxide minerals are complexed by H^+, Mg^{2+}, Ca^{2+}, Na^+, and K^+ (Balistrieri and Murray, 1982), modifying the pH_{ZPC} of the surface and promoting anion adsorption. The majority of manganese oxide adsorption studies to date have been carried out in freshwater/low ionic strength solution, groundwater, drinking water, or solutions containing specific divalent cations/anions and transition metal ions; studies in seawater are lacking. Yao and Millero (1996) in a study of 10 μM phosphate adsorption on 1 mM δ-MnO_2 in seawater, observed that adsorption of phosphate was initially very rapid (60 % complete in 5 minutes) but only reached near equilibrium (~95 %) after 10 hours. Bajpai and Chaudhuri (1999) studied the removal of arsenic from groundwater and found that the adsorption of 1.0 mg/L arsenate onto 10 g/L δ-MnO_2 coated sand was rapid and close to completion (~95 %) after 2 hours. The total arsenate removal was about 65 %. Ouvrard et al. (2001) investigated the individual adsorption of arsenate and phosphate from drinking water through column experiments with a natural manganese oxide (71 % w. MnO_2, 4 % Fe, 6 % Al_2O_3, particle size 600 μm and surface area 17 m^2/g, pH_{ZPC} = 4.7). They concluded that the natural manganese oxide studied had a greater affinity for arsenate than for phosphate. This was deduced from single component adsorption experiments (0.5-1300 μM As(V), 470-4800 μM phosphate). Manning et al. (2002) observed that following arsenite

oxidation, a significant amount of arsenic was adsorbed as arsenate (20-30 %) onto synthetic birnessite in drinking water during stirred flow reactions (experimental solution continuously stirred by a magnetic stir bar during the experiment). Katsoyiannis et al. (2004) observed 80 % arsenate removal (initial arsenate concentration 42 μg/L) by a column filled with beads coated with hydrous manganese oxide, formed by manganese-oxidizing bacteria, and 90 % arsenate removal for a similar column with iron oxide, also formed by bacteria.

In summary, both arsenate and phosphate are expected to adsorb onto hydrous manganese oxide in seawater. Previous studies confirm that arsenate has a stronger affinity than phosphate for HMO and a natural manganese oxide, and since the oxyanions have similar chemical properties, the adsorption kinetics are anticipated to be similar. Hongshao and Stanforth (2001) and Luengo (2007) found that the adsorption of both arsenate and phosphate on goethite followed a two-phase pattern with rapid initial adsorption followed by a slower reaction. Gao and Mucci (2003) and Kanematsu et al. (2013) also observed similar individual adsorption behaviours for arsenate and phosphate onto goethite. Table 2 presents the relative adsorption capacity of goethite for arsenate and phosphate.

Table 2: Relative adsorption capacity of goethite for phosphate and arsenate in a 0.7 M NaCl solution (25°C). Data from Gao (2001). The specific surface area of goethite was 33.5 m^2/g.

Adsorbate	pH	μmol/g	μmol /m^2
Phosphate	7.0	54	1.6
	8.5	38	1.2
Arsenate	7.0	61	1.8
	8.5	46	1.4

2.2. Surface complexation

The specific adsorption reaction mechanisms of arsenate and phosphate on HMO have not yet been examined, but surface complexation of oxyanions onto metal oxides can occur through different bonding and stoichiometries, including the formation of inner-sphere monodentate (1:1; one lone pair of electrons on the adsorbate binding to one site on the adsorbent), inner-sphere bidentate mononuclear (1:2; two lone pairs on the adsorbate binding to one site on the adsorbent), and inner-sphere bidentate binuclear (2:2; two lone pairs on the adsorbate binding to two sites on the adsorbent) and outer-sphere complexes (non-specific, electrostatic attraction between a charged surface and an oppositely charged ion in solution) (Hingston et al., 1972). Inner-sphere complexation involves specific and stronger interactions (chemical) with the solid surface than outer-sphere complexation (physical/electrostatic). These binding mechanisms and their respective balanced reactions are presented in Table 3. Manning et al. (2002) confirmed, through Extended X-ray Absorption Fine Structure (EXAFS) analysis, that the adsorption of arsenate onto birnessite (MnO_2) occurs through the formation of an inner-sphere bidentate binuclear complex, and the reaction can be written as:

$$2(\text{Mn-OH}) + H_3AsO_4 = (MnO)_2AsOOH + 2H_2O \qquad (1)$$

where Mn-OH represents the reactive hydroxyl group on the manganese oxide surface, and $(MnO)_2AsOOH$ represents the resulting surface complex. Katsoyiannis et al. (2004) suggested a similar adsorption reaction of arsenate onto a biogenic (hydrous) manganese oxide whereas Lafferty et al. (2010a), based on an EXAFS investigation, concluded that arsenate is bound to δ-MnO_2 as bidentate-binuclear

and monodentate-mononuclear complexes. In contrast, Yao and Millero (1996) suggested that phosphate is likely to form outer-sphere complexes ($MnOH_2^+$-$H_2PO_4^-$ and $MnOH_2^+$-HPO_4^{2-}) on δ-MnO_2, as defined in the context of a triple-layer model, in seawater and similarly high ionic strength solutions. Their adsorption data did not fit an inner-sphere model, but the outer-sphere model gave a good fit in 0.7 M NaCl. They did not do an EXAFS analysis of the reacted δ-MnO_2 surface, which might have confirmed their conclusion.

The bidentate-binuclear complex has been proposed as the dominant surface complex between arsenate on goethite, but a monodentate complex may also form at very low concentrations (Waychunas et al., 1993; Fendorf et al., 1997; Antelo et al., 2005). Tejedor-Tejedor and Andersen (1990) reported that phosphate, like arsenate, forms inner-sphere complexes on goethite including monodentate and bidentate complexes, whereas Persson et al. (1996) concluded that phosphate only forms monodentate complexes on goethite.

The presence of Mg^{2+} and Ca^{2+} may promote the adsorption of arsenate and phosphate onto HMO through ternary complexation. Ternary complexes form when cations (e.g. Mg^{2+} or Ca^{2+}) adsorb onto the negatively-charged surface of HMO, altering its pH_{ZPC} and promoting the electrostatic adsorption of the negatively-charged oxyanion (e.g. Yao and Millero, 1996; Ouvrard et al., 2002a). The cations serve as a bridging entity. The formation of ternary complexes of arsenate and phosphate with sodium (Gao and Mucci, 2001) and potassium (Antelo et al., 2005) on the surface of HMO has also been proposed.

Table 3: Possible surface complexes that form upon the adsorption of arsenate and phosphate onto a metal oxide.

Complex formations	References
Monodentate mononuclear complex (inner-sphere)	Min et al. 2009
Bidentate mononuclear (inner-sphere)	
Bidentate binuclear (inner-sphere)	
Inner-sphere	
$Mn(IV)OH + PO_4^{3-} + H^+ \longleftrightarrow Mn(IV)\text{-}PO_4^{2-} + H_2O$	Yao and Millero (1996)
$Mn(IV)OH + PO_4^{3-} + 2H^+ \longleftrightarrow Mn(IV)\text{-}HPO_4^- + H_2O$	
$Mn(IV)OH + PO_4^{3-} + 3H^+ \longleftrightarrow Mn(IV)\text{-}H_2PO_4 + H_2O$	
$2Mn(IV)OH + PO_4^{3-} + 2H^+ \longleftrightarrow Mn(IV)_2\text{-}PO_4^- + 2H_2O$	
$Mn(IV)OH + H_3AsO_4^0 \longleftrightarrow Mn(IV)\text{-}H_2AsO_4^0 + H_2O$	Stollenwerk (2003)
$Mn(IV)OH + H_2AsO_4^- \longleftrightarrow Mn(IV)\text{-}HAsO_4^- + H_2O$	
$Mn(IV)OH + HAsO_4^{2-} \longleftrightarrow Mn(IV)\text{-}AsO_4^{2-} + H_2O$	
Outer-sphere	
$Mn(IV)OH + PO_4^{3-} + H^+ \longleftrightarrow Mn(IV)OH_2^+\text{-}PO_4^{3-}$	
$Mn(IV)OH + PO_4^{3-} + 2H^+ \longleftrightarrow Mn(IV)OH_2^+\text{-}HPO_4^{2-}$	Yao and Millero (1996)
$Mn(IV)OH + PO_4^{3-} + 3H^+ \longleftrightarrow Mn(IV)OH_2^+\text{-}H_2PO_4^-$	
$2Mn(IV)OH + PO_4^{3-} + 2H^+ \longleftrightarrow (Mn(IV)OH_2^+)_2\text{-}PO_4^{3-}$	
Ternary complexes (* L = ligand, M = divalent cation)	
$Mn(IV)OH + M^{2+} + L^{2-} \longleftrightarrow Mn(IV)\text{-}M^{2+}\text{-}L^{2-} + OH$	
$Mn(IV)OH + L^{2-} + M^{2+} \longleftrightarrow Mn(IV)\text{-}OM^{2+}\text{-}L^{2-} + H^+$	Stumm (1993)

2.3. Competitive adsorption of phosphate and arsenate onto manganese oxides

There are few competitive adsorption experiments with arsenic and phosphate onto manganese oxides in the literature, and no studies have been conducted in seawater. Based on results of individual adsorption experiments, it could be expected that both arsenate and phosphate will compete for adsorption sites on HMO and that adsorption will likely favour arsenate since it has a higher affinity for these surfaces. However, published observations are contradictory. Driehaus et al. (1995) concluded that the oxidation of 6.7 μM arsenite as well as the subsequent adsorption of arsenate onto 92 μM δ-MnO_2 in freshwater was not affected by the presence of 0.03-0.1 mM phosphate. In contrast, Chiu and Herring (2000) observed that the extent and rate of arsenite (29 μM) oxidation by 94 μM manganite (γ-MnOOH) was reduced in the presence of 200 μM phosphate. Katsoyiannis (2004) stated that the reduced conversion of 0.3-0.7 μM arsenite to arsenate (decreased from 80 % to 30 %) on the surface of biogenic hydrous manganese oxide in the presence of 6.3 μM phosphate was not due to diminished oxidation, but rather to the competitive adsorption of arsenite and phosphate for adsorption sites on the oxide. Parikh et al. (2010) observed reduced total arsenic adsorption and arsenate production when 1-15 mM arsenite was oxidized by ~ 0.5 M hydrous manganese oxide (δ-MnO_2) in the presence of 1-15 mM phosphate. They concluded that phosphate and arsenate compete for adsorption onto the HMO.

The competitive adsorption of arsenate and phosphate has been examined more extensively on iron oxides including goethite (Gao and Mucci 2003; Hongsaho and Stanforth, 2001; Liu et al., 2001) and ferrihydrite (Jain and Loeppert, 2000), and iron ore (Zhang et al., 2004). Jain and Loeppert (2000) found that arsenate (2.08

mM) and phosphate (2.08, 20.8, 104 mM) compete for similar surface sites on ferrihydrite (2 g/L); the presence of phosphate caused a significant decrease in arsenate and arsenite adsorption at all concentrations studied at pH>7. At equimolar concentrations, both arsenate and phosphate adsorption decreased. The decrease was greatest at pH 9, with 20 % reduced arsenate adsorption (relative to maximum adsorption in a single-ion system). At a arsenate:phosphate molar ratio of 1:10, arsenate adsorption dropped 30-50 % over the entire pH range (3-10), whereas at 1:50 it did not exceed 11 % at pH 3.5 and was <1 % at pH 10.5. Liu et al. (2001) concluded that, at a As:P molar ratio of 1:1 and pH < 6, slightly more arsenate than phosphate was adsorbed on goethite. When arsenate was added before phosphate to solutions with pH ranging from 3 to 8.5, arsenate inhibited phosphate adsorption to a greater extent than when phosphate was added to the arsenate solution first. Furthermore, compared to the decrease in arsenate adsorption when the phosphate concentration was increased, the phosphate adsorption decreased more when the arsenate concentration was increased. Hongshao and Stanforth (2001) studied the competitive adsorption of phosphate (40 μM) and arsenate (40 μM) on goethite by simultaneous and sequential additions. Sequential additions revealed that the extent of exchange for the first oxyanion depended on the equilibration time before the second oxyanion was introduced – the longer the equilibration time, the greater the exchange. For example, after 1 hour of equilibration between phosphate and goethite, only 24 % of the phosphate was replaced by an equimolar addition of arsenate, but after 288 hours, 38 % of the phosphate was replaced by an equimolar addition of arsenate (relative to total adsorption, pH 5). Similarly, after 1 hour of equilibration between arsenate and goethite, only 2 % of the arsenate was replaced by equimolar additon of phosphate (relative to total adsorption, pH 5), whereas after 288 hours, 24 % of the arsenate was replaced. This indicates that different bonding mechanisms exist and that these result in either rapid irreversible

adsorption of anions, or slower adsorption of exchangeable anions. Results of simultaneous additions revealed that the two oxyanions were adsorbed about equally, but that the total surface coverage when using both ions simultaneously was slightly greater than for either individual ion. This observation is consistent with results from Hingston (1971) who also found that the amount of oxyanion adsorbed onto a metal oxide was greater in a mixed ion system, although it is dependent on the concentration of the adsorbate and adsorbent. Gao and Mucci (2001) observed that the adsorption of 9.0 μM arsenate on goethite from a 0.7 M NaCl solution was greatly reduced in the presence of phosphate (9.0, 22.5, 45 μM) and that the decrease was proportional to the phosphate concentration. Phosphate adsorption was less affected by the presence of arsenate in competitive experiments. On the other hand, competitive adsorption studies in artificial seawater revealed that, in simultaneous additions at a 1:2.5 (As:P) molar ratio at pH 8, there was no apparent change in arsenate adsorption, whereas phosphate adsorption was reduced by about 10 % relative to individual adsorption (Gao and Mucci, 2003). At a 1:5 (As:P) molar ratio, arsenate adsorption was reduced by 10 % whereas phosphate adsorption was reduced by 20 % relative to individual adsorption. On the other hand, Zhang et al. (2004) concluded that, irrespective of the As:P ratio, arsenate adsorption onto natural iron ores (64.1 % Fe, 3.5 % SiO_2, 1.8 % Al, 0.12 % MgO) in distilled water was reduced in the presence of phosphate. These results indicate that the composition of the solution and the nature of the solid surface may influence the competitive adsorption between arsenate and phosphate. For example, the pH of the solution determines the speciation of phosphate and arsenate and affects the surface charge of the solid. In seawater and groundwater there are many potential cations and anions that can interfere with the adsorption of arsenate and phosphate (some enhance adsorption, others inhibit adsorption). Antelo et al. (2005) concluded that phosphate adsorption is more affected by changes in pH compared

to arsenate adsorption, and this causes reduced phosphate adsorption in basic media. According to the CD-MUSIC model (0.1 KNO_3), phosphate complexation at the goethite surface gradually decreases from 2.4 μmol/m^2 at pH 3, to 1.8 μmol/m^2 at pH 8 and to about 1.25 μmol/m^2 at pH 10. In comparison, arsenate complexation was unchanged at 2.1 μmol/m^2 between pH 3-8, and decreased to 1.5 at pH 10. They suggest the effect is due to electrostatic differences between arsenate and phosphate (different location of charge on the oxyanions). In summary, studies of the competitive adsorption of arsenate and phosphate onto metal oxides have yielded different and conflicting conclusions. More research is clearly needed.

2.4. Desorption of phosphate and arsenate from metal oxides

Few studies have investigated the ability of various ions to desorb previously adsorbed arsenate or phosphate from manganese oxides (e.g. Lafferty et al., 2011) and few studies to date have examined the reversibility of the adsorption reaction (Hongshao and Stanforth, 201). Lafferty et al. (2011) found that phosphate, Ca^{2+}, and a solution of 10 mM NaCl and 5 mM MOPS (3-(N-morpholino)propanesulfonic acid (buffer)) to be efficient in desorbing arsenate from a poorly crystalline manganese oxide. After 4 hours of arsenite oxidation followed by arsenate adsorption, roughly 67 % of the adsorbed arsenate was mobilized. In most experiments, phosphate caused the greatest desorption of arsenate, but under all the experimental conditions investigated by Lafferty et al. (2011), a fraction of the arsenate always remained on the surface.

3. MATERIALS AND METHODS

3.1. Solution preparation

All glassware was acid washed in a 10 % nitric acid-bath for a minimum of 24 hours followed by thorough Milli-Q water rinse. Plastic bottles and other plastics were acid-washed in a 10 % HCl acid-bath for a minimum of 24 hours followed by thorough Milli-Q water rinse. Volumetric flasks were capped after rinsing whereas other glassware was dried at room temperature under a dust cover. All syringes and pipettes tips were disposable and only used once.

The seawater used for the experiments was collected in the St. Lawrence Estuary at STA-21 (49°05.4'N; 67°16.9'W) at a depth of 270 m on 19 May 2011 using 12-L Niskin bottles mounted on a CTD-rosette onboard the R/V Coriolis II. The practical salinity (S_p) determined by the conductivity probe (Seabird SBE-911) at the time of sampling was 34.334. Before analysis and experimental work, the seawater was filtered through a 0.45 μm HA Millipore filter and stored in Nalgene plastic bottles. The pH_{SWS} of the seawater was determined (method described in section 3.3.3.) after the seawater had been stored for 47 months, filtered, and equilibrated with the atmosphere for 48 hours and was 7.9. The soluble reactive phosphate (SRP) and silicate concentrations were 2.1 μM ± 0.1 μM and 11.8 ± 0.5 μM, respectively (methods described in section 3.3.2.). Silicate was measured after 12 months of storage and SRP several times between 12-46 months of storage. Total dissolved arsenic was determined 14.5 nM ± 3 nM by AAS (method described in section 3.3.1) after 12 months storage, which was near or below the detection limit.

The amorphous hydrous manganese oxide (HMO) (method described in section 3.2) was prepared using ACS grade reagents (NaOH, $KMnO_4$, $MnCl_2$) purchased from Fisher Scientific. The solutions were prepared in distilled water. A ~100 ppm arsenate stock solution was prepared by dissolving 0.0759 g of $As_2O_5 \cdot 5H_2O$ (99.99 %, Aldrich) in 500 mL Milli-Q water. This stock solution was diluted to the desired arsenate concentration for each experiment. A 10 mM orthophosphate stock solution was prepared by dissolving 1360.9 mg of potassium dihydrogenphosphate (KH_2PO_4; 99.5 % analytical reagent, Analar) in 1 litre of Milli-Q water to which 2 mL of a 4.5 M sulphuric acid solution were added. The phosphate salt had been dried in an oven for 1 hour at 110°C prior to use and the solution was stored refrigerated in a volumetric flask covered by aluminium foil.

3.2. Synthesis

3.2.1. Amorphous hydrous manganese oxide (HMO)

The synthetic manganese oxide suspension was prepared according to the method described by Laha and Luthy (1990) (originally developed by Murray, 1974). A suspension of approximately 10 mM amorphous hydrous manganese oxide (HMO) was prepared by combining 80 mL of 0.1 M NaOH (0.008 mol) with 40 mL of 0.1 M $KMnO_4$ (0.004 mol) under constant stirring by a suspended magnetic stir bar. The volume was adjusted to 500 mL with distilled water before 60 mL of 0.1 M $MnCl_2$ (0.006 mol) was added slowly. A dark brown precipitate formed quickly and the solution was stirred with a suspended magnetic stir bar for another 30 minutes to allow complete reaction and for the suspension to settle out. The solid was separated by vacuum filtration on a Millipore 0.45 μm HA Membrane filter and washed several times with Milli-Q water. The wet solid was immediately

resuspended in 1 L of seawater water yielding a slurry of ~10 mM HMO. To account for aging and change in reactivity over time, the suspension was used after 24 hours of preparation (Stone and Morgan, 1984; Laha and Luthy, 1990) and within 1 month (Catts and Langmuir, 1986). The suspension was additionally sonicated for 60 minutes to separate particles/homogenize the suspension as much as possible prior to the experiments (Ying et al., 2012), and stored at 4°C until use (Lafferty et al. 2010c). The solid to volume ratio was determined for each batch by filtering 10-12 of 20 mL aliquots of the stock suspensions through a 0.45 μm HA Millipore filter weighing the collected solid after it had been dried at room temperature for 48 hours. These values were used to determine how much HMO was added to each experiment (Table 3). In the current literature there is little information about the stability of amorphous manganese oxide suspensions, but it is suggested to store the suspension at low temperature and to use it within a month to avoid the effect of altered crystallinity, surface area and mineralogy (Stone and Morgan, 1984; Catts and Langmuir, 1986; Lafferty et al., 2010c).

The mineralogy of two of the seven batches of HMO (Batch # 1 and 4) was verified by X-ray diffraction (XRD) analysis two weeks and 6 months after the suspension was prepared. The suspension was filtered, rinsed with distilled water to remove salts, dried, and mounted on the sample stage. The diffractograms (example presented in Fig. A-1 of Appendix 1) were recorded using a Siemens (Bruker) D5000 Diffractometer and Co with Ni filter cathode at an accelerating voltage of 40kV/30mA and a scanning rate of 2 degrees 2 theta/minute. The two-week old suspension showed no distinct peaks, which indicates that the structure is completely amorphous, whereas the 6-month old suspension yielded small spurious potential peaks around 10.5°, 20.5° and 31° 2θ (CoKα) that could not readily be matched to a specific mineral upon EVA (Evaluation) software with ICDD (International Centre

for Diffraction Data) standards. The closest matches where the hydrated manganese iron phosphate minerals stewartite (41.97 % match) and laueite (13.71 % match) both with the chemical formula $Mn^{2+}Fe^{3+}{}_2(PO_4)_2(OH)_2 \cdot 8H_2O$. Murray's (1974) XRD analysis of the prepared hydrous manganese oxide showed a low degree of crystallinity with reflection points at 7.4, 4.04, 2.43 and 1.63 Å, corresponding to a structure similar to birnessite. Cui et al. (2009) obtained two predominant peaks at 15° and 32° 2θ (FeKα) for various types of synthetic Na- and K-birnessite. The specific surface area of the HMO (Batch # 7) was determined on a standard Acorn Area Particle Surface Area Analyzer using AreaQuant software (version 0.9.2.) by Xigo Nanotools Laboratory. This method measures the surface area of suspensions using a patented NMR (Nuclear Magnetic Resonance) technique. The suspension was stirred prior to measurement due to particle settling and the surface area was estimated using a T_2 measurement obtained from a CPMG (Carr-Purcell-Meiboom-Gill) sequence with 436 echo cycles and $T = 0.5$ ms, averaging 4 scans with a recycle delay of 3500 ms. The specific surface area was estimated at 272.5 m^2/g of solids, based on a T_2 value of 746.6 ms, a specific surface relaxivity, K_a, of 0.001168 $g/m^2/ms$, a bulk relaxation time of 2600 ms, and a volume ratio (solid-to-liquid) of 0.0030 in de-ionized water.

Table 4: Solid to volume ratios of the HMO batches.

Batch #	solid:volume ratio
1	0.71 g/L ± 0.07
2	1.08 g/L ± 0.18
3	1.33 g/L ± 0.29
4	0.94 g/L ± 0.30
5	2.05 g/L ± 0.08
6	1.28 g/L ± 0.06
7	1.61 g/L ± 0.45

3.3. Analytical Methods

3.3.1. Atomic Absorption Spectrometry

The total dissolved arsenic concentrations were determined by flameless atomic absorption spectrometry (AAS). Arsenic was determined by hydride generation following the method of Aggett and Aspell (1976). The analysis was conducted on a Perkin-Elmer Aanalyst 100 equipped with an AS 90 autosampler, a FIAS 400 flow injection system and an electrodeless discharge lamp (EDL). The sample cell was heated to 900°C, the EDL was set to 385 milliamps and the detector at a wavelength of 197.3 nm. Arsenic samples were pre-treated with a 5 % (w/v) ascorbic acid/KI solution and 10 % trace-metal free HCl for at least 1 hour to reduce all arsenate to arsenite. The sample to 5 % ascorbic acid/5 % KI to 10 % HCl ratio was 1:3:10. Arsenite was reduced to arsine by reaction with a solution containing 0.2 % (w/v) sodium borohydride ($NaBH_4$) and 0.05 % (w/v) sodium hydroxide (NaOH). Additional information about the reagents is presented in Appendix 1.

Calibration curves were constructed using external standards prepared by appropriate dilution of the stock solution (described in 3.1) with Milli-Q water. Standard calibration curves were determined after every 12-15 samples and always at an r^2 level of at least 0.999. Samples were run in triplicate and only the mean values are reported. Sample concentration measurements with a %RSD above 10 % were rejected and re-analyzed. The detection limit ranged from 8-35 nM (0.6-2.6 ppb) calculated from three times the highest blank and the slope of the calibration curve. An arsenate calibration curve is presented in Appendix 2.

3.3.2. Absorption spectrometry

Soluble Reactive Phosphate (SRP)

Phosphate was measured on the day of sampling or within 24 hours. Soluble reactive phosphate (SRP) concentrations were determined colorimetrically as the molybdenum blue complex following the procedure described in Grasshoff et al. (1999) (original procedure developed by Murphy and Riley, 1962). In the presence of arsenate exceeding 0.05 μM, the arsenate ion is reduced to arsenite by the addition of 0.5 mL of 2.4 % (w/v) thiosulfate per 25 mL sample (Grasshoff et al., 1999) to avoid interference with the SRP analysis. For samples containing up to 2 μM arsenic, 1 mL of the ascorbic acid and 0.5 mL of the thiosulfate solution was added and mixed thoroughly. After 15 minutes of reaction time, 1 mL of the mixed reagent was added and the solution mixed well, and the absorbance was read after 15 minutes and within 30 minutes.

The analysis was performed manually on a Hewlett-Packard Agilent 8453 UV-visible spectrophotometer, operating in the 190 to 1100 nm (± 0.5 nm) range, using a 10-cm cell. The absorbance at a wavelength of 880 nm is linear up to an absorbance of about 1.800 (approximately 8 μM phosphate) and the reagents are effective up to a phosphate concentration of 50 μM. The detection limit is 2-3 nM (Wurl, 2009) and the method is assumed free of salt effect (<1 %, according to Murphy and Riley, 1962). Calibration curves were constructed by successive dilution of the 10 mM standard phosphate stock solution with Milli-Q water. The r^2 value of the calibration curves was always at least 0.999. Concentrations higher than 6 μM were diluted to prevent non-linearity. A phosphate calibration curve is presented in Fig. A-2 of Appendix 2.

Dissolved Inorganic Silicate

The concentration of dissolved inorganic silicate was determined by the method described in Grasshoff et al. (1999). The method is based on the formation of a yellow β-silicomolybdic acid when a sample is treated with a molybdate solution under acidic conditions (pH ~ 1.5). The silicomolybdic acid is then reduced by ascorbic acid to form a blue coloured complex, followed by the addition of oxalic acid to avoid reduction of excess molybdate and to eliminate the influence of phosphate. The analysis was performed manually on a Hewlett-Packard Agilent 8453 UV-visible spectrophotometer and a 1-cm cell. The absorbance of the complex was measured at 810 nm. It is linear up to 200 μM (Grasshoff et al., 1999), and the detection limit is below 0.03 μM (Taylor, 1990). The instrument was calibrated using external solutions prepared by suitable dilution of a standard silicate stock solution (50 mM). The latter was prepared by dissolving 0.4700 g of disodium hexafluorosilicate in 50 mL of Milli-Q water. The silicate salt had been dried in an oven at 105°C for 1 hour before use and the solution was prepared two days prior to the analysis to ensure complete dissolution. A silicate calibration curve is presented in Fig. A-3 of Appendix 2.

3.3.3. Temperature, Salinity and pH

All experiments were carried out at room temperature (23±3°C), and the temperature of the experimental solution was monitored during several adsorption experiments. The salinity of the experimental solution was determined by titration with a $AgNO_3$ solution standardized against IAPSO standard seawater. The pH of the experimental solution on the seawater scale (pH_{SWS}) was determined spectrophotometrically with a Hewlett-Packard Agilent 8453 UV-visible spectrophotometer and a 1-cm cell. Phenol red was used as indicator and

absorbances were measured at 433 nm and 558 nm after 1.5 minutes of reaction. A TRIS buffer solution with a salinity of 35.0 was used for calibration, and the pH_{sws} was calculated using molar absorbance values and pK(phenol red) from Baldo (1985), K(HSO_4) from Khoo (1977), and K(HF) from Dickson (1990).

Samples for salinity and pH analysis were taken at "time zero" of the experiments and 48 hours into the experiments. This was done to ensure that there was no significant change in the pH or salinity over the course of the experiments.

3.4. Experimental Protocols

Several experiments were conducted to determine the individual and competitive adsorption and adsorption kinetics of arsenate and phosphate onto HMO from seawater, and the desorption of arsenate- or phosphate-laden hydrous manganese oxide in seawater. Assuming no adsorption onto the vessel walls, all experiments were performed at room temperature (23±3°C) and at the pH of seawater. Only dissolved concentrations were measured due to limitations with the methods and instruments.

3.4.1. Phosphate adsorption onto amorphous hydrous manganese oxide from seawater

The experiments were conducted at initial phosphate concentrations ranging from 2.0 to 46 μM, whereas the concentration of HMO was kept constant at approximately 0.15 g/L (~ 1 mM). The initial solution was prepared by adding the required volume of the 10 mM phosphate stock solution to 500 mL of filtered seawater and this solution was left open to the atmosphere and stirred for about 15

minutes before an aliquot was taken for determination of the "time zero" concentration. Fifty five mL of the HMO suspension, which was pre-equilibrated with seawater between 1-31 days, was then added to solution to obtain an approximate solid to solution ratio of 0.15 g/L. At set time intervals, 25 mL samples of the solution were withdrawn, filtered through a 0.45 μm HA filter and analyzed for their soluble reactive phosphate (SRP) content. All samples were collected using a 60 cc plastic syringe that was immersed directly into the experimental solution. These experiments were replicated with the same HMO batch and with HMO from different syntheses. The results showed that sonication of the HMO suspensions and sampling the suspension with a pipette while it was being stirred by a suspended magnetic stir bar yielded more reproducible adsorption kinetic results. A control experiment was also carried out under the same conditions but in the absence of HMO to confirm the stability of the solution and lack of significant adsorption to the walls of the container. Aliquots of the control solution were sampled and analysed on 8 occasions over a 44-hour period (Appendix 3). The initial SRP concentration (2.1 μM) remained the same within 0.02 μM (SD) or 1.1 % (RSD) throughout the control experiment, confirming that there was no significant phosphate adsorption to the walls of the container or the magnetic stir bar. Hence, whereas the HMO was not analysed after the adsorption experiment, it was assumed that adsorption of phosphate was onto HMO only. The reproducibility of the spectrophotometric SRP measurements, estimated by determining the concentrations of six 5 μM phosphate solutions prepared by dilution of the same stock solution with Milli-Q water, was 0.04 μM (SD) or 0.78 % (RSD).

The kinetic experiments were followed over a 48-hour period and samples were taken at set time intervals (0, 0.0833, 0.167, 0.25, 0.5, 1, 2, 4, 6, 8, 10, 24, and 48 hours after the HMO addition). Maximum adsorption concentrations for the

isotherm were measured after 30 hours. All experiments were conducted at room temperature in a 1L Pyrex beaker equipped with a suspended stir bar, and with a glass lid to prevent evaporation and contamination from dust (but open to the atmosphere). The solution was stirred at a constant rate (~100 rpm), enough to keep the solution homogeneous, but without a visible vortex. Luengo et al. (2007) found that the stirring rate did not affect the adsorption kinetics of phosphate and arsenate on goethite.

3.4.2. Arsenate adsorption onto amorphous hydrous manganese oxide from seawater

Kinetic adsorption experiments for arsenate were performed the same way as with phosphate (described in section 3.4.1.). The initial arsenate concentrations in seawater ranged from 0.6-6 μM. At the set time intervals, 25 mL samples were withdrawn with a syringe, filtered through a 0.45μm HA Millipore membrane filter and analyzed as described in section 3.3.1. The reproducibility of the flameless AAS measurements, estimated by determining the concentrations of six 2 μM arsenate solutions prepared from the same stock solution, was 0.02 μM (SD) or 0.79 % (RSD).

3.4.3. Competitive adsorption of arsenate and phosphate onto amorphous hydrous manganese oxide from seawater

The kinetics of the competitive adsorption of arsenate and phosphate onto HMO was examined through simultaneous and sequential addition of phosphate and arsenate to a seawater solution in the presence of HMO. In simultaneous addition experiments, the ions compete for the same adsorption sites, whereas in sequential

addition experiments one ion is adsorbed before the second is introduced to the solution and can displace the other on the surface of the HMO.

Simultaneous addition

Three sets of kinetic experiments were performed using simultaneous additions of phosphate and arsenate, and the experimental conditions are summarized in Table 5. The combined phosphate and arsenate seawater solutions were stirred for about 15 minutes before two individual 25-mL aliquots were withdrawn to determine the exact initial phosphate and arsenate concentrations ("time zero"). Next, 100 mL of the HMO suspension was added to the solutions to obtain an approximate solid to solution ratio of 0.15 g/L (identical to individual adsorption experiments). The phosphate and arsenate adsorption kinetics were monitored over 48 hours and samples were taken at the frequency as for the individual adsorption experiments. Samples for phosphate and arsenate analysis were collected simultaneously using two syringes and filtered through 0.45 μm HA Millipore membrane filters. Two syringes were used because each 0.45 μm HA Millipore membrane filter could only separate about 40 mL of the experimental solution before it clogged. The samples were analyzed following the methods described in section 3.3.1 and 3.3.2.

Sequential additions

Two experiments were carried out to examine the effect of exposing HMO sequentially to phosphate and arsenate. The arsenate to phosphate ratio was 1:10 for both experiments (1 μM arsenate, 10 μM phosphate). The required volume of phosphate or arsenate stock solution was added to 875 mL of seawater and an aliquot was taken after 15 minutes of stirring to determine the initial oxyanions concentration. Next, 100 mL of the HMO suspension was added to obtain an approximate solid to solution ratio of 0.15 g/L (identical to individual adsorption

experiments). After 48 hours, an aliquot of the solution was withdrawn to determine the equilibrium oxyanion concentration and the appropriate volume of the second oxyanion stock solution was added. The kinetics of the competing adsorption was followed over the next 48 hours as the mixed solution was sampled at the same frequency as for the individual adsorption experiments and both oxyanion concentrations determined according to the methods described in 3.3.1 and 3.3.2.

3.4.4. Desorption of arsenate- or phosphate-laden amorphous hydrous manganese oxide in seawater

Several experiments were performed to investigate the kinetics of arsenate or phosphate desorption from HMO in seawater. First, 55 mL of the HMO suspension was added to 500 mL of seawater (solid to solution ratio: 0.15 g/L) containing either 31 μM of phosphate or 6 μM of arsenate. The solution was stirred and allowed to equilibrate for 48 hours before the equilibrium oxyanion concentration was determined. The phosphate- or arsenate-laden HMO was then filtered through a 0.45 μm HA Millipore membrane filter and immediately transferred to 500 mL of seawater. The desorption kinetics of the oxyanion was monitored over the next 48 hours and samples taken at the same frequency as for the individual adsorption experiments and the oxyanion concentration analyzed following the methods described in 3.3.1 and 3.3.2.

Table 5: Summary of experimental conditions during simultaneous additions. The experimental solutions were prepared by additions of appropriate volumes of stock solutions of 900 mL of seawater.

	Arsenate (μM)	Phosphate (μM)	Ratio
1	2.0	5.0	1:2.5
2	0.5	5.0	1:10
3	0.5	50	1:100

4. RESULTS

The results obtained using the experimental protocol in section 3.4 are described below. The data are presented graphically and all the numerical data can be found in Appendices 3-7. Errors are shown as the standard deviation or percent standard deviation.

4.1.Temperature, salinity and pH

4.1.1. Temperature

The temperature of the experimental solutions was monitored during some of the 48-hour adsorption experiments. It typically increased by 4°C, from 22-26°C, in the first 5 hours of reaction time and remained nearly invariant to the end of a 48-hour experiment. When the cold manganese oxide suspension was added, the temperature of the experimental solution dropped by about 1°C within minutes, but increased steadily after about 30 minutes. The increase in temperature is likely due to heating by the stirrer, and the evolution of the solution temperature during one competitive adsorption experiment is shown in Fig. 6.

4.1.2. Salinity

The salinity of the experimental solutions was monitored over the course of several adsorption experiments. Samples were taken at time zero and at the end of the experiment (after 48 hours). The practical salinity of the initial experimental solution was 33.39 (± 0.43) and typically increased only slightly (33.57 ± 0.40) by the end of the experiment, most likely as a result of evaporation.

4.1.3. pH

The pH_{sws} of the experimental solution was measured during several adsorption experiments at time zero and after 48 hours. Insignificant changes in pH were noted, with the average initial pH being 7.72 ± 0.06 and the final pH equal to 7.74 ± 0.05.

Figure 6: Temperature of the experimental solution over the course of one competitive adsorption experiment (48 hours).

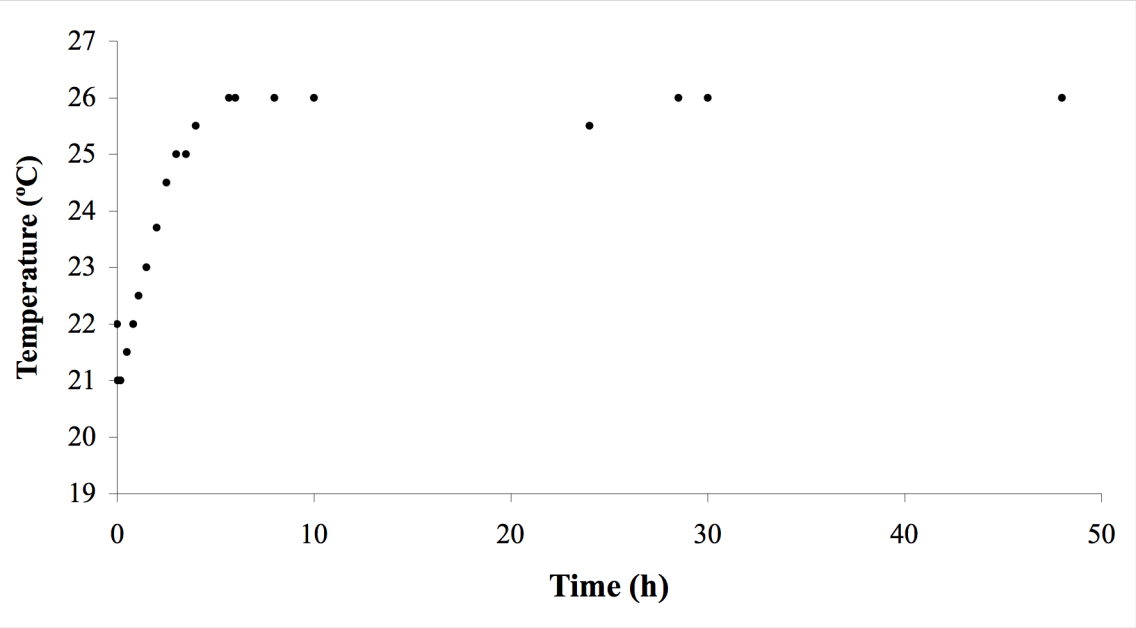

4.2 Adsorption of phosphate onto amorphous hydrous manganese oxide from seawater at 23(±3)°C

4.2.1. Reproducibility of the experiments

The kinetics of phosphate adsorption onto amorphous hydrous manganese oxide (HMO) was first evaluated over 8 hours through replicate experiments with different batches of HMO at 23 (±3)°C (Fig. 7). This was done to ensure that the experiment was reproducible and that there were no significant variations in the rate of adsorption or the amount of adsorbed material for the different batches of HMO. Experiments with the first HMO batch showed that the reaction was rapid and close to completion after 8 hours, and therefore these experiments were only monitored over 8 hours. The results show good reproducibility and precision within a given batch, and similar adsorption results between batches. The replicate experiments were only done with phosphate due to more rapid determination relative to arsenate. Moreover, the range of arsenate concentrations studied are lower than phosphate since in the marine environment, phosphate is naturally more abundant. The amount of phosphate and arsenate adsorbed is reported as a percentage to show the relative change.

4.2.2. Kinetics of phosphate adsorption over 48 hours

Phosphate adsorption onto HMO (Batch # 5) from seawater was monitored over 48 hours with an initial phosphate concentration of 6 μM and solid:solution ratio of 0.15 g/L. The amount of adsorption was determined by subtracting $[SRP]_{solution}$ from $[SRP]_{initial}$, and the percent adsorption was calculated by dividing $[SRP]_{adsorbed}$ by $[SRP]_{solution}$ and multiplying by 100. The adsorption reaction was initially rapid and

was 75 % complete within 4 hours (Fig. 8). The rate of phosphate adsorption decreased with time and the reaction was 91 % complete after 24 hours. The total percent adsorption (at equilbrium) was 31 % .

4.2.3. Phosphate adsorption isotherms

Langmuir and Freundlich adsorption isotherms were constructed for phosphate concentrations ranging from 2.0-46 μM and a [HMO]:solution ratio of 0.15 g/L. The adsorption data was fit to a Langmuir adsorption isotherm (Fig. 9) of the form:

$$\Gamma = \Gamma_{max} \times (K_{ads}[SRP]_{equilibrium})/(1+K_{ads}[SRP]_{equilibrium}) \qquad (2)$$

where $[SRP]_{equilibrium}$ is reported in μM and Γ is plotted as the amount of adsorbed phosphate (μmol) times the volume of solution, divided by the specific surface area (m^2/g) times the mass of adsorbent. Γ_{max} and K_{ads} were obtained by plotting $1/\Gamma$ versus the reciprocal concentration of the adsorbate (Fig. 10). Their values were 0.34 (Γ_{max}) $\mu mol/m^2$ (calculated as 1/intercept) and 0.07 (K_{ads}) $m^2/\mu mol$ (calculated as $1/(\text{slope} \times \Gamma_{max})$) respectively (Table 6). The Freundlich adsorption isotherm was fitted to the form:

$$\Gamma = K_f \times [SRP]_{equilibrium}^{(1/n)} \qquad (3)$$

where $[SRP]_{equilibrium}$ and Γ are plotted as above (Langmuir). K_f and n were obtained by plotting the $\log(\Gamma)$ versus the $\log[SRP]_{equilibrium}$ (Fig. 11) and their values were 0.03 $\mu mol/m^2$ (calculated as $10^{intercept}$) and 1.5 (calculated as 1/slope), respectively (Table 6). The models were compared to the experimental values by the RSQ excel function, which is a function that returns the r^2 or the square of the correlation

coefficient. This function showed that n = 1.3 gave the best fit to the experimental data, which are fitted well by both isotherms, but overall, the Freundlich isotherm provides the best fit.

The percent adsorption versus $[SRP]_{equilibrium}$ was plotted to examine the fraction (percent) phosphate adsorption relative to the initial phosphate concentration. The plot showed that the fraction (percent) of phosphate adsorption decreased with increasing initial phosphate concentration, which was expected. Percent adsorption ranged from 44 % ($[SRP]_{initial}$ = 2.0 μM) to 21-25 % for $[SRP]_{initial}$ = 15-46 μM (Fig. 12).

Table 6: Parameters of Langmuir and Freundlich isotherms for the adsorption of phosphate and arsenate onto HMO (23 ± 3°C).

		Langmuir			Freundlich	
Adsorbate	Range of concentration	Γ_{max} μmol/m^2	K_{ads} m^2/μmol	r^2	K_f μmol/m^2	r^2
Arsenate	0.6-6 μM	0.21	0.32	0.977	0.06	0.996
Phosphate	2-46 μM	0.34	0.07	0.968	0.03	0.994

Figure 7: Adsorption of SRP onto two different batches of HMO from seawater at 23(±3)°C over the first 8 hours. The [HMO]:solution ratio was 0.15 g/L for all experiments (Batch # 2 and 5).

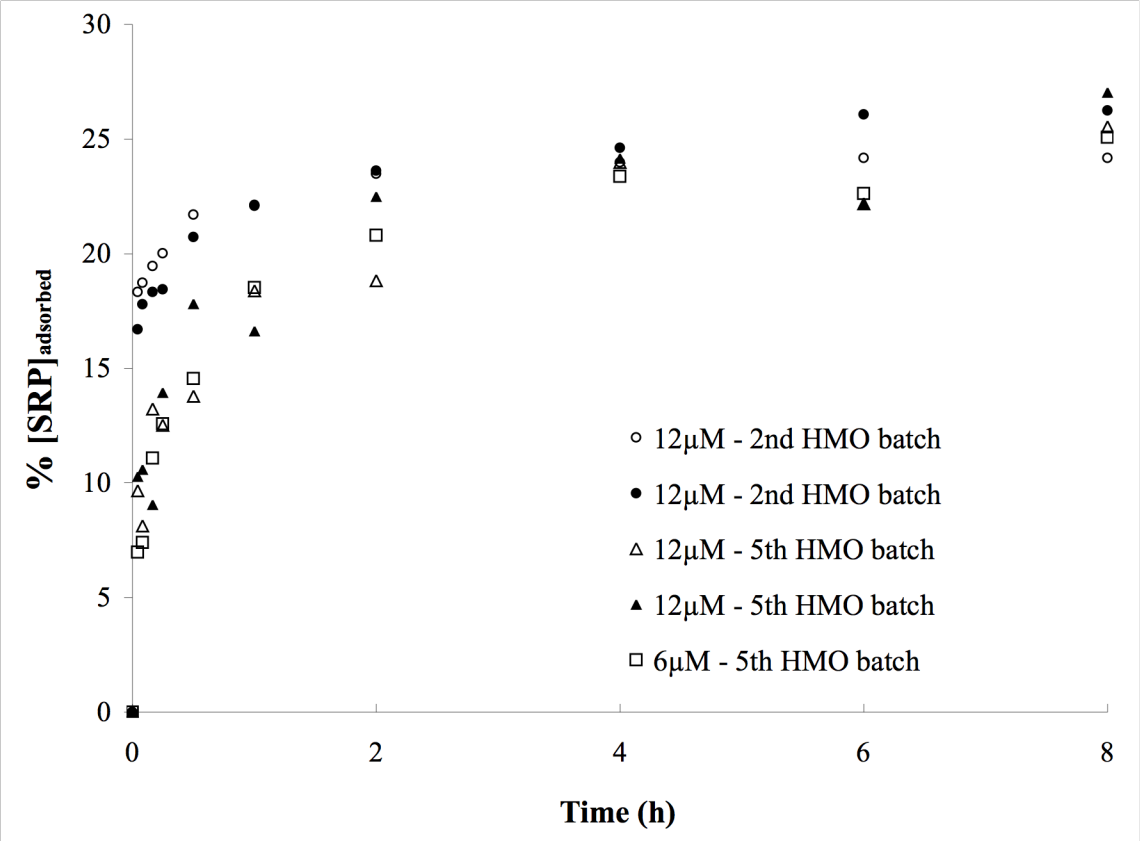

Figure 8: Percent phosphate adsorption onto HMO from seawater at 23(±3)°C over 48 hours. $[SRP]_{initial}$ = 6 µM, [HMO]:solution ratio = 0.15 g/L (Batch #5).

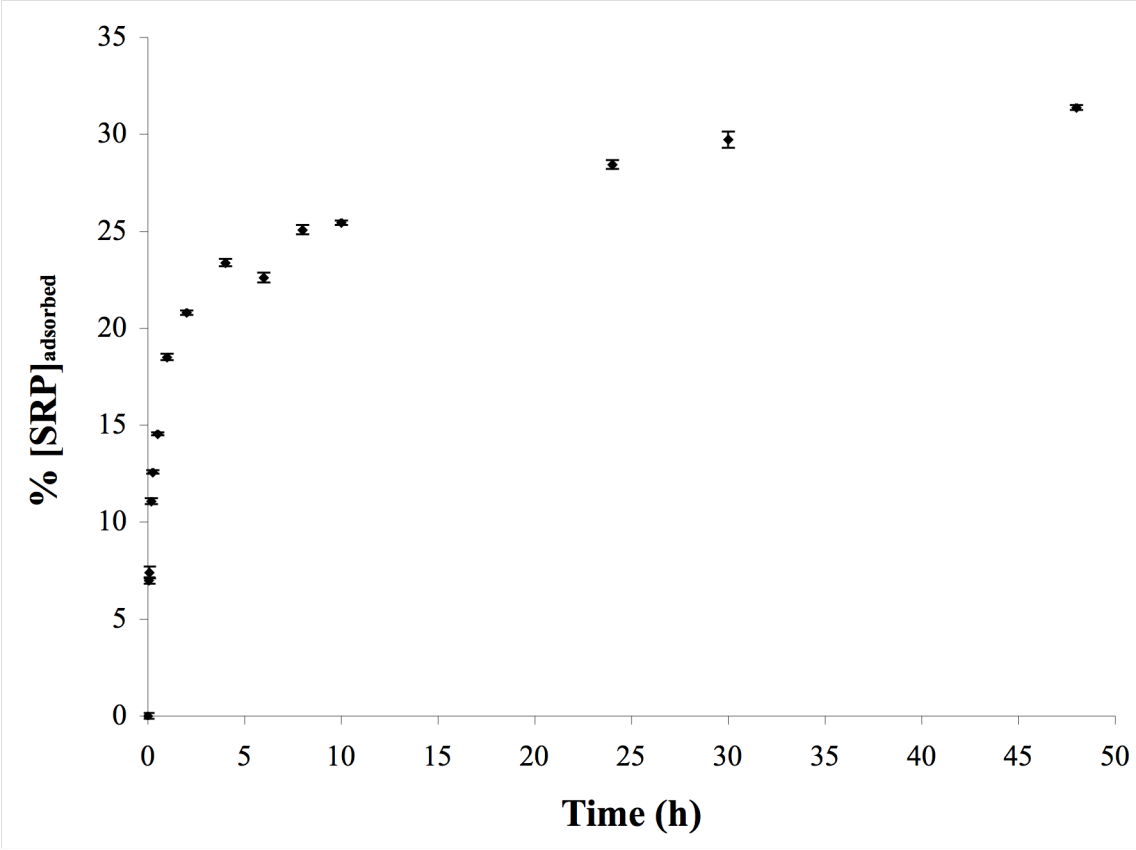

Figure 9: Langmuir- and Freundlich-type phosphate adsorption isotherms at 23(±3)°C, [HMO]:solution ratio = 0.15 g/L, (Batch # 4, 6 and 7), $[SRP]_{initial}$ = 2.0-46 µM.

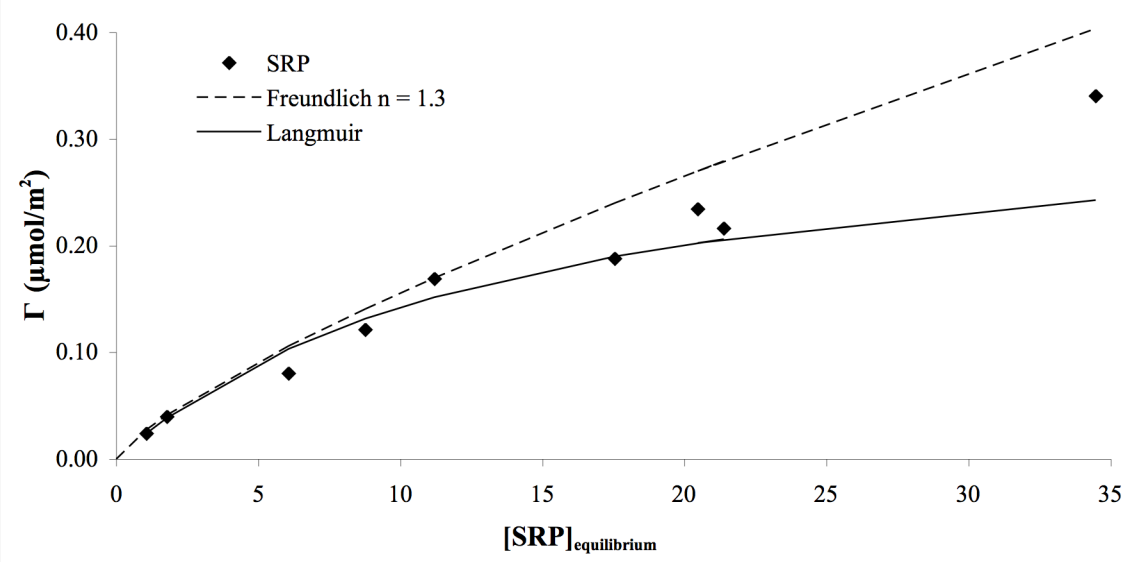

Figure 10: Reciprocal Langmuir-type phosphate adsorption isotherm at 23(±3)°C, [HMO]:solution ratio = 0.15 g/L, (Batch # 4, 6 and 7), $[SRP]_{initial}$ = 2.0-46 µM.

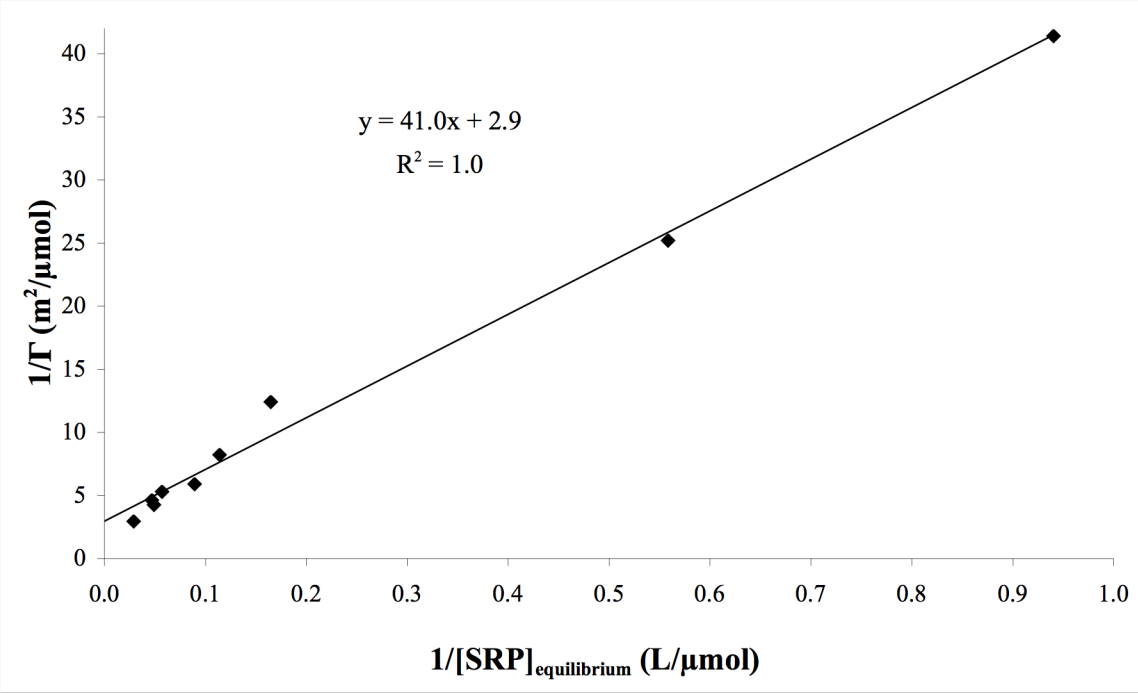

Figure 11: Logarithmic Freundlich-type phosphate adsorption isotherm at 23(±3)°C, [HMO]:solution ratio = 0.15 g/L, (Batch # 4, 6 and 7), $[SRP]_{initial}$ = 2.0-46 μM.

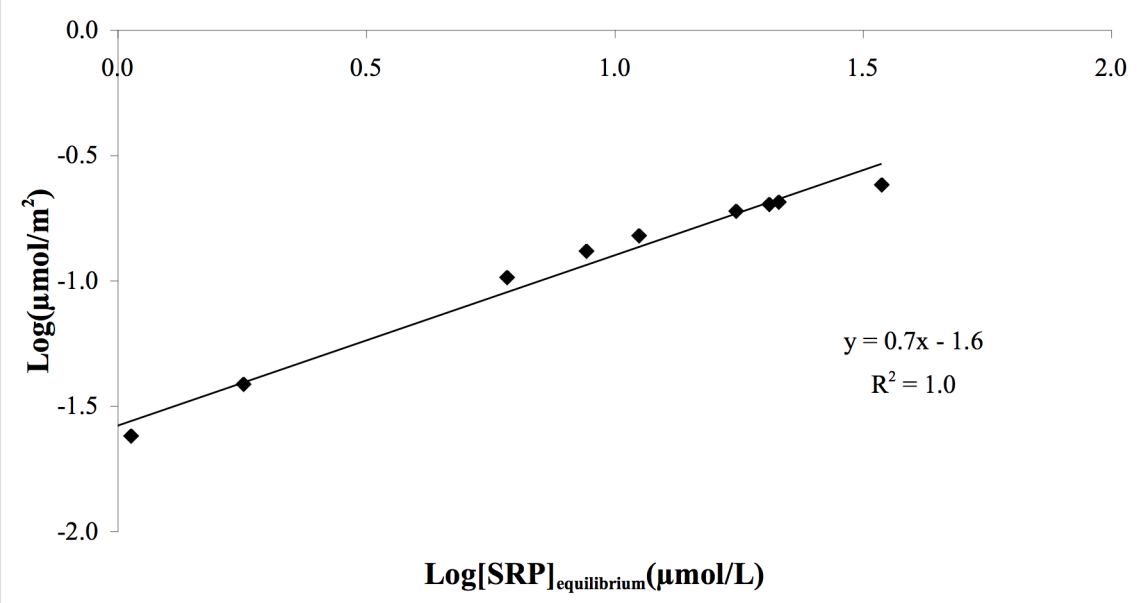

Figure 12: Percent phosphate adsorption at equilibrium and 23(±3)°C, [HMO]:solution ratio = 0.15 g/L, (Batch # 4, 6 and 7), $[SRP]_{initial}$ = 2.0-46 μM.

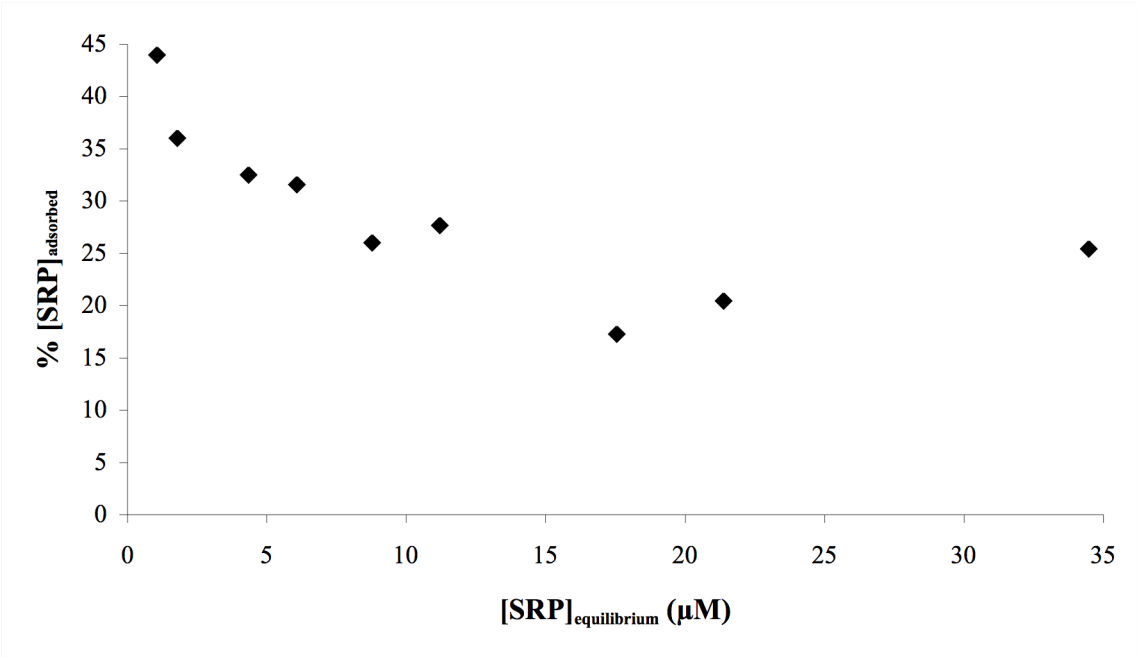

4.3. Arsenate adsorption onto amorphous hydrous manganese oxide from seawater at 23(±3)°C

4.3.1. Kinetics of arsenate adsorption over 48 hours

Arsenate adsorption onto amorphous hydrous manganese oxide (HMO) was monitored over 48 hours from an initial 0.6 μM arsenate concentration in seawater and a [HMO]:solution ratio of 0.15 g/L (Batch # 5) (Fig. 13). The adsorption reaction was initially rapid, 90 % complete after 4 hours and 98 % complete after 8 hours. The amount of adsorption of arsenate by HMO was determined by subtracting $[As(V)]_{solution}$ from $[As(V)]_{initial}$, and the fraction (percent) adsorption was calculated by dividing $[As(V)]_{adsorption}$ by $[As(V)]_{solution}$ and multiplying by 100. The total adsorption was 79 %.

4.3.2. Arsenate adsorption isotherms

Langmuir and Freundlich adsorption isotherms were constructed using arsenate concentrations in the range 0.6-6 μM at a [HMO]:solution ratio of 0.15 g/L. The adsorption data were fit to a Langmuir and Freundlich adsorption isotherms (Fig. 14) in the same form as phosphate and described in section 4.2.3. The obtained Γ_{max} and K_{ads} values were 0.21 μmol/m^2 and 0.32 m^2/μmol respectively (Fig. 15-16) (Table 6). The n value obtained from the log(Γ) versus the $\log[As(V)]_{equilibrium}$ plot was 1.0, but the RSQ function indicated that the best fit was with n = 0.78. Both isotherms fit well to the experimental data, but overall, the Freundlich isotherm fit is better.

The percent adsorption versus $[As(V)]_{equilibrium}$ was plotted to examine the fraction (percent) arsenate adsorption relative to the initial arsenate concentration. As with

phosphate, the highest total percent As(V) adsorption was obtained at the lowest $[As(V)]_{initial}$ concentration, but there was no obvious trend of decreasing total percent As(V) adsorption with increasing initial arsenate concentration over the range of concentrations studied. The percent adsorption ranged from 79 % ($[As(V)]_{initial}$ = 0.6 μM) to 70-77 % ($[As(V)]_{initial}$ = 1.0-6.0 μM) (Fig. 17).

Figure 13: Percent arsenate adsorption onto HMO from seawater at 23(±3)°C over 48 hours. $[As(V)]_{initial}$ = 0.6 μM, [HMO]:solid solution ratio = 0.15 g/L, (Batch # 5).

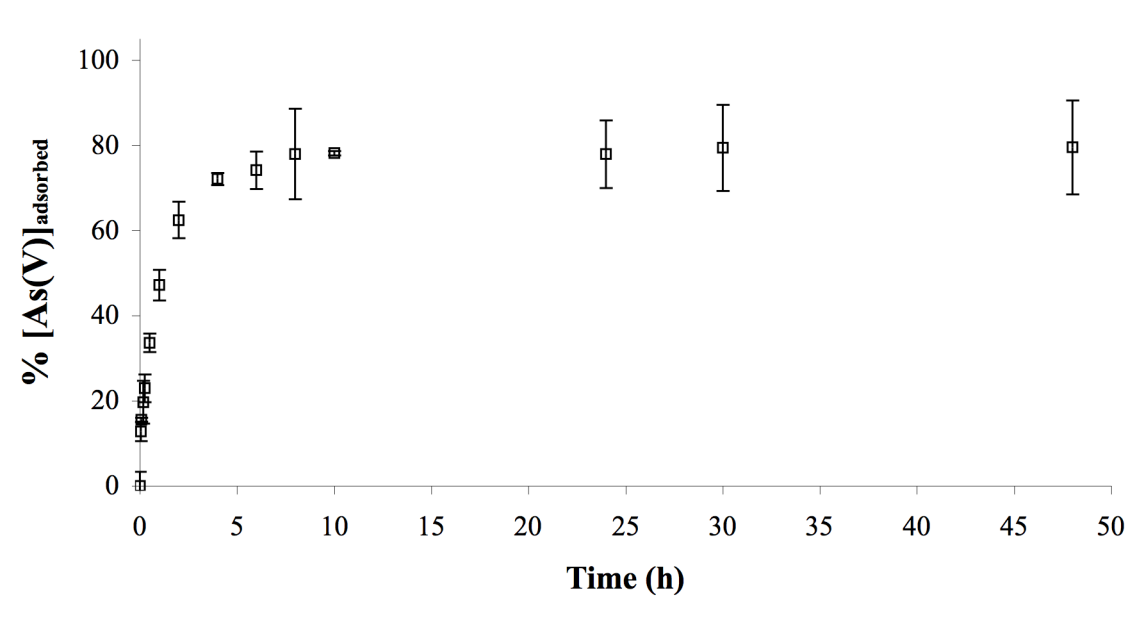

Figure 14: Langmuir- and Freundlich-type arsenate adsorption isotherms at 23(±3)°C, $[As(V)]_{initial}$ = 0.6-6 µM, [HMO]:solid solution ratio = 0.15 g/L, (Batch # 5-6).

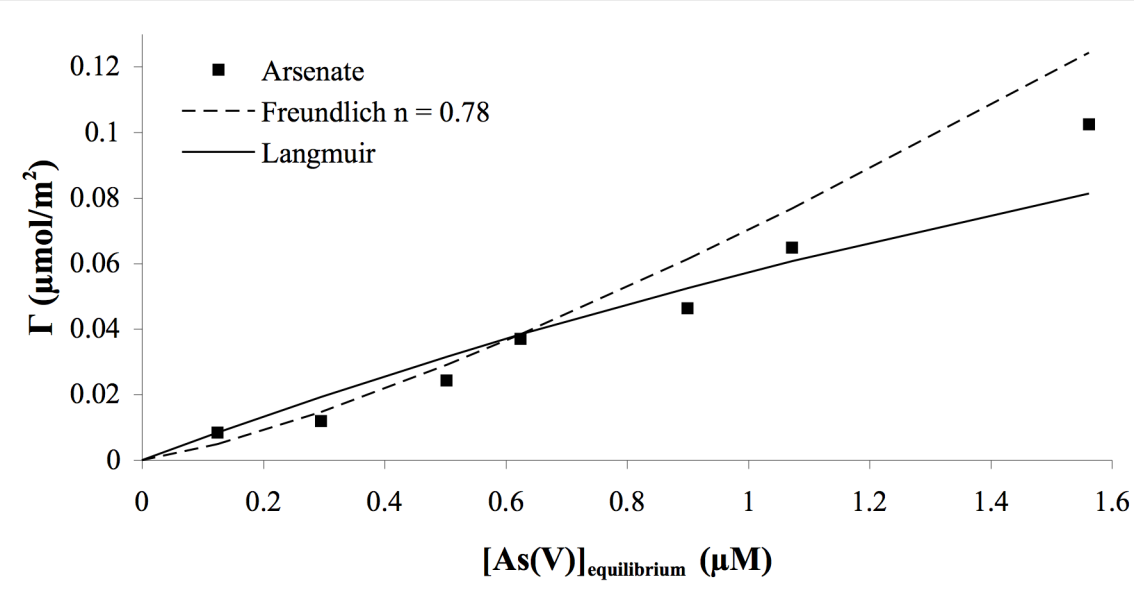

Figure 15: Reciprocal Langmuir-type arsenate adsorption isotherm at 23(±3)°C, $[As(V)]_{initial}$ = 0.6-6 µM, [HMO]:solid solution ratio = 0.15 g/L, (Batch # 5-6).

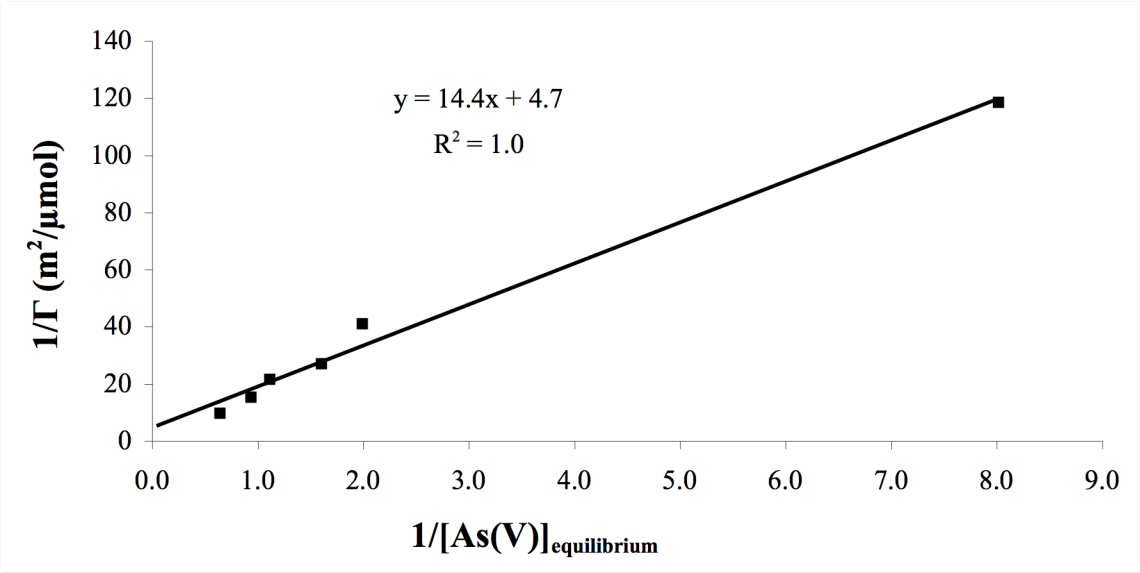

Figure 16: Logarithmic Freundlich type arsenate adsorption isotherm at 23(±3)°C, $[As(V)]_{initial}$ = 0.6-6 µM, [HMO]:solid solution ratio = 0.15 g/L, (Batch # 5-6).

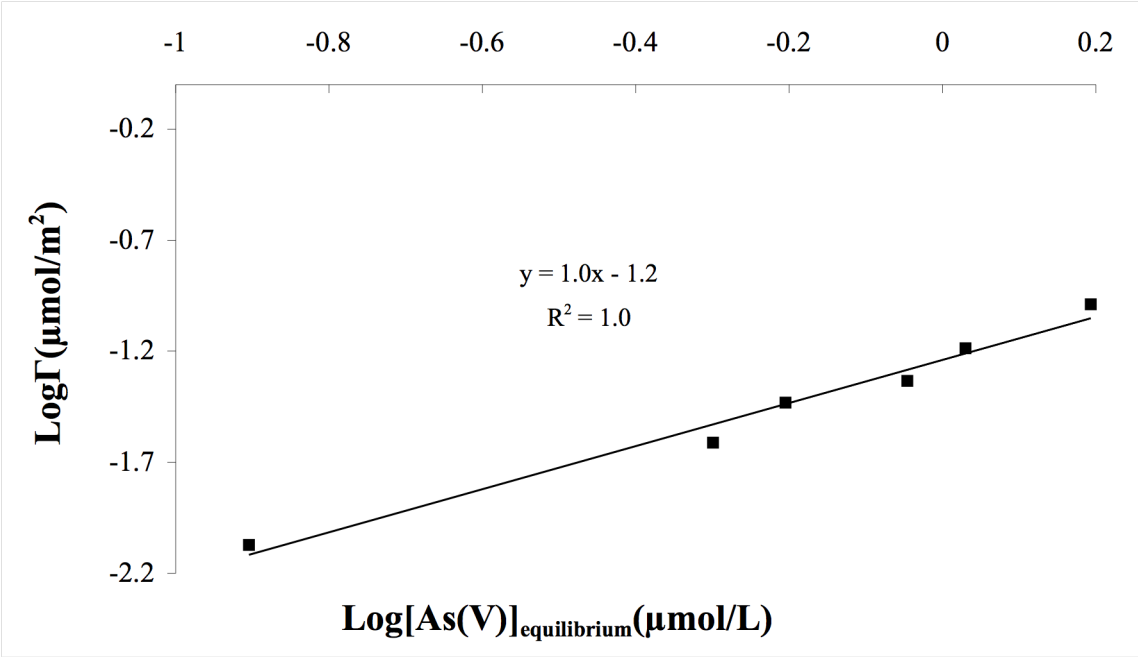

Figure 17: Percent arsenate adsorption at 23(±3)°C, $[As(V)]_{initial}$ = 0.6-6 µM, [HMO]:solid solution ratio = 0.15 g/L, (Batch # 5-6).

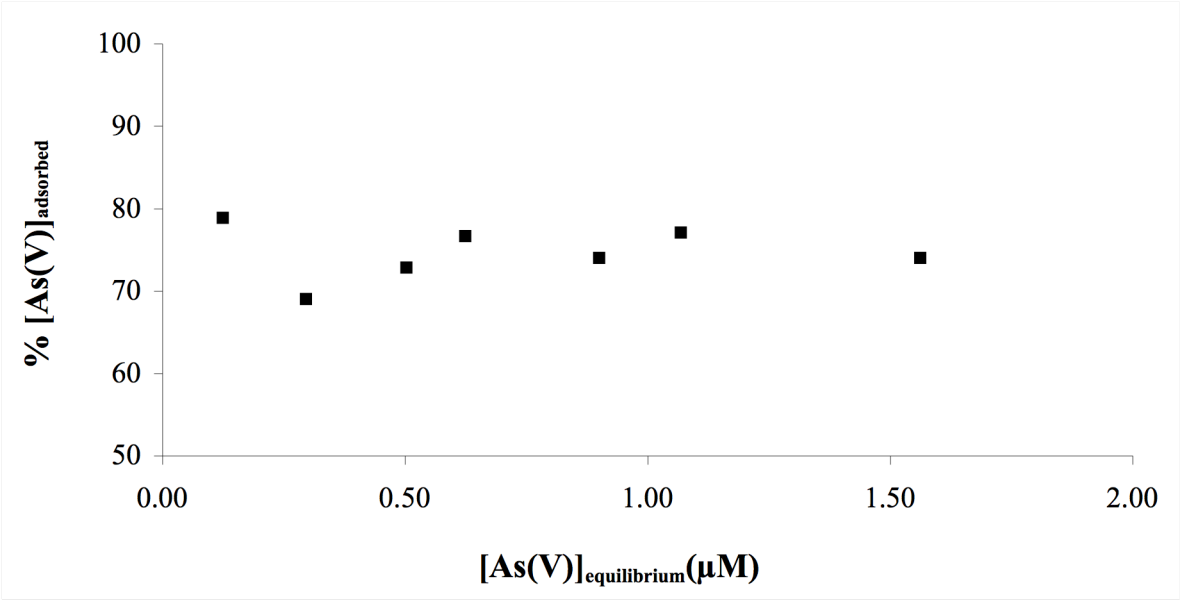

4.4. Competitive adsorption of arsenate and phosphate onto amorphous hydrous manganese oxide from seawater at 23(±3)°C

4.4.1. Simultaneous additions

The competitive adsorption of arsenate and phosphate onto amorphous hydrous manganese oxide (HMO) (Batch # 5-6) was evaluated over 48 hours and compared to individual adsorption experiments. The experimental set up is presented in Table 5, and the results are presented in Fig. 18-21.

For the [As(V)]:[SRP] = 1:2.5 and 1:10 ratio experiments, there was no obvious competition between arsenate and phosphate in terms of percent adsorption. In fact, surprisingly, there was more adsorption of each oxyanion in the presence of each other compared to the individual adsorption isotherms. For example, in the 1:2.5 and 1:10 experiments, percent adsorption of SRP reached a maximum of 45 % and 40 %, respectively, compared to 31 % for the individual adsorption of 6 μM SRP (%RSD <1 %), whereas the arsenate adsorption maximum reached 82 % (1:2.5 and 1:10), compared to 79 % for the individual adsorption of 0.6 μM As(V). Nevertheless, the %RSD of arsenate in the 1:2.5 and 1:10 experiments was 3 % and 5 %, respectively, and therefore the difference in adsorption between the competitive and individual experiments is not significant. The increase in the total adsorption could be due to small variations in the amount of HMO in suspension (i.e. solid:solution ratio or surface area), but given that the same batch of HMO was used for the 1:2.5 competitive experiment and the two individual adsorption experiments highlighted in the comparison, it is unlikely that the outcome was a result of the differential behaviour of the adsorbent. In contrast, the [As(V)]:[SRP] = 1:100 ratio experiment displayed effective competition with reduced adsorption of

both phosphate and arsenate, with 4 % less phosphate adsorption, and 18 % less arsenate adsorption compared to individual adsorption experiments at the same concentration.

The rate of arsenate adsorption showed a trend similar to the individual adsorption experiment for all three competitive adsorption experiments (1:2.5, 1:10, and 1:100), with rapid initial adsorption followed by a slower reaction. On the other hand, the rate of phosphate adsorption showed significant fluctuations, particularly in the first 2 hours for all three experiments. In the first 8 hours of the 1:2.5 and 1:10 experiments, SRP concentrations initially decreased rapidly, but increased noticeably before resuming a more progressive decline. The rate of phosphate adsorption in the 1:100 experiment reached equilibrium after only 2 hours, which was much faster than the individual adsorption experiment. These observations likely reflect competition and competing adsorption kinetics with arsenate or the formation of multi-component (ternary or quaternary) surface complexes.

Figure 18: Simultaneous competitive adsorption of arsenate and phosphate onto HMO (0.15 g/L) from seawater at 23(±3)°C at various initial [As(V)]:[SRP] ratios: 1:2.5 (2.0 μM and 5.0 μM), 1:10 (0.5 μM and 5 μM) , 1:100 (0.5 μM and 50 μM). Adsorption results from one individual adsorption experiment of arsenate ($[As]_{initial}$ = 0.6 μM) and phosphate ($[SRP]_{initial}$ = 6 μM) are included for comparison, and represented with open symbols.

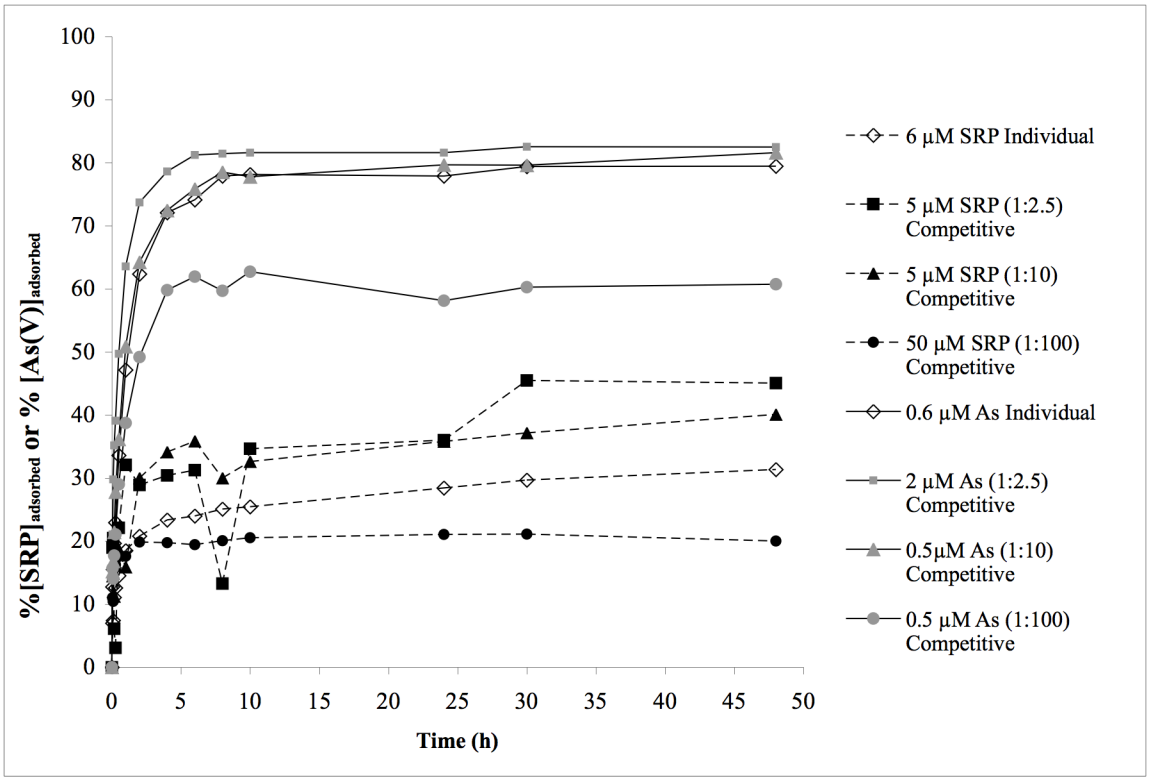

Figure 19: Percent phosphate adsorption following simultaneous competitive adsorption of arsenate and phosphate onto 0.15 g HMO/L from seawater at 23(±3)°C at various initial [As(v)]:[SRP] ratios: 1:2.5 (2.0 μM and 5.0 μM), 1:10 (0.5 μM and 5 μM), 1:100 (0.5 μM and 50 μM). Adsorption results from one individual adsorption experiment of phosphate ($[SRP]_{initial}$ = 6 μM) is included for comparison and represented with open symbols.

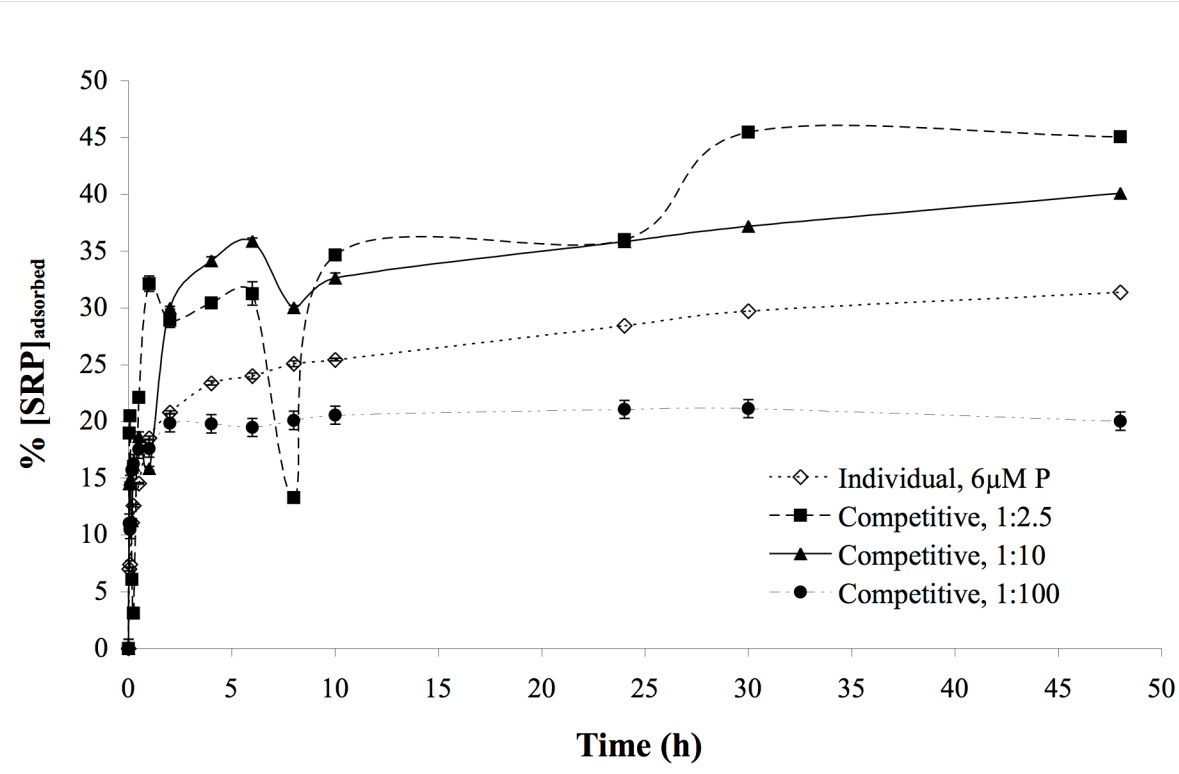

Figure 20: Percent phosphate adsorption during simultaneous competitive adsorption of arsenate and phosphate onto HMO (0.15 g/L) in seawater at 23(±3)°C at various initial [As(v)]:[SRP] ratios: 1:2.5 (2.0 μM and 5.0 μM), 1:10 (0.5 μM and 5 μM), 1:100 (0.5 μM and 50 μM) for the first 2 hours of reaction.

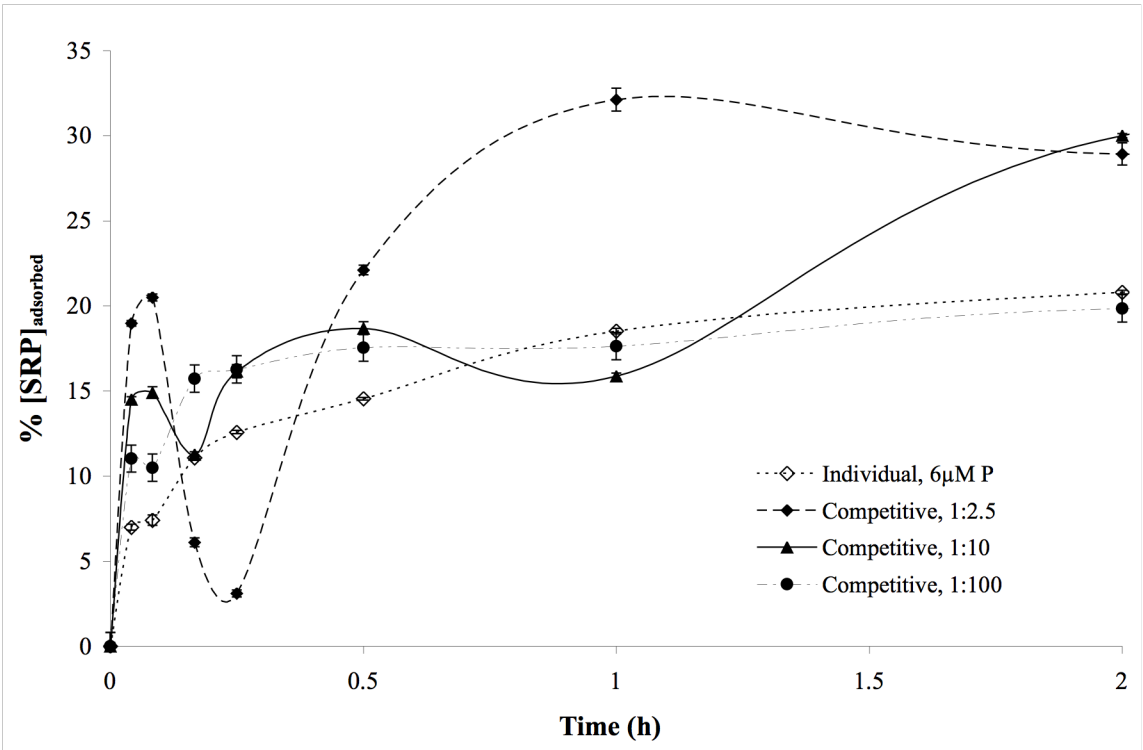

Figure 21: Percent arsenate adsorption during simultaneous competitive adsorption of arsenate and phosphate onto HMO (0.15 g/L) in seawater at various initial [As(v)]:[SRP] ratios: 1:2.5 (2.0 μM and 5.0 μM), 1:10 (0.5 μM and 5 μM), 1:100 (0.5 μM and 50 μM). Adsorption results from one individual adsorption experiment of arsenate ($[As]_{initial}$ = 0.6 μM) is included for comparison and represented by open symbols.

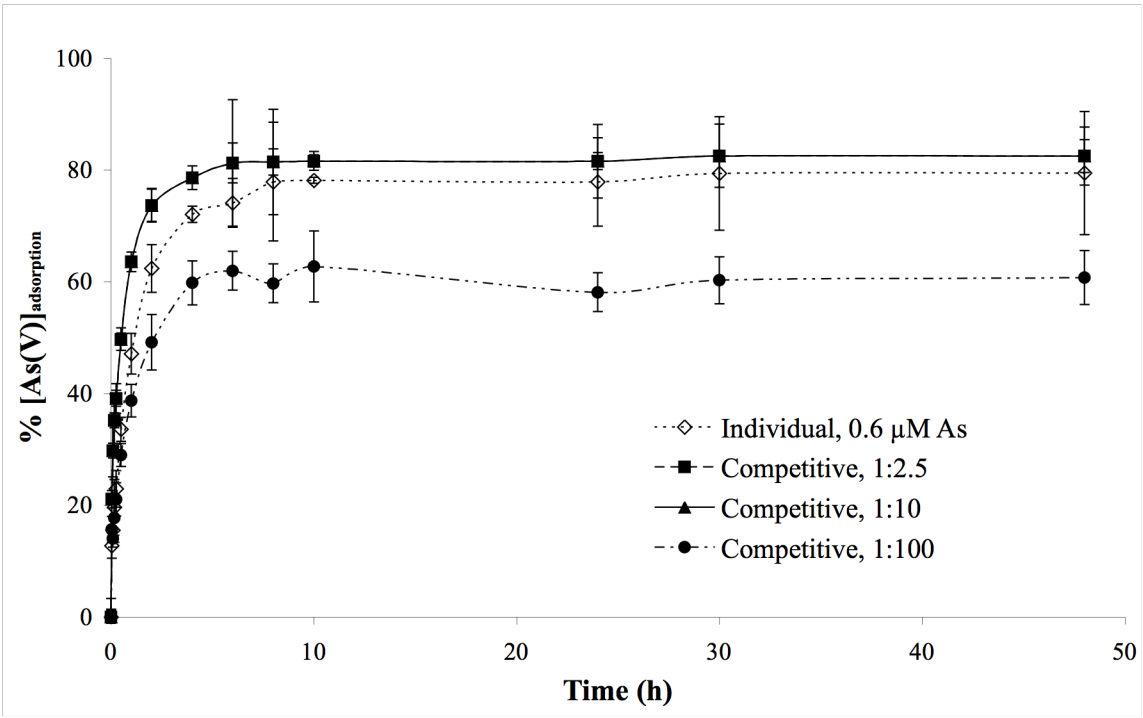

4.4.2. Sequential additions

In sequential addition the oxyanions are added one at a time – the first anion is allowed to equilibrate with the solid for a set amount of time before the second anion is introduced. This gives different competition compared to simultaneous addition where both anions are added at the same time and likely compete for the same sites. The kinetics of the competitive adsorption of arsenate and phosphate onto amorphous hydrous manganese oxide (HMO) was evaluated over 48 hours by sequential additions of the two oxyanions. In the first experiment, 10 μM phosphate was allowed to equilibrate with HMO for 48 hours before 1 μM arsenate was added. The addition of arsenate appeared to have no overall effect on phosphate adsorption (Fig. 22). There were some minor increases of [SRP] in the first 10 hours following the addition of the As(V), but upon longer equilibration the [SRP] was nearly identical to the value prior the arsenate addition. This was an unexpected and interesting phenomenon since an increase in the adsorption of phosphate also occurred upon simultaneous addition. The total arsenate adsorbed to phosphate-preconditioned HMO was reduced by 10 %, from 80 % to 70 %, when added as the competing oxyanion, but the rate of reaction was similar to the individual adsorption.

In the second experiment, 1 μM arsenate was allowed to equilibrate with HMO for 48 hours before 10 μM phosphate was added. The addition of phosphate caused a 5 % reduction in the total amount of arsenate adsorbed (Fig. 23). Forty eight hours after the phosphate addition, the total amount of dissolved arsenate was still steadily decreasing from 80 % to 75 % and did not appear to have reached equilibrium. In comparison, the equilibrium value in simultaneous addition (1:2.5 and 1:10) was 82 %. The total amount of adsorbed phosphate was reduced by about 5 %, from 31 %

to 26 %, when added as the competing oxyanion, but the rate of reaction was similar to the individual adsorption.

Figure 22: Percent adsorption of arsenate and phosphate following the sequential addition of 1 μM of arsenate to a seawater solution previously equilibrated at $[SRP]_{initial}$ = 10 μM and a [HMO]:solution ratio of 0.15 g/L for 48 hours. Batch # 7.

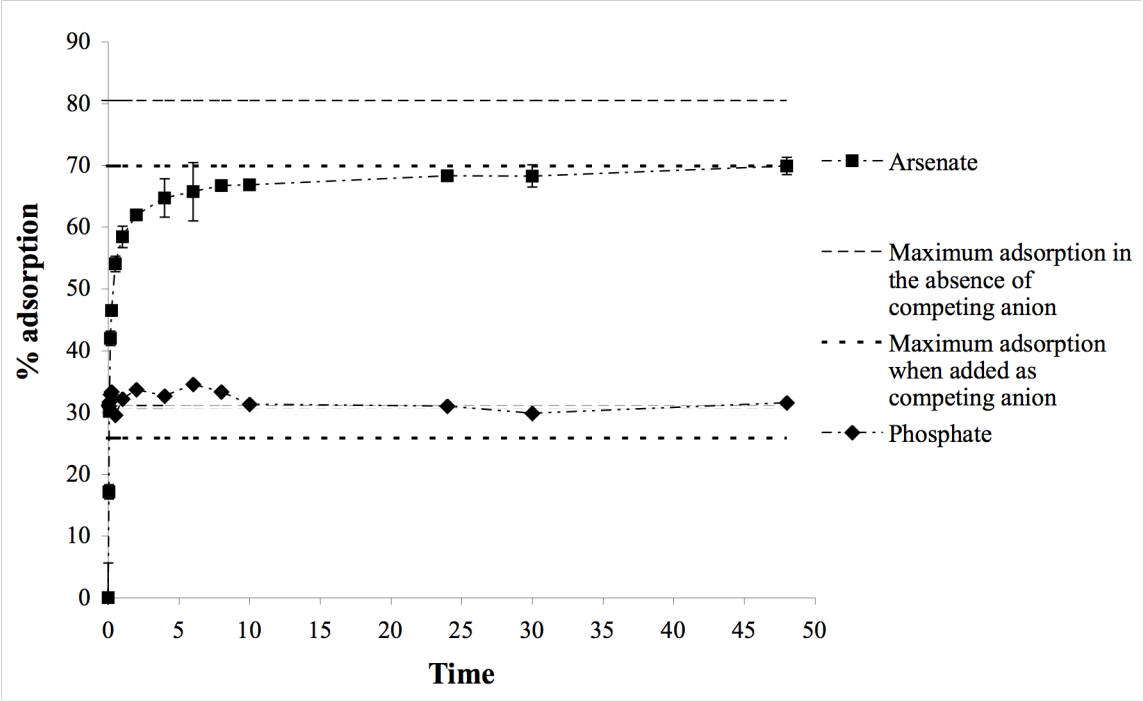

Figure 23: Percent adsorption of arsenate and phosphate following the sequential addition of 10 μM of phosphate to a seawater solution previously equilibrated at $[As(V)]_{initial}$ = 1 μM and a [HMO]:solution ratio of 0.15 g/L for 48 hours. Batch # 7.

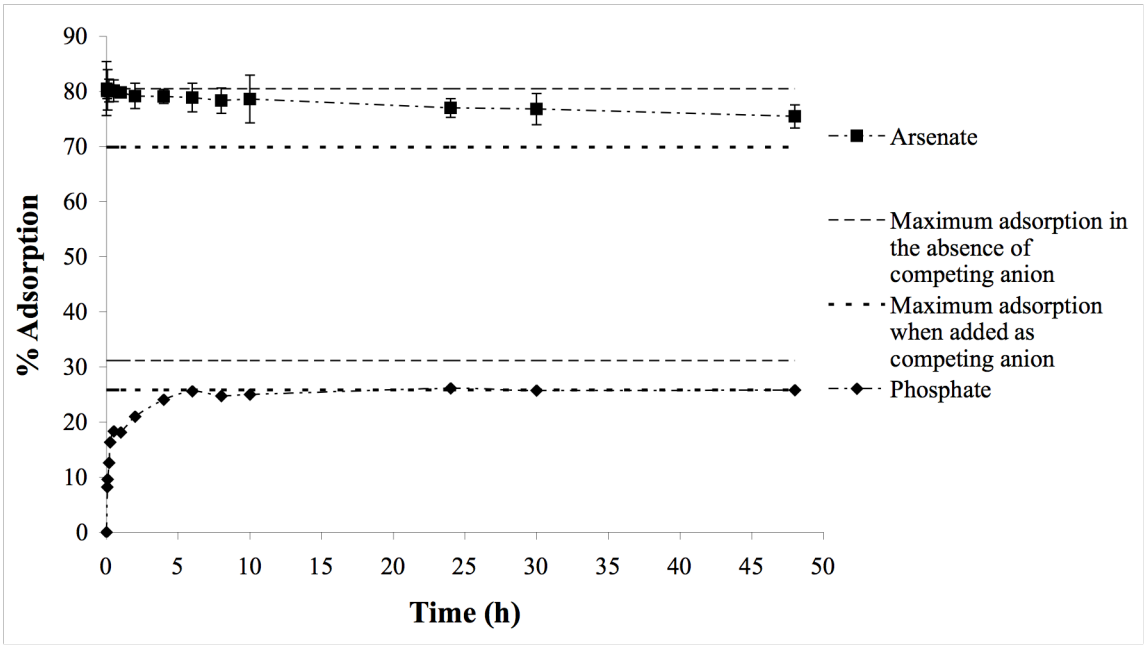

4.5. Desorption of arsenate- or phosphate-laden amorphous hydrous manganese oxide in seawater

4.5.1. Desorption of phosphate

Seawater spiked with 31 μM phosphate was first allowed to equilibrate with [HMO] = 0.15 g/L for 48 hours (Batch # 7). After this period, 33 % of the SRP had been adsorbed to the solid, which was a few percent higher compared to the adsorption isotherm. Next, the phosphate-laden HMO was filtered on a 0.45 μM Millipore membrane and the solid transferred to seawater containing 2.1 μM phosphate. The desorption of phosphate was monitored over 48 hours. The desorption reaction followed a reverse, but similar trend to the individual SRP adsorption reaction, including a rapid initial desorption rate followed by a slower equilibration (Fig. 24). After 48 hours, 49 % of the adsorbed phosphate was desorbed to the solution.

4.5.2. Desorption of arsenate

Seawater spiked with 6 μM arsenate was first allowed to equilibrate with [HMO] = 0.15 g/L (Batch # 7) for 48 hours. After this period, 74 % of the As(V) had been adsorbed to the solid, which was equal to the adsorption isotherm. Next, the arsenate-laden HMO was filtered on 0.45 μM Millipore membrane and the solid transferred to seawater containing 14 nM arsenate and the desorption of arsenate was monitored over 48 hours. The desorption reaction followed a reverse, but similar trend to the individual As(V) adsorption reaction, including a rapid initial desorption rate followed by a slower equilibration. After 48 hours, 24 % of the adsorbed arsenate was desorbed to the seawater solution (Fig. 24).

Figure 24: Percent desorption of phosphate- or arsenate-laden HMO in seawater at 23(±3)°C over 48 hours. $[SRP]_{initial}$ = 31 µM, $[SRP]_{ads}$ = 10 µM, $[SRP]_{desorbed}$ = 5 µM. $[As(V)]_{initial}$ = 6 µM, $[As(V)]_{ads}$ = 4 µM, $[As(V)]_{desorbed}$ = 1 µM. [HMO]:solution ratio = 0.15 g/L, (Batch # 7).

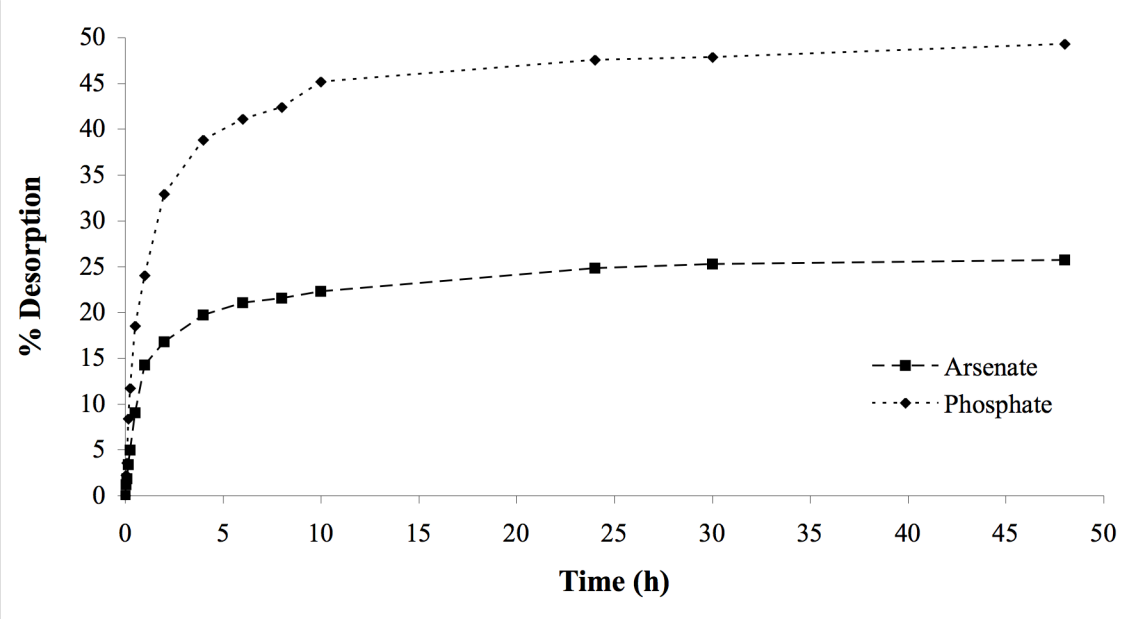

5. DISCUSSION

The outcome of the individual and competitive adsorption experiments of phosphate and arsenate onto HMO, including a comparison with the literature results are presented in this section. The objectives of the study were to evaluate the individual and competitive adsorption of arsenate and phosphate on amorphous hydrous manganese oxide (HMO) in seawater at environmentally-relevant concentrations. The experimental results provide insights into the relative importance of manganese oxides as adsorbents for phosphate and arsenate in seawater, as well as the relative affinity and interactions of arsenate and phosphate with the HMO surface. Adsorption of arsenate and phosphate onto HMO and the adsorption kinetics are modelled using classical concepts. Finally, the desorption of phosphate- or arsenate-laden HMO is analyzed.

5.1 Modelling the adsorption results

The individual arsenate and phosphate adsorption experiments in seawater can be described by both Freundlich and Langmuir isotherms (correlation coefficients greater than 0.97) (Table 6). For both oxyanions, the Langmuir isotherm underestimated adsorption at the highest concentrations, whereas the Freundlich slightly overestimated the adsorption at these concentrations. The Langmuir and Freundlich isotherm models fit the data equally well at lower concentrations (below equilibrium [SRP] ~10 μM and [AsV] ~ 0.7 μM). Nevertheless, overall, the data fit best to the Freundlich isotherm model with n = 0.78 for arsenate (r^2 = 0.996) and n = 1.3 for phosphate (r^2 = 0.994). This indicates, as would be expected, that the surface of HMO is populated by adsorption sites of varying energies (heterogeneous surface) as opposed to identical sites (homogeneous surface) as assumed in the

Langmuir isotherm model. The Γ_{max} value from the Langmuir adsorption isotherm represents the adsorption capacity of HMO for phosphate and arsenate, and is useful in comparing the amount of adsorption on different adsorbents, although the constants are specific to the experimental conditions. The Freundlich constant K_f indicates the extent of arsenate or phosphate removal from solution and is also a measure of the adsorption capacity. According to the Langmuir model, HMO has a greater adsorption capacity for phosphate (Γ_{max} = 0.34 $m^2/\mu mol$, r^2 = 0.992) than arsenate (Γ_{max} = 0.21 $m^2/\mu mol$, r^2 = 0.989), but the K_f value of the Freundlich model indicates that the extent of removal is greater for arsenate (0.06 $\mu mol/m^2$, r^2 = 0.977) than phosphate (0.03 $\mu mol/m^2$, r^2 = 0.980). Nevertheless, given the differences in the ranges of concentrations examined in this study (0.6-6 μM for arsenate and 2-46 μM for phosphate), the difference between the adsorption characteristics of the two oxyanions might not be significant; the values are not widely different, as expected from their similar chemistries. The adsorption parameter *n* in the Freundlich isotherm indicates adsorption intensity and is a measure of the preferential adsorption of one adsorbate over another (Okeola and Odebunmi, 2010). A small *n* value reflects a strong bond between adsorbent and the adsorbate and favourable adsorption. The derived *n* values indicate that the adsorption of arsenate (n = 0.78) is favoured over the adsorption of phosphate (n = 1.3) onto HMO under the experimental conditions of this study.

Driehaus et al. (1995) fit the adsorption data of arsenate onto δ-MnO_2 from a 20 mM $NaNO_3$ solution at pH 7.5 to a Freundlich isotherm (n = 0.5-0.54), and found a near-linear relationship between the amount of arsenate adsorbed and the equilibrium solution concentration. Dutta et al. (2004) fit the adsorption data of arsenate onto two distinct samples of titanium dioxide in pure water to a Langmuir isotherm. They obtained Γ_{max} (Q_{sat}) values of 0.90 $\mu mol/m^2$ (pH 4) and 0.36 $\mu mol/m^2$

(pH 9) (specific surface area, S = 334 m^2/g), and 1.13 μmol/m^2 (pH 4) and 0.42 μmol/m^2 (pH 9) (S = 55 m^2/g) for the two TiO_2 samples. They also fit their data to a Freundlich adsorption isotherm and found that the data obtained at pH 9 fit better to a Freundlich isotherm, whereas the data generated at pH 4 was better described by a Langmuir adsorption isotherm. In comparison, the Γ_{max} values derived in this study were 0.21 μmol/m^2 for arsenate onto HMO (S = 270 m^2/g and pH 7.7). The adsorption capacity for phosphate we obtained from the Langmuir isotherm is similar to results by Yao and Milleo (1996) who studied the adsorption of phosphate onto δ-MnO_2 in seawater and obtained a value of 0.24 μmol/m^2 compared to 0.34 μmol/m^2 in this study. Other studies have reported adsorption capacities for various manganese oxides (Table 7), but did not report the specific surface areas of the solids and, therefore, the values cannot be readily compared. For instance, Zhang et al. (2011) fit the adsorption data of arsenate onto γ-MnO_2 from water to a Langmuir isotherm model and reported a Γ_{max} of 11 μmol/g at pH 7. Thanabalasingam and Pickering (1986) reported adsorption capacities of 10 μmol/g arsenate onto HMO from water. In comparison, we obtained adsorption capacities of 58 μmol/g or 0.21 μmol/m^2 for arsenate and 93 μmol/g or 0.34 μmol/m^2 for phosphate at pH 7.7.

As mentioned earlier, arsenate was expected to have a greater affinity (the degree to which a substance combines with another) than phosphate for HMO and this was confirmed in our experiments. For example, the total phosphate adsorption at 2 μM and 6 μM was 44 % and 31 %, respectively, whereas for arsenate, at the same initial concentrations, adsorption was 73 % and 74 %, respectively. The reason why arsenate has a higher affinity for manganese oxides is not fully understood, but it has been postulated that because arsenate is larger than phosphate it interacts more strongly with the solid (Lumsdon et al., 1984). In other words, it may be related with charge density. The distance of the arsenate As-O and the phosphate P-O bonds in

Table 7: Capacity of various metal oxides/hydroxides to adsorb arsenate.

Adsorbent	Solution	Sorption capacity		pH	SSA*	Reference
		μmol/g	μmol/m^2		g/m^2	
Cryptomelane (α-MnO_2)	water	25	n/a	6.5	n/a	Thanabalasingam and Pickering (1986)
Pyrolusite (β-MnO_2)	water	10	n/a	6.5	n/a	Thanabalasingam and Pickering (1986)
γ-MnO_2	water	11	n/a	7	n/a	Zhang et al. (2011)
HMO	water	10	n/a	6.5	n/a	Thanabalasingam and Pickering (1986)
HMO	seawater	58	0.21	7.7	270	This study
Iron-oxide-coated sand	water	0.1	n/a	5-9	n/a	Ramakrishna et al. (2006)
Iron-oxide-coated quartz sand	water	0.15	0.13	5-8	1.2	Hsu et al. (2008)
Iron-oxide-coated Mn-ore sand	0.01 M $NaNO_3$	39	4.3	7	9.18	Wu et al. (2011)
Ferrihydrite	water	59	n/a	7	n/a	Zhang et al. (2011)
Fe(III) coagulant	water	143	n/a	7	n/a	Zhang et al. (2011)
Fe(III)/Al(III) coagulant	water	214	n/a	7	n/a	Zhang et al. (2011)
Fe-Zr binary oxide	0.01M $NaNO_3$	329	0.97	7	339	Ren et al. (2011)
MnO_2-doped Al_2O_2	0.01M $NaNO_3$	714	16	7	44.7	Wu et al. (2012)

*Specific surface area

inner-sphere bidentate complexation may also be critical in determining their relative affinity for HMO (Tawfik and Viola, 2011). Thus the steric-fit on the adsorption site may be an important factor in determining the amount of adsorption and explain why some oxyanions have a stronger affinity for metal oxide surfaces. For example, it explains why selenite has a higher affinity (strongly bound complexes) compared to selenate (weakly bound complexes) onto iron oxide (α-FeOOH) (Hayes et al., 1987) and hydrous aluminium oxide (Peak, 2006). Given the stronger affinity of arsenate for HMO observed in this study, the adsorption capacity of arsenate was expected to be larger than for phosphate, but slightly higher values were obtained for phosphate. The discrepancy could be due to the different range of concentrations investigated for each oxyanion, and/or the different size of the oxyanions (stearic hindrance) and a lower Γ_{max} for arsenate than expected. Nevertheless, the sizes of the oxyanions are quite similar: the ionic radius for phosphate (as HPO_4^{2-}, dominant species in seawater) is 2.38 Å and that of arsenate (as $HAsO_4^{2-}$, dominant species in seawater) is 2.48 Å (Frausto da Silva and Williams, 1997; Tawfik and Viola, 2011).

5.2. Adsorption kinetics

The kinetics of phosphate and arsenate adsorption onto HMO from seawater was anticipated to be similar, as they are for adsorption onto goethite (Hongshao and Stanforth, 2001; Gao and Mucci, 2003; Luengo et al., 2007), and this was verified by the 48-hour individual experiments. In both cases, the adsorption reaction could be described as a two-step process; an initial rapid adsorption followed by a slower reaction. For instance, at an initial concentration of 6 μM, the phosphate adsorption reaction was 75 % complete after 4 hours and 91 % complete after 24 hours. In comparison, at an initial concentration of 0.6 μM, the arsenate adsorption reaction

was 90 % complete after 4 hours and 98 % complete after 8 hours. The faster adsorption reaction of arsenate is consistent with its higher affinity for HMO. Grossl and Sparks (1995) proposed that the two-step adsorption kinetics reflects a rapid initial formation of a monodentate surface complex by ligand exchange with OH groups, followed by a slower adsorption reaction resulting in the formation of a bidentate complex. The slow second step has also been attributed to diffusion-controlled mass transfer of the oxyanions to adsorption sites into a porous structure, such as ferrihydrite, or within aggregated particles, such as a soil (Willett et al., 1988).

The results we obtained from the phosphate adsorption experiments are similar to those of Yao and Millero (1996). They used similar adsorbate and adsorbent concentrations in seawater and observed a 60 % completion of the adsorption after 5 minutes and 95 % completion after 10 hours. In comparison, we found that 27 % of the initial phosphate concentration ($[SRP]_{init}$ = 6 μM) was adsorbed after 5 minutes, and 82 % after 10 hours. The rate of arsenate adsorption was similar to that obtained by Bajpai and Chaudhuri (1999), who studied the removal of 13 μM arsenate (initial) by 10 g/L manganese dioxide-coated quartz sand from groundwater. After 1 hour, the adsorption of arsenate was 74-77 % complete, and had reached equilibrium after 4 hours. In this study, the adsorption of arsenate ($[As(V)]_{init}$ = 0.6 μM) to HMO from seawater was 59 % complete after 1 hour and 90 % complete after 4 hours.

Numerous models have been used to describe the kinetics and reaction order of adsorption from solution (e.g. Saiers et al., 1994; O'Shannessy and Winzor, 1996; Zaror, 1997; Mohan et al., 2002; Chu and Hashim, 2003), including Lagergren's

first-order reaction (Lagergren, 1898) and Ho's second-order expression (Ho, 1995; Ho and McKay, 1998a, 1999, 2000):

Lagergren's original equation (Lagergren, 1898) is given by:

$$dq/dt = k_1(q_e - q_t) \qquad (4)$$

where dq/dt is the rate of change in adsorption density, q_e and q_t ($\mu mol/m^2$) are the adsorption densities at equilibrium and at time t, respectively, and k_1 (1/h) is the first-order adsorption rate constant.

Ho's second-order expression (Ho and McKay, 2000) is:

$$dq/dt = k_2(q_e - q_t)^2 \qquad (5)$$

where k_2 ($m^2/\mu mol\,h$) is the second-order adsorption rate constant.

The rate of the reaction is measured via the rate of change in adsorbate concentration with time, and reaction order and rate constants must be determined experimentally. Lagergren's pseudo-first-order model has been widely used to describe the adsorption of pollutants (e.g. metal ions, dyes and organics) from aqueous solutions onto various adsorbents (Ho, 2004), including kaolinite (Atun and Sismanoglu, 1996), magnetite (Ortiz et al., 2001) and Fe(III)/Cr(III) hydroxide (Namasivayam et al., 1994). Ho's pseudo-second-order model has been successfully applied to a multitude of adsorbent-adsorbate systems in solution, including the adsorption of dye and divalent metals onto peat and wood (e.g. Ho and McKay, 1998a,b), arsenic(III + V) onto iron oxide-coated quartz sand (Thirunavukkarsu et

al., 2003; Wu et al., 2011), arsenic(III + V) onto manganese oxide-doped aluminum oxide (Wu et al., 2012), and phosphate onto mesoporous silicate (Shin et al., 2004). Both models have been termed "pseudo" to distinguish them from kinetic expressions based solely on the solute concentrations or the adsorption capacity of the solid (Ho, 2006).

5.3 Modelling the adsorption kinetics

The models described by equation (4) and (5) did not fit well to our adsorption data. However, the rewritten forms suggested by Wu et al. (2011, 2012) fit well. Therefore, the adsorption data from this study were fitted to the same pseudo-first-order model and a pseudo-second-order model from their studies. The analytical solutions to the rate equations described above (Eqns. 4 & 5) are presented in equations 6 and 7:

Pseudo-first-order model (Ho, 2006):

$$q_t = q_e(1-e^{-k_1 t}) \qquad (6)$$

Pseudo-second-order model (Ho and McKay, 1998b):

$$t/q_t = t/q_e + 1/(k_2 q_e) \qquad (7)$$

The rate constants, k_1 and k_2, were determined from adsorption data acquired during the first 2 hours of the reaction, and q_e was obtained from the adsorption isotherms. The derived kinetic parameters are presented in Table 8.

Table 8: Parameters of pseudo-first-order and pseudo-second-order kinetic models for the adsorption of arsenate and phosphate by amorphous hydrous manganese oxide (HMO) from seawater.

			Pseudo-first-order		Pseudo-second-order	
Adsorbate	Initial concentration	q_e ($\mu mol/m^2$)	k_1 (1/h)	r^2	k_2 ($m^2/\mu mol\,h$)	r^2
Arsenate	0.6 μM	0.0085	0.752	0.998	1.329	0.995
Phosphate	6 μM	0.036	0.496	0.921	2.01	0.942

As shown in Fig. 25, the arsenate adsorption data can be fitted well to both the pseudo-first-order and pseudo-second-order kinetic models. The pseudo-first-order and pseudo-second-order kinetic models did not fit as well the phosphate adsorption data (Fig. 26), especially between 5 and 24 hours. As expected, the derived adsorption rate constant for arsenate (k_1 = 0.75/h, r^2 = 0.832) was larger than for phosphate (k_1 = 0.50/h, r^2 = 0.700). Based on the correlation coefficients (r^2), the pseudo-first-order model fits the arsenate adsorption data best, whereas the pseudo-second-order model provides a better fit to the phosphate adsorption. Nevertheless, the difference in the goodness of the fits is marginal and one should favour the simplest model (i.e. the pseudo-first-order model). More experimental data would be required to distinguish between the two models and draw conclusions about the rate-determining steps. First-order kinetics indicates that the rate is solely dependent on the concentration of arsenate or phosphate in solution, whereas second-order kinetics implies that more than one rate controlling step defines the adsorption rate of these oxyanions onto HMO. Wu et al. (2011) fit the results of their study of arsenate adsorption onto iron-oxide-coated manganese sand (manganese sand is an industrial material made of natural manganese ore) and iron-

oxide-coated quartz sand from a 0.01 M $NaNO_3$ solution at pH 7 to both models and obtained similarly good fits to both.

All our experiments, like most other studies reported to date, were conducted at room temperature. Few studies have investigated the effect of temperature on the rate and amount of arsenate and phosphate adsorption onto various metal oxides and other solids (e.g. Bartell et al., 1951; Yao and Millero, 1996; Fitzpatrick, 1998; Gao, 2001; Zhang and Huang, 2011). Gao (2001) observed an increase in the rate of arsenate adsorption onto goethite in artificial seawater, whereas the rate of phosphate adsorption was unaffected. Yao and Millero (1996) investigated the adsorption of phosphate onto δ-MnO_2 in seawater at various temperatures (5-35°C) and found that an increase in temperature increases the adsorption. Their result was unexpected since adsorption is an exothermic process and an increase in temperature should cause a decrease in adsorption (Bartell et al., 1951). Increasing temperatures typically increase the solubility and stability of the adsorbate, which is unfavourable for adsorption. Bartell et al. (1951) suggested that the effect of temperature on adsorption is also a function of concentration. At lower adsorbate concentrations, the adsorption decreases with increasing temperature, whereas at higher adsorbate concentrations the reverse is often the case.

Figure 25: Kinetics of arsenate adsorption by amorphous hydrous manganese oxide from seawater at 23(±3)°C over 48 hours. $[As(V)]_{initial}$ = 0.6 µM, [HMO]:solution ratio = 0.15 g/L.

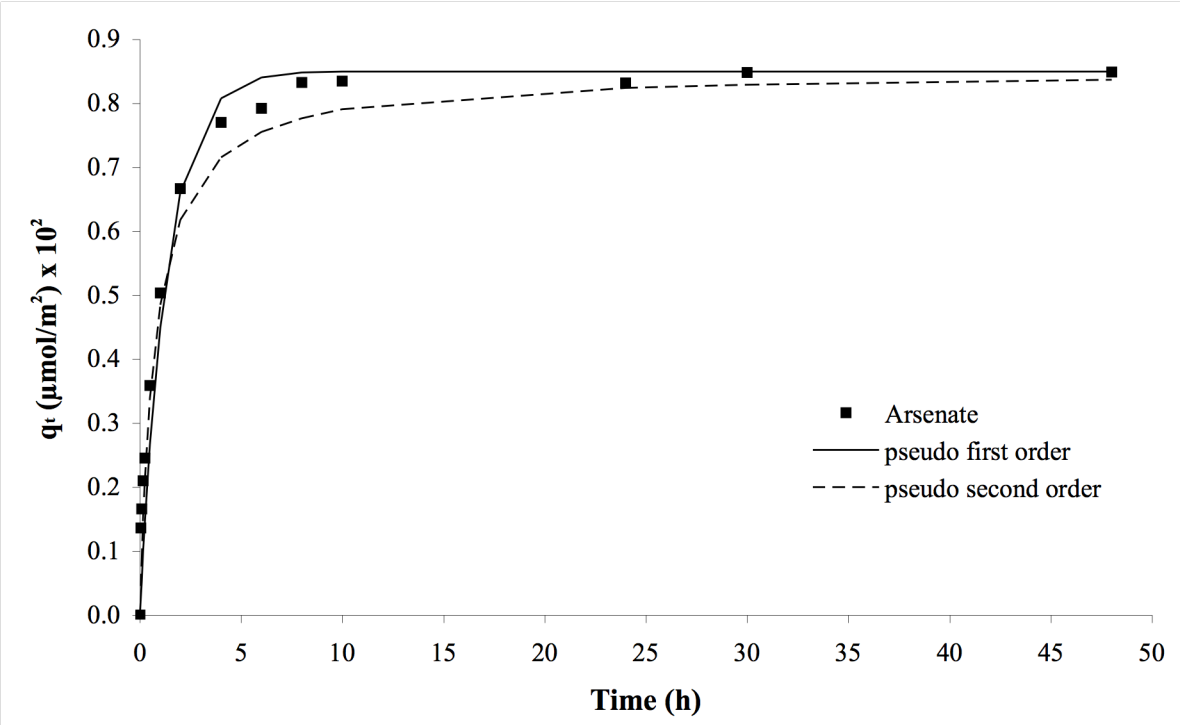

Figure 26: Kinetics of phosphate adsorption by amorphous hydrous manganese oxide from seawater at 23(±3)°C over 48 hours. $[SRP]_{initial}$ = 6 µM, [HMO]:solution ratio = 0.15 g/L.

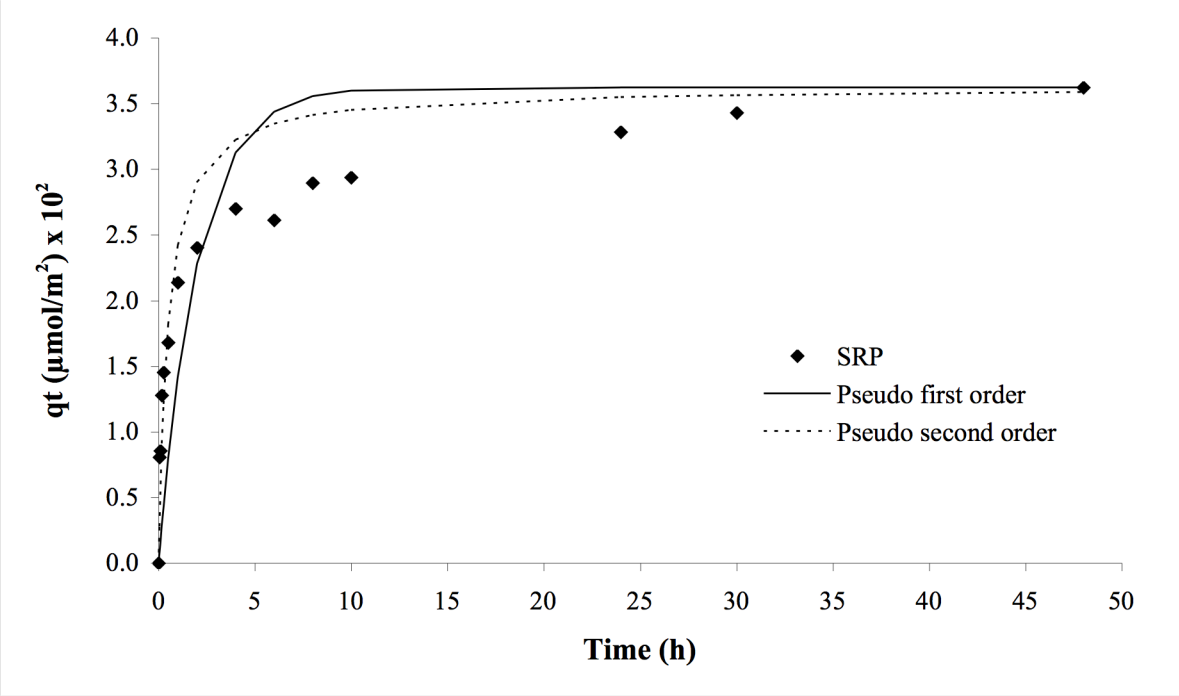

5.4. Simultaneous competitive adsorption

Given its greater affinity for the HMO surface, arsenate was expected to compete effectively with phosphate for adsorption onto HMO, and this was confirmed in our competitive adsorption experiments. During the simultaneous addition experiments, the adsorption of arsenate was unaffected by the presence of phosphate at [As(V)]:[SRP] = 1:2.5 and 1:10 molar ratios, but when the ratio reached 1:100, arsenate adsorption was reduced to 61 % (compared to 79 % in individual adsorption). Other studies have reported reduced adsorption of arsenate onto ferrihydrite from 0.1 M NaCl at [As(V)]:[HPO_4^{2-}] = 1:1 (Jain and Loeppert, 2000), reduced adsorption of arsenate onto iron ores in water at all [As(V)]:[HPO_4^{2-}] ratios (Zhang et al., 2004), and reduced arsenate adsorption onto iron-oxide-coated manganese sand from 0.01 M $NaNO_3$ at [As(V)]:[HPO_4^{2-}] = 1:20 (from 95.5 % in the absence of phosphate to 49.8 %) and slightly less adsorption at [As(V)]:[HPO_4^{2-}] = 1:200 (from 95.5 % to 42.6 %) (Wu et al., 2011). Gao and Mucci (2003) observed no reduction of arsenate adsorption onto goethite from artificial seawater at [As(V)]:[HPO_4^{2-}] = 1:2.5, but a 10 % reduction at [As(V)]:[HPO_4^{2-}] = 1:5 (from 50 % in the absence of phosphate to 40 %). Competition between arsenate and phosphate appears to be dependant on the oxyanion concentration ratio as well as the nature of the metal oxide and supporting electrolyte solution.

When the oxyanions were added simultaneously, an increase in the adsorption relative to their individual adsorption maximum was observed for both oxyanions at [As(V)]:[SRP] = 1:2.5 and 1:10. This was unexpected, although Hingston et al. (1971) and Hongshao and Stanforth (2001) also observed similar results when studying the competitive adsorption of phosphate and arsenate on gibbsite and/or goethite from 0.125 M NaCl and 0.001 M NaCl, respectively. When phosphate and

arsenate were added simultaneously, the total surface coverage was slightly greater than for either oxyanion alone. This observation is consistent with the hypothesis that there exists preferential adsorption surface sites for each oxyanion, plus non-specific sites where both oxyanions can adsorb (Hingston et al., 1971; Liu et al., 2001), but the synergistic effect observed at low [As(V)]:[SRP] ratios may reflect some interaction between the two oxyanions and the HMO surface, including the formation of polyphosphoarsenate complexes, although there is no mention of this in the literature.

The rate of arsenate adsorption was similar to the individual adsorption experiment in all three competitive adsorption experiments (1:2.5, 1:10, and 1:100), whereas the rate of phosphate adsorption showed significant (and reproducible) fluctuations (abrupt desorption and re-adsorption), particularly in the first 2 hours of all three experiments. The peculiar behaviour of phosphate may be explained by the presence of preferential arsenate adsorption sites on the HMO surface, the displacement of phosphate in the early stages of the experiments and the re-adsorption of phosphate at non-specific or lower arsenate-affinity sites.

5.5 Sequential competitive adsorption

In the sequential adsorption experiments, addition of arsenate was expected to replace a portion of the pre-adsorbed phosphate because arsenate has a stronger affinity for the HMO surface. Conversely, phosphate addition was expected to have little effect on pre-adsorbed arsenate. These expectations were not born out by the experiments. For example, the addition of arsenate to a phosphate-equilibrated HMO suspension, did not significantly affect phosphate adsorption: after 48 hours, the amount of adsorbed phosphate remained the same as before arsenate was

added. Nevertheless, during the first 10 hours after arsenate addition, there were some further phosphate adsorption followed by desorption similar to what was observed in the simultaneous addition experiment, which may be attributed to a greater total surface coverage in the mixed oxyanion system or the formation of polyphosphoarsenate complexes. The presence of adsorbed phosphate caused a 10 % reduction in arsenate adsorption (from 80 % in the absence of phosphate to 70 % 48-hours after phosphate was added), but it had no effect on the rate of arsenate adsorption.

The addition of phosphate to an arsenate-equilibrated HMO suspension caused a 5 % reduction in the amount of adsorbed arsenate (from 80 % before phosphate was added to 75 %, although this is close to the %RSD ranging from 1.3-5 % in this experiment) after 48 hours. Moreover, the presence of pre-adsorbed arsenate caused a 5 % reduction in phosphate adsorption (from 31 % to 26 %, and %RSD < 1 %), but the rate of reaction was similar to the individual adsorption experiments. In both experiments, the total amount of adsorption was around 35 % after 48 hours of competitive adsorption ($([AsV]_{ads} + [SRP]_{ads})/([AsV]_{initial} + [SRP]_{initial}) \times 100$ %) or 0.081 μmol/m^2. Barrow (1974) investigated the adsorption-desorption of arsenate and phosphate on soil (naturally phosphate deficient, never fertilized) from water and found that arsenate desorbed some of the previously adsorbed phosphate, but most of the adsorbed phosphate remained adsorbed. Likewise, in experiments similar to our competitive experiments, Hongshao and Stanforth (2001) found that only a fraction of the initially adsorbed anion was replaced by competing anions on goethite in 0.001 M NaCl (phosphate-arsenate system), and that the exchangeable fraction was concentration dependent. Conversely, Liu et al. (2001) observed an opposite trend when they examined the competitive adsorption of arsenate and phosphate onto goethite in water. They found that arsenate was more effective at

inhibiting phosphate adsorption than phosphate was at inhibiting arsenate adsorption, which is what was expected. They investigated the competitive adsorption at equimolar concentrations, whereas experiments in this study were carried out at [As(V)]:[SRP] = 1:10, which may account for the apparently contradictory observations.

5.6. Desorption of phosphate and arsenate from HMO

The amount of phosphate desorbed from a phosphate-equilibrated HMO was expected to be greater than that of arsenate desorbed from an arsenate-equilibrated HMO suspension, and this was confirmed in this study. When 0.15 g/L of a phosphate-equilibrated seawater HMO suspension ($[SRP]_{init}$ = 31 μM, $[SRP]_{equil}$ = 20 μM and q_e = 0.036 μmol/m^2) was resuspended in seawater ($[SRP]_{SW}$ = 2.1 μM), 49 % or 2.8 μmol of the adsorbed phosphate (5.7 μmol) was desorbed within 48 hours. In comparison, when 0.15 g/L of an arsenate-equilibrated seawater HMO suspension ($[As(V)]_{init}$ = 6 μM, $[As(V)]_{equil}$ = 2 μM and q_e = 0.0085 μmol/m^2) was resuspended in seawater ($[As(V)]_{SW}$ = 14 nM), only 24 % or 0.6 μmol of the adsorbed arsenate (2.5 μmol) was desorbed within 48 hours. This means that HMO is likely to desorb a larger fraction of phosphate than arsenate upon a change in the solution concentration of these oxyanions (e.g. following sediment resuspension). Ouvrard et al. (2002a) investigated the reversibility of phosphate adsorption from a column packed with biogenic manganese oxide. They eluted a phosphate-free 1 mM NaCl solution through the column and recovered all the adsorbed phosphate (q_e = 6.13 μmol/g).

The desorption kinetics in this study were similar for the two oxyanions including an initially fast desorption followed by a slower reaction, and the reaction was close to

equilibrium after 10 hours. Millero et al. (2001) found similar phosphate desorption kinetics from calcium carbonate resuspended in seawater, with a fast initial reaction (less than 30 minutes) followed by a much slower process (lasting more than 1 week). Up to 80 % phosphate was desorbed over 24 hours. Sundby et al. (1992) investigated the desorption of phosphate from natural oxic sediments and found that phosphate was always desorbed when the seawater contained < 20 μM phosphate at 25 °C. They observed that the desorption was fast and reached near equilibrium after 1 day.

The effect of varying phosphate and arsenate concentrations on the desorption from HMO was not investigated in this study, but based on limited preliminary results, one can assume that more phosphate and arsenate would be desorbed if the oxyanion-laden HMO was either exposed to lower phosphate or arsenate concentrations or pre-equilibrated with solutions of higher oxyanion concentrations. Froelich (1988) found that phosphate concentrations in some estuarine waters were higher than expected based on the mixing of surface water with river water. He ran laboratory experiments with suspended particles and sediments and concluded that the additional phosphate was likely released from bottom sediments or particles in suspension (phosphate buffer mechanism). Puls and Powell (1992) found that the percent desorption of arsenate from Fe_2O_3 in 0.01 M $NaClO_4$ at pH 7 was directly proportional to the amount of adsorbed arsenate. From an initial arsenate concentration of 2.7 μM, about 2.4 μM (16 μmol/g) was adsorbed and only 2 % of this was desorbed. For an initial arsenate concentration of 40.8 μM, about 14.4 μM (82 μmol/g) was adsorbed and 6 % was desorbed.

During our desorption experiments, a larger fraction of phosphate remained adsorbed to the HMO after 48 hours of desorption compared to the equilibrium

concentrations in individual adsorption experiments after a similar period of equilibration (e.g. $[SRP]_{adsorbed}$:$[SPR]_{solution}$ = 1:1 in desorption experiment and 1:2 for individual adsorption experiments at identical equilibrium solution concentrations). In contrast, Millero et al. (2001) found that the amount of phosphate left adsorbed on calcium carbonate after 24 hours of desorption was close to the equilibrium adsorption value. For arsenate, the equilibrium concentration was similar for the desorption and the individual adsorption experiments ($([As(V)]_{adsorbed}$:$[As(V)]_{solution}$ ~ 3:1). This indicates that phosphate is more strongly bound (irreversibly) either through inner-sphere or co-precipitation (incorporation in the solid) to the HMO surface compared to arsenate. This outcome was unexpected since results of individual and simultaneous competitive experiments implied that arsenate has a stronger affinity for HMO than phosphate, although sequential competitive experiments revealed that the effect of the arsenate addition had little effect on adsorbed phosphate.

6. CONCLUSION

Results of our adsorption and desorption experiments indicate that HMO can act as both a source and sink of phosphate and arsenate in seawater and thus buffer the concentration of oxyanions in surrounding waters. The adsorption rate of phosphate and arsenate onto HMO from seawater is similar (arsenate is faster) with rapid initial adsorption (minutes) followed by a slower adsorption reaction (hours). Likewise, the desorption of arsenate and phosphate is fast when HMO is exposed to a seawater solution of lower concentration than the equilibrium concentrations. Hence, in oxic marine sediments, porewater arsenate and phosphate will be depleted or replenished by adsorption or desorption and porewater concentrations will be buffered by these reactions. The adsorption data fit well to Freundlich and Langmuir isotherms and could be described by both pseudo-order- and second-order-rate laws. Adsorption modelling revealed that the surface of HMO is likely populated by adsorption sites of various energies and affinities. Nevertheless, the adsorption capacities for arsenate and phosphate are similar. Arsenate has a stronger affinity for HMO than phosphate and this is reflected by faster adsorption kinetics and greater adsorption at the same initial concentrations. Accordingly, in simultaneous competitive experiments, adsorption of phosphate is more affected by the presence of arsenate than the reverse. This was confirmed by significant fluctuations, especially in the first 2 hours of phosphate adsorption in all competitive experiments, whereas arsenate adsorption appeared unaffected at [As(V)]:[SPR] = 1:2.5 and 1:10 . Effective competition was observed at [As(V)]:[SRP] = 1:100 with reduced adsorption of both oxyanions. Conversely, when the oxyanions are added sequentially, phosphate is less affected by the addition of arsenate to phosphate-equilibrated suspension, whereas arsenate is more affected by the addition of phosphate to an arsenate-equilibrated suspension. In simultaneous competitive

experiments, the presence of both oxyanions in solution increases the adsorption of both oxyanions at [As(V)]:[SRP] = 1:2.5 and 1:10, indicating synergistic effects possibly resulting from interaction between the two oxyanions and the HMO surface, such as the formation of polyphosphoarsenate complexes. Overall, the extent of competition between the two oxyanions depends on their concentration ratio in solution. Phosphate is more abundant than arsenate in the marine environment and, therefore, the adsorption of arsenate to HMO might be lower than expected due to competition with phosphate and vice versa. Desorption experiments reveal that arsenate adsorption to HMO is perfectly reversible, whereas a fraction of the phosphate is bound irreversibly to its surface.

7. FUTURE WORK

The objectives of this study were to evaluate the individual and competitive adsorption of arsenate and phosphate on amorphous hydrous manganese oxide (HMO) from seawater, including the kinetics of adsorption and the reversibility of the reaction. These objectives were met. To go further, it would be interesting to evaluate the influence of phosphate and arsenate adsorption on the adsorption and oxidation kinetics of arsenite to arsenate by HMO in seawater. Arsenite is readily adsorbed and oxidized by HMO (e.g. Oscarson et al., 1983), even in the absence of oxygen (Scott and Morgan, 1995; Rahman, 2004), and several studies have reported reduced adsorption or oxidation of arsenite in the presence of phosphate (e.g. Chiu and Hering, 2000; Katsoyiannis et al., 2004) and calcium (e.g. Driehaus et al., 1995). In marine sediments, arsenate is reduced to arsenite once carrier phases (iron and manganese oxides) are buried below the oxic-anoxic redox boundary and arsenate is released to porewaters. Arsenite is more mobile than arsenate (Smedley and Kinniburgh, 2002) and migrates upwards along the concentration gradient towards the oxic zone where it encounters metal oxides and can become (re)adsorbed and oxidized to arsenate (or migrates downwards where it may be trapped or co-precipitation in a sulfide phase) (Mucci et al., 2000). To date, most studies of the adsorption and oxidation of arsenite by manganese oxides have been carried out in fresh water. Therefore, examining the adsorption and oxidation of arsenite by HMO in seawater, including the effect of phosphate addition, could add to the understanding of the cycling of arsenic during early diagenesis. The surface complexation of adsorbed arsenate and phosphate onto HMO in seawater and the nature of the complexes should be confirmed by EXAFS. Conducting experiments at various temperatures could provide insights on its effect on arsenate and phosphate adsorption onto HMO. Our experiments were run at room temperature,

whereas most marine sedimentary environments are much colder. In our experiments, the desorption of arsenate and phosphate from HMO was only investigated at a single concentration of each oxyanion ($[SRP]_{equilibrium} = 20\ \mu M$ and $[As(V)]_{equilibrium} = 2\ \mu M$). To better understand the buffer capacity of HMO for these oxyanions, it would be necessary to run these experiments at various oxyanion concentrations, i.e. vary the concentration of the oxyanions in solution, or the amount of adsorbed oxyanions on the pre-equilibrated HMO. Sundby et al. (1992) reported that the concentration of dissolved phosphate in sediment porewaters increases significantly across the sediment-water interface in the Gulf of St. Lawrence, and the same has been reported for total dissolved arsenic in the Saguenay Fjord Estuary (Mucci et al. 2000). Furthermore, Sundby et al. (1992) observed that the porewater phosphate concentrations remain nearly constant down to 5-15 cm depth, and this observation was attributed to phosphate buffering by adsorption-desorption equilibrium with the solid sediment. Below the metal-oxide redox boundary, the phosphate and arsenate concentrations increase as the metal oxides dissolve and release adsorbed species to the porewater (Mucci et al., 2000). The maximum buffer capacity for each solid component of the sediment was not investigated in the Sundby et al. (1992) or Mucci et al. (2000) experiments. Therefore, it would be interesting to determine the maximum buffer capacity of HMO, a ubiquitous component of oxic marine sediments, to elucidate its significance in the buffering of porewater oxyanions by the solid sediments.

8. LIST OF REFERENCES

Aggett, J., Aspell, A.C. (1976). The determination of arsenic(III) and total arsenic by atomic-absorption spectroscopy. Analyst, 101:341-347.

Antelo, J., Aven, M., Fiol, S., Lopez, R., Arce, F. (2005). Effects of pH and ionic strength on the adsorption of phosphate and arsenate at the goethite-water interface. Journal of Colloid and Interface Science, 285:476-486.

Arai, Y., Sparks, D.L., Davis, J.A. (2004). Effects of dissolved carbonate on arsenate adsorption and surface speciation at the hematite-water interface. Environmental Science ad Technology, 38:817-824.

Atun, G., Sismanoglu, T. (1996). Adsorption of 4,4'isopropylidene diphenol and diphenylolpropane 4,4'-dioxyacetic acid from aqueous solution on kaolinite. Journal of Environmental Science and Health Part A: Environmental Science and Engineering, 31:2055-2069.

Bajpai, S., Chaudhuri, M. (1999). Removal of arsenic from ground water by manganese dioxide-coated sand. Journal of Environmental Engineering, 125:782-787.

Baldo, G.R., Morris. M.J., Robert, Byrne, R.H. (1985). Spectrophotometric determination of seawater pH using phenol red. Analytical Chemistry, 57:2564-2567.

Balistrieri, L.S., Murray, J.W. (1982). The surface chemistry of δMnO_2 in major ion seawater. Geochimica et Cosmochimica Acta, 46:1041-1052.

Barrow, N.J. (1974). On the displacement of adsorbed anions from soil: 2. Displacement of phosphate by arsenate. Soil Science, 117:28-33.

Bartell, F.E., Thomas, T.L., Fu, Y. (1951). Thermodynamics of adsorption from solution. IV. Temperature dependence of adsorption. Journal of Physical Chemistry, 55:1456-1462.

Boujeben, N., Bouzid, J., Elouear, Z., Feki, M., Jamoussi, F., Montiel, A. (2008). Phosphorus removal from aqueous solution using iron coated natural and engineered sorbents. Journal of Hazardous Materials, 151:103-110.

Brookins, D.G. (1988). Eh-pH diagrams for geochemistry. New York: Springer-Verlag.

Burdige, D.J. (1993). The biogeochemistry of manganese and iron reduction in marine sediments. Earth-Science Reviews, 35:249-284.

Burdige, D.J. (2006). Geochemistry of Marine Sediments. Princeton Woodsock: Princeton University Press.

Caldwell, B.K., Caldwell, J.C., Mitra, S.N., Smith, W. (2003). Searching for an optimum solution to the Bangladesh arsenic crisis. Social Science & Medicine, 56:2089-2096

Canfield, D.E. (1989). Sulfate reduction and oxic respiration in marine sediments: implications for organic carbon preservation in euxinic environments. Deep-Sea Research, 36:121-138.

Canfield, D.E., Thamdrup, B., Hansen, J.W. (1993). The anaerobic degradation of organic matter in Danish coastal sediments: Fe reduction, Mn reduction, and sulfate reduction. Geochimica et Cosmochimica Acta, 57:3867-3883.

Catts, J.G., Langmuir, D. (1986). Adsorption of Cu, Pb, and Zn by δMnO_2: Applicability of the site binding-surface complexation model. Applied Geochemistry, 1:255-264.

Chu, M., Hashim, M. (2003). Modeling batch equilibrium and kinetics of copper removal by crab shell. Separation Sciene and Technology, 38:3927-3950.

Chiu, V.Q., Hering, J.G. (2000). Arsenic adsorption and oxidation at manganite surfaces. 1. Method for simultaneous determination of adsorbed and dissolved arsenic species. Environmental Science and Technology, 34:2029-2034.

Dickson, A.G. (1990). Thermodynamics of the dissociation of boric acid in synthetic seawater from 273.15 to 318.15 K. Deep Sea Research Part A. Oceanographic Research Papers, 37:755-766.

Driehaus, W., Seith, R., Jekel, M. (1995). Oxidation of arsenate(III) with manganese oxides in water treatment. Water Research, 29:297-305.

Dutta, P.K., Ray A.K., Sharma, V.K., Millero, F.J. (2004). Adsorption of arsenate and arsenite on titanium dioxide suspensions. Journal of Colloid and Interface Science, 248:270-275.

Edenborn, H.M., Belzile, N., Mucci, A., Lebel, J., Silverberg, N. (1986). Observations on the diagenetic behaviour of arsenic in a deep coastal sediment. Biogeochemistry, 2:359-376.

Feely, R.A., Trefry, J.H., Massoth, G.J., Metz,Z. (1991). A comparison of the scavenging of phosphorus and arsenic from seawater by hydrothermal iron oxyhydroxides in the Atlantic and pacific oceans. Deep Sea-Research, 38:617-623.

Fendorf, S., Eick, M.J., Grossl, P., Sparks, D.L. (1997). Arsenate and chromate retention mechanisms on goethite. Environmental Science and Technology, 31:315.

Ferguson, J.F., Gavis, J. (1972). A review of the arsenic cycle in natural waters. Water Research, 6:1259-1274.

Fitzpatrick, A.J. (1998). Adsorption of arsenate and phosphate on gibbsite from artificial seawater. M.Sc. Thesis, Department of Earth and Planetary Sciences, McGill University, Montreal.

Frausto da Silva, J.J.R., Williams, R.J.P. (1997). The biological chemistry of the elements: The inorganic chemistry of life, 1st ed., Oxford University Press, Oxford, U.K.

Froelich, P.N., Klinkhammer, G.P., Bender, M.L., Luedtke, N.A., Heath, G.R., Cullen, D., Dauphin, P. (1979). Early oxidation of organic matter in pelagic sediments of the eastern equatorial Atlantic: suboxic diagenesis. Geochimica et Cosmochimica Acta, 43:1075-1090.

Froelich, P.N. (1988). Kinetic control of dissolved phosphate in natural rivers and estuaries: A primer on the phosphate buffer mechanism. Limnology and Oceanography, 33:649-668.

Gao, Y. (2001). Surface electrical properties of goethite and adsorption of phosphate and arsenate on iron oxyhydroxides in high ionic strength solutions. Ph.D. Dissertation, Department of Earth and Planetary Sciences, McGill University, Montreal.

Gao, Y., Mucci, A. (2001). Acid base reactions, phosphate and arsenate complexation, an their competitive adsorption at the surface of goethite in 0.7 M NaCl solution. Geochimica et Cosmochimica Acta, 65:2361-2378.

Gao, Y., Mucci, A. (2003). Individual and competitive adsorption of phosphate and arsenate on goethite in artificial seawater. Chemical Geology, 199:91-109.

Grasshoff, K., Kremling, K., Ehrhardt, M. (Eds.) (1999). Methods of seawater analysis, 1st Ed., Verlag Chemie, New York.

Grossl, P.R., Sparks, D.L. (1995). Evaluation of contaminant ion adsorption/desorption on goethite using pressure-jump relaxation kinetics. Geoderma, 67:87-101.

Hayes, K.F, Roe, A.L., Brown, G.E., Hodgson, K.O, Leckie, J.O, Parks, G.A. (1987). In situ x-ray absorption study of surface complexes: selenium oxyanions on αFeOOH. Science, 238:783-786.

Hem, J.D. (1978). Redox processes at surfaces of manganese oxide and their effects on aqueous metal ions. Chemical Geology, 21:199-218.

Hingston, F.J., Posner, A.M., Quirk, J.P (1971). Competitive adsorption of negatively charged ligands on oxide surfaces. Discussions of the Faraday Society, 52:334-342.

Hingston, F.J., Posner, A.M., Quirk, J.P. (1972). Anion adsorption by goethite and Gibbsite. I. The role of the proton in determining adsorption envelopes. Journal of Soil Science, 23:177-192.

Ho, Y.S., Wase, D.A.J., Forster, C.F. (1995). Batch nickel removal from aqueous solution by sphagnum moss peat. Water Research, 29:1327-1332.

Ho, Y.S., McKay, G. (1998a). Kinetic models for the sorption of dye from aqueous solution by wood. Process Safety and Environmental Protection, 76:183-191.

Ho, Y.S., McKay, G. (1998b). Sorption of dye from aqueous solution by peat. Chemical Engineering Journal, 70:115-124.

Ho, Y.S., McKay, G. (1999). Pseudo-second order model for sorption processes. Process Biochemistry, 34:451-465.

Ho, Y.S., McKay, G. (2000). The kinetics of sorption of divalent metal ions onto sphagnum moss peat. Water Research, 34:735-742.

Ho, Y.S., Wang, C.C. (2004). Pseudo-isotherms for the sorption of cadmium ion onto tree fern. Process Biochemistry, 39:759-763.

Ho, Y.S. (2006). Review of second-order models for adsorption systems. Journal of Hazardous Materials, 136:681-689.

Hongshao, Z., Stanforth, R. (2001). Competitive adsorption of phosphate and arsenite on goethite. Environmental Science and Technology, 35:4753-4757.

Hsu, J., Lin, C., Liao, C., Chen. S. (2008). Removal of As(V) and As(III) by reclaimed iron-oxide coated sands. Journal of Hazardous Materials, 153:817-826.

Hu, C., Tsou, T. (2002). Ideal capacitive behaviour of hydrous manganese oxide prepared by anodic deposition. Electrochemistry Communications, 4:105-109.

Jain, A., Loeppert, R.H. (2000). Effect of competing anions on the adsorption of arsenate and arsenite by ferrihydrite. Journal of Environmental Quality, 29:1422-1430.

Jenne, E.A. (1968). Controls on Mn, Fe, Co, Ni, Cu, and Zn concentrations in soils and water: The significant role of hydrous Mn and Fe oxides. In: Trace inorganics in water, Baker, R.A. (Ed.). American Chemical Society, Volume 73, Chapter 21.

Kanematsu, M., Young, T.M., Fakushi, K., Green, P.G., Darby, J.L. (2013). Arsenic(III, V) adsorption on a goethite-based adsorbent in the presence of major co-existing ions: Modeling competitive adsorption consistent with spectroscopic and molecular evidence. Geochimica et Cosmochimica Acta, 106:404-428.

Katsoyiannis, I.A., Zouboulis, A.I., Jekel, M. (2004). Kinetics of bacterial As(III) oxidation and subsequent As(V) removal by sorption onto biogenic manganese oxides during groundwater treatment. Industrial & Engineering Chemical Research, 43:486-493.

Kawashima, M., Tainaka, Y., Hori, T., Koyama, M., Takamatsu, T. (1986). Phosphate adsorption onto hydrous manganese(IV) oxide in the presence of divalent cations. Water Research, 20:471-475.

Khoo, K.H., Ramette, R.N., Culberson, C.H., Bates, R.G. (1977). Determination of hydrogen ion concentrations in seawater from 5 to 40°C: Standard potentials as salinities from 20 to 45. Analytica Chemistry, 49:29-34.

Krauskopf, K.B. (1956). Factors controlling the concentrations of thirteen rare metals in sea-water. Geochimica et Cosmochimica Acta, 9:1-32.

Lafferty, B.J., Ginder-Vogel, M., Sparks, D.L. (2010a). Arsenite oxidation by a poorly crystalline manganese-oxide 1. Stirred-flow experiments. Environmental Science and Technology, 44:8460-8466.

Lafferty, B.J., Ginder-Vogel, M., Zhu, M., Livi, K.J.T., Sparks, D.L. (2010b). Arsenite oxidation by a poorly crystalline manganese-oxide 2. Results from x-ray absorption spectroscopy and x-ray diffraction. Environmental Science and Technology, 44:8467-8472.

Lafferty, B.J., Ginder-Vogel, M., Zhu, M., Livi, K.J.T., Sparks, D.L. (2010c). Arsenite oxidation by a poorly crystalline manganese-oxide. Supporting information. Environmental Science and Technology, 44:8467-8472.

Lafferty, B.J., Ginder-Vogel, M., Sparks, D.L. (2011). Arsenite oxidation by a poorly-crystalline manganese oxide. 3. Arsenic and manganese desorption. Environmental Science and Technology, 45:9218-9233.

Lagergren, S. (1898). Zur theorie der sogenannten adsorption gelöster stoffe. Kungliga Svenska Vetenskapsakaddemiens Handlingar, 24:1-39.

Laha, S., Luthy, R.G. (1990). Oxidation of aniline end other primary aromatic amines by manganese dioxide. Environmental Science and Technology, 24:363-373.

Li, Y.-H, Schoonmaker, J.E. (2005). Chemical composition and mineralogy of marine sediments. In: Sediments, diagenesis and sedimentary rocks: treatise on geochemistry, Volume 7, 1st ed, Fred T. Mackenzie (Ed.). Elsevier.

Liu, F., De Christofaro, A., Violante, A. (2001). Effect of pH, phosphate and oxalate on the adsorption/desorption of arsenate on/from goethite. Soil Science, 166:197-208.

Luengo, C., Brigante, M., Avena, M. (2007). Adsorption kinetics of phosphate and arsenite on goethite. A comparative study. Journal of Colloid and Interface Science, 311:354-360.

Lumsdon, D.G., Fraser, A.R., Russell, J.D., Livesey, N.T. (1984). New infrared band assignments for the arsenate ion adsorbed on synthetic goethite (α-FeOOH). Journal of Soil Science, 35:381-386.

Maity, S., Chakravarty, S., Bhattacharjee, S., Roy, B.C. (2005). A study on arsenic adsorption on polymetallic sea nodule in aqueous medium. Water Research, 39:2579-2590.

Manning, B.A., Fendorf, S.E., Bostick, B., Suarez, D.. (2002). Arsenic(III) oxidation and arsenic(V) adsorption reactions on synthetic birnessite. Environmental Science and Technology, 36:976-981.

Manning, B.A., Goldberg, S. (1996). Modeling competitive adsorption of arsenate with phosphate and molybdate on oxide minerals. Soil Science Society of America Journal, 60:121-131.

McKenzie, R.M. (1981). The surface charge on manganese dioxides. Australian Journal of Soil Research, 19:41-50.

Millero, F.J, Schreiber, D.R. (1982). Use of the ion pairing model to estimate activity coefficients of the ionic components of natural waters. American Journal of Science, 282:1508-1540.

Millero, F., Huang, F., Zhu, X., Liu, X., Zhang, J. (2001). Adsorption and desorption of phosphate on calcite and aragonite in seawater. Aquatic Geochemistry, 7:33-56.

Min, S., Kim, B., Park, S., Chang, Y., Yang, J. (2009). Removal efficiency of arsenic by adsorbents having different type of metal oxides. Korean Society of Environmental Engineers, 14:134-139.

Mohan, S.V., Rao, N.C., Karthikeyan, J. (2002). Adsorptive removal of direct azo dye from aqueous phase onto coal based sorbents: a kinetic and mechanistic study. Journal of Hazardous Materials, 90:189-204.

Mok, W.M., Wai, C.M. (1994). Mobilization of arsenic in contaminated river waters. In: Arsenic in the environment, Part I: Cycling and characterization, Nriagy, J.L. (Ed.), Wiley, New York, pp. 99-118.

Moore, J.N., Walker, J.R., Hayes, T.H. (1990). Reaction Scheme for the oxidation of As(III) to As(V) by birnessite. Clays and Clay Minerals, 38:549-555.

Mucci, A., Richard, L., Lucotte, M., Guignard, C. (2000). The differential geochemical behaviour of arsenic and phosphorus in the water column and sediments of the Saguenay fjord estuary, Canada. Aquatic Geochemistry, 6:293-324.

Murphy, J., Riley, J.P. (1962). A modified single solution method for the determination of phosphate in natural waters. Analytical Chimica Acta, 27:31-36.

Murray, J.W. (1974). The surface chemistry of hydrous manganese dioxide. Journal of Colloid and Interface Science, 46:357-371.

Murray, J.W. (1975). The interactions of metal ions at the manganese dioxide-solution interface. Geochimica et Cosmochimica Acta, 39:505-519.

Mustafa, S., Zaman, M. I., Khan, S. (2008). Temperature effect on the mechanism of phosphate anions sorption by β-MnO_2. Chemical Engineering Journal, 141:51-57.

Namasivanyam, C., Thamaraiselvi, K., Yamuna, R.T. (1994). Removal of paraquat by adsorption on “waste” Fe(III)/Cr(III) hydroxide: adsorption rates and equilibrium studies. Pesticide Science, 41:7-12.

Nagarajah, S., Posner, A.M., Quirk, J. P. (1968). Desorption of phosphate from kaolinite by citrate and bicarbonate. Soil Science Society of America Journal, 32:507-510.

O'Shannessy, D.J., Winzor, D.J. (1996). Interpretation of deviations from pseudo-first-order kinetic-behaviour in the characterization of ligand binding by biosensor technology. Analytical Biochemistry, 236:275-283.

Okeola, F.O., Odebunmi, E.O. (2010). Freundlich and Langmuir isotherms parameters for adsorption of methylene blue by activated carbon derived from agrowastes. Advances in Natural and Applied Sciences, 4:281-288.

Ortiz, N., Pires, M.A, Bressiani, J.C. (2001). Use of steel converter slag as nickel adsorber to wastewater treatment. Waste Management, 21:631-635.

Oscarson, D.W., Huang, P.M., Defosse, C., Herbillon, A. (1981a). Oxidative power of Mn(IV) and Fe(III) oxides with respect to As(III) in terrestrial and aquatic environments. Nature, 291:50-51.

Oscarson, D.W., Huang, P.M., Liaw, W.K . (1981b). Role of manganese in the oxidation of arsenite by freshwater lake sediments. Clays and Clay Minerals, 29:219-225.

Oscarson, D.W., Huang, P.M., Liaw, W.K., Hammer, U.T. (1983a). Kinetics of oxidation of arsenite by various manganese dioxides. Soil Science Society of America Journal, 47:644-648.

Oscarson, D.W., Huang, P.M., Hammer, U.T., Liaw, W.K. (1983b). Oxidation and sorption of arsenite by manganese dioxide as influenced by surface coatings of iron and aluminium oxides and calcium carbonate. Water, Air, and Soil Pollution, 20:233-244.

Ouvrard, S., Simonnot, M, Sardin, M. (2001). Removal of arsenate from drinking water with a natural manganese oxide in the presence of competing anions. Water Science and Technology: Water Supply, 1:167-173.

Ouvrard, S., Simonnot, M., Sardin, M. (2002a). Reactive behaviour of natural manganese oxide toward the adsorption of phosphate and arsenate. Industrial & Engineering Chemical Research, 41:2785-2791.

Ouvrard, S., Simonnot, M., Donato, P., Sardin, M. (2002b). Diffusion-controlled adsorption of arsenate on a natural manganese oxide. Industrial & Engineering Chemistry Research, 41:6194-6199.

Parikh, S., Lafferty, B.L., Meade, T.G., Sparks, D.L. (2010). Evaluating environmental influences on As(III) oxidation kinetics by a poorly crystalline Mn-Oxide. Environmental Science and Technology, 44:3772-3778.

Parks, G.A. (1965). The isoelectric points of solid oxides, solid hydroxides, and aqueous hydroxo complex systems. Chemical Reviews, 65:177-198.

Peak, D. (2006). Adsorption mechanism of selenium oxyanions at the aluminium oxide/water interface. Journal of Colloid and Interface Science, 303:337-345.

Persson, P., Nilsson, N., Sjoberg, S. (1996). Structure and binding of orthophosphate ions at the iron oxide-aqueous interface. Journal of Colloidal and Interface Science, 177:263-275.

Pierce, M.L, Moore, C.B (1982). Adsorption of arsenite and arsenate on amorphous iron hydroxide. Water Research, 16:1247-1253.

Posselt, H.S., Anderson, F.J. (1968). Cation sorption on colloidal hydrous manganese dioxide. Environmental Science and Technology, 2:1087-1093.

Post, J.E. (1999). Manganese oxide minerals: Crystal structures and economic and environmental significance. Proceedings of the National Academy of Sciences, 96:3447-3454.

Puls, R.W., Powell, R.M. (1992). Transport of inorganic colloids through natural aquifer material: implications for contaminant transport. Environmental Science and Technology, 26:614-621.

Radu, T., Subacz, J.L., Phillippi, J.M., Barnett, M.O. (2005). Effects of dissolved carbonate on arsenic adsorption and mobility. Environmental Science and Technology, 39:7875-7882.

Rahman, S. (2004). Oxidation of arsenite by dissolved oxygen, manganese and iron oxyhydroxides in aqueous solutions. M.Sc. Thesis, Department of Earth and Planetary Sciences, McGill University, Montreal.

Ramakrishna, D.M., Viraraghavan, T., Jin, Y. (2006). Iron oxide coated sand for arsenic removal: investigation of coating parameters using factorial design approach. Practice Periodical of Hazardous, Toxic, and Radioactive Waste Management, 10:198-206.

Ren, Z., Zhang, G., Chen, J.P. (2011). Adsorption removal of arsenic from water by an iron-zirconium binary oxide adsorbent. Journal of Colloid and Interface Science, 358:230-237.

Riedel, G.F. (1993). The annual cycle of arsenic in a temperate estuary. Estuaries, 16:533-540.

Saiers, J.E., Hornberger, G.M., Liang, L. (1994). First-and second-order kinetics approaches for modelling the transport of colloidal particles in porous media. Water Resource Research, 30:2499-2506.

Schindler, D.W., Armstrong, F.A., Holmgren, S.K., Brunskill, G.J. (1971). Eutrophication of lake 227, experimental lakes area, Nothwestern Ontario, by addition of phosphate and nitrate. Journal of the Fisheries Research Board of Canada, 28:1763-1782.

Schindler, D.W. (1974). Eutrophication and recovery in experimental lakes: Implications for lake management. Science, 184:897-899.

Scott, M.J., Morgan, J.J. (1995). Reactions at oxide surfaces. 1. Oxidation of As(III) by synthetic birnessite. Environmental Science and Technology, 29:1898-1905.

Shin, E.W., Han, J.S., Jang, M. Min, S.H., Park J.K., Rowell, R.M. (2004). Phosphate adsorption on aluminum-impregnated mesoporous silicates: Surface structure and behaviour of adsorbents. Environmental Science and Technology, 38:912-917.

Smedley, P.L., Kinniburgh, D.G. (2002). A review of the source, behaviour and distribution of arsenic in natural waters. Applied Geochemistry, 17:517-568.

Smil, V. (2000). Phosphorus in the environment: natural flows and human interferences. Annual Review of Energy and the Environment, 25:53-88.

Stachowicz, M., Hiemstra, T., van Riemsdija, W.H. (2007). Arsenic-bicarbonate interaction on goethite particles. Environmental Science and Technology, 41:5620-5625.

Stollenwerk, K.G. (2003). Geochemical processes controlling transport of arsenic in ground water: A review of adsorption. Arsenic in Ground Water, pp. 69-100.

Stone, A.T., Morgan, J.J. (1984). Reduction and dissolution of manganese(III) and manganese(IV) oxides by organics. 1. Reaction with hydroquinone. Environmental Science and Technology, 18:450-456.

Stumm, W. (1993). Aquatic colloids as chemical reactants: Surface structure and reactivity. Colloids and Surfaces A: Physiochemical and Engineering Aspects, 73:1-18.

Sundby, B., Gobeil, C., Silverberg, N., Mucci, A. (1992). The phosphorus cycle in coastal marine sediments. Limnology and Oceanography, 37:1129-1145.

Takamatsu, T., Kawashima, M., Koyama, M. (1985). The role of Mn2+-rich hydrous manganese oxide in the accumulation of arsenic in lake sediments. Water Research, 19:1029-1032.

Tan, W., Lu, S., Liu, F., Feng, X., He, J., Koopal, L.K. (2008). Determination of the point-of-zero charge of manganese oxides with different methods including an improved salt titration method. Soil Science, 173:277-286.

Tanabalasingam, P., Pickering, W.F. (1986). Effect of pH on interaction between As(III) or As(V) and manganese(IV) oxide. Water, Air, and Soil Pollution, 29:205-216.

Tawfik, D.S., Viola, R.E. (2011). Arsenate replacing phosphate: Alternative life chemistries and ion promiscuity. Biochemistry, 50:1128-1134.

Tebo, B.M., Bargar, J.R., Clement, B.G., Dick, G.J., Murray, K.J., Parker, D., Verity, R., Webb, S.M. (2004). Biogenic manganese oxides: Properties and mechanisms of formation. Annual Review of Earth and Planetary Science, 32:287-328.

Tejedor-Tejedor, M.I., Anderson, M.A. (1990). Protonation of phosphate on the surface of goethite as studies by CTR-FTIR and electrophoretic mobility. Langmuir, 6:602-611.

Tessier, A., Fortin, D., Belzile, N., DeVitre, R.R., Leppard, G.G. (1996). Metal sorption to diagenetic iron and manganese oxyhydroxides and associated organic matter: Narrowing the gap between field and laboratory measurements. Geochimica et Cosmochimica Acta, 60:387-404.

Thirunavukkarasu, O.S. Viraraghavan, T., Subramanian, K.S. (2003). Arsenic removal from drinking water using iron-oxide coated sand. Water, Air, and Soil Pollution, 142:95-111.

Tournassat, C., Charlet, L., Bosbach, D., Manceau, A. (2002). Arsenic(III) oxidation by birnessite and precipitation of manganese(II) arsenate. Environmental Science and Technology, 36:493-500.

Van Riemsdijk, W.H., Lyklema, J. (1980). Reaction of phosphate with gibbsite ($Al(OH)_3$) beyond the adsorption maximum. Journal of Colloid and Interface Science, 76:55-66.

Waychunas, G.A., Rea, B.A., Fuller, C.C., Davis, J.A. (1993). Surface chemistry of ferrihydrite: Part I. EXAFS studies of the geometry of coprecipitated and adsorbed arsenate. Geochimica et Cosmochimica Acta, 57:2251-2269.

Whiting, K.S. (1992). The thermodynamics and geochemistry of arsenic, with application to subsurface waters at the Sharon Steel Superfund Site at Midvale, Utah. M.Sc. Thesis, Colorado School of Mines.

Willet, I.R., Chartres, C.J., Nguyen, T.T. (1988). Migration of phosphate into aggregated particles of ferrihydrite. Journal of Soil Science, 39: 275-282.

Wu, K., Liu, R., Liu, H., Zhao, X., Qu, J. (2011). Arsenic(III,V) adsorption on iron-oxide-coated manganese sand and quartz sand: Comparison of different carriers and adsorption capacities. Environmental Engineering Science, 28: 643-651.

Wu, K., Liu, T., Xue, W., Wang, X. (2012). Arsenic(III) oxidation/adsorption behaviours on a new bimetal adsorbent of Mn-oxide-doped Al oxide. Chemical Engineering Journal, 192:343-349.

Wurl, O. (2009). Practical guidelines for the analysis of seawater. Boca Raton, FL., CRC Press.

Yao, W., Millero, F.J. (1996). Adsorption of phosphate on manganese dioxide in seawater. Environmental Science and Technology, 30:536-541.

Ying, S.C., Kocar, B.D., Fendorf, S. (2012). Oxidation and competitive retention of arsenic between iron- and manganese oxides. Geochimica et Cosmochimica Acta, 96:294-303.

Zaror, C.A. (1997). Enhanced oxidation of toxic effluents using simultaneous ozonation and activated carbon treatment. Journal of Chemical Technology and Biotechnology, 70:21-28.

Zhang, W., Singh, P., Paline, E., Delides, S. (2004). Arsenic removal from contaminated water by natural iron ores. Minerals Engineering, 17: 517-524.

Zhang, J., Huang, X. (2011). Effect of temperature and salinity on phosphate sorption on marine sediments. Environmental Science and Technology, 45:6831-6837.

APPENDIX 1: Materials, reagents and XRD of HMO suspensions

Reagents used to prepare the HMO suspension included 0.1 M NaOH, 0.1 M $KMnO_4$ and 0.1 M $MnCl_2$, and were prepared by dissolving 2.0241 g NaOH in 0.5 L of distilled water, 7.9011 g $KMnO_4$ in 0.5 L o distilled water, and 9.9032 g $MnCl_2 \cdot 4H_2O$ in 0.5 L of distilled water.

Reagents used for AAS included sodium hydroxide (NaOH; MW=40 g/mol, ACS grade, Fisher Scientific), sodium borohydride ($NaBH_4$; MW=37.8 g/mol, 99 %, Aldrich), potassium iodide, (KI; MW=166 g/mol, ACS, Fisher Scientific), ascorbic acid ($C_6H_8O_6$; MW=176 g/mol, 99+%, Sigma Aldrich) and concentrated trace metal-free hydrochloric acid. All solids were dissolved and prepared in Milli-Q water.

Reagents used for visible spectrometry included sulphuric acid (H_2SO_4, diluted to 4.5 M with MilliQ water, ACS grade, ACP), ammonium heptamolybdate tetrahydrate ($(NH_4)_6Mo_7O_{24} \cdot 4H_2O$; MW=1236 g/mol, ACS grade, Fisher Scientific), potassium antimony(III) oxide tartrate ($K(SbO)C_4H_4O_6$; MW=325 g/mol, 99+%, Aldrich Chemical company), ascorbic acid ($C_6H_8O_6$; MW=176 g/mol, 99+%, Sigma Aldrich), potassium dihydrogenphosphate (KH_2PO_4; MW=136.09 g/mol, 99.5 %, AnalaR, BHD), oxalic acid dihydrate ($(COOH)_2 \cdot 2H_2O$; MW=126.07 g/mol, ACS grade, Fisher Scientific), disodium hexafluorosilicate (Na_2SiF_6; MW=188.06 g/mol, d. 268, Aldrich). The sulphuric acid stock solution (4.5 M), was prepared by slowly adding 250 ml concentrated sulphuric acid to 750 ml of Milli-Q water followed by dilution to 1 L after cooling. The ascorbic acid reagent was prepared by dissolving 10.0 g ascorbic acid in 50 ml Milli-Q water followed by addition of 50 ml of 4.5 M sulphuric acid. This solution was prepared fresh for every experiment or stored cold and dark for up to 3 days (replaced if any coloration appeared). The mixed reagent

was prepared by dissolving 12.5 g of ammonium heptamolybdate tetrahydrate in 125 ml Milli-Q water, which was slowly added to 350 ml of 4.5 M sulphuric acid while stirring. To this solution, 0.5 g potassium antimony oxide tartrate dissolved in 20ml Milli-Q water was added. This resulted in the mixed reagent, which was stored in a glass bottle and stored up to 3 months and replaced if any precipitation occurred.

The salinity of the experimental solution was determined by titrating 3.5 ml aliquots with 3.5 mL 0.022 M K_2CrO_4 (indicator) against 0.3 M $AgNO_3$ solution.

$$\text{Salinity of sample} = \frac{\text{ml } AgNO_3 \text{ of sample}}{\text{ml } AgNO_3 \text{ Standard}} \times \text{salinity of standard}$$

The pH of the experimental solution was determined spectrophotometrically by adding 0.022 ml of Phenol red to 10 ml aliquots and mesured as described in 3.3.3.

Figure A-1: X-ray diffractograms of a fresh (2 weeks old) HMO suspension (top graph) (Batch # 4) and an aged (6 month old) HMO suspension (bottom graph) (Batch # 1).

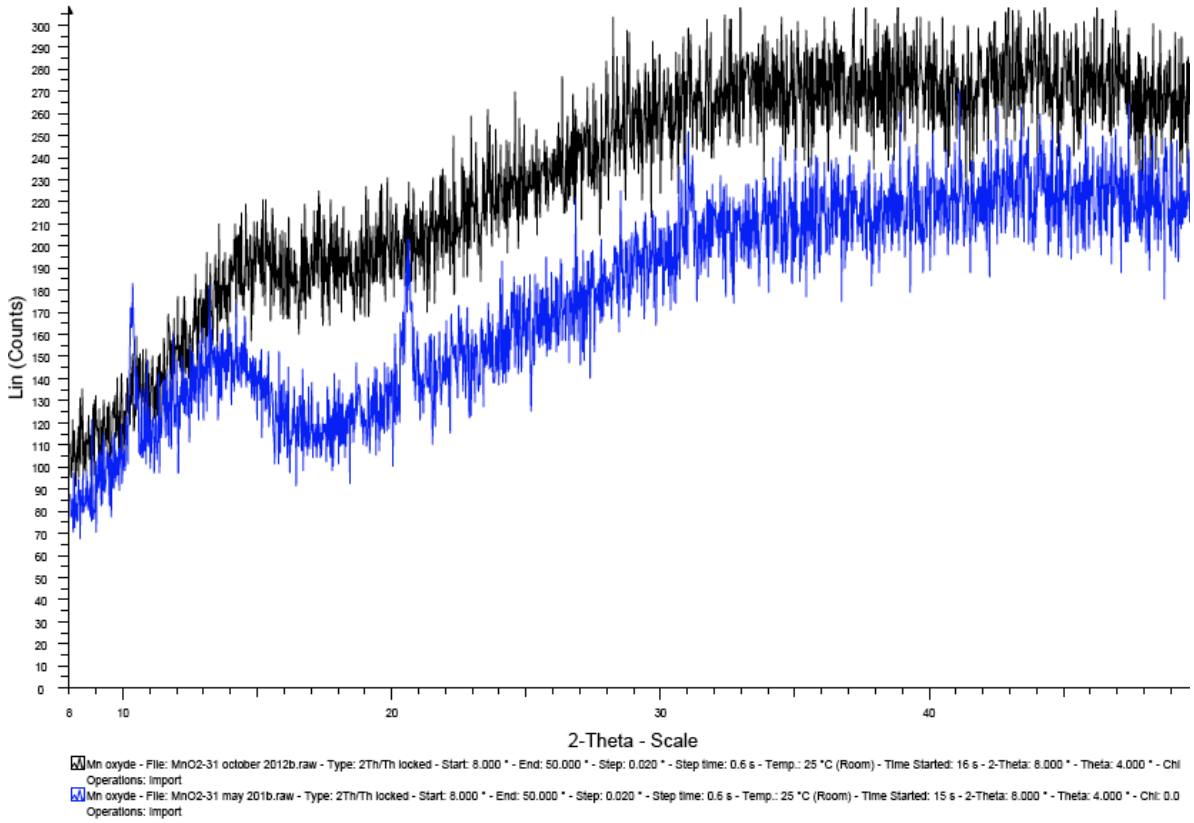

APPENDIX 2: Calibration curves

Figure A-2: Phosphate calibration curve, as described in 3.3.2. [SRP] = 0-12.5 µM, absorbance at 880 nm using a 10-cm cell. The points above 8 µM were excluded from the calibration curve as they showed non-linearity at high SRP concentration. Concentrations above 6 µM were diluted.

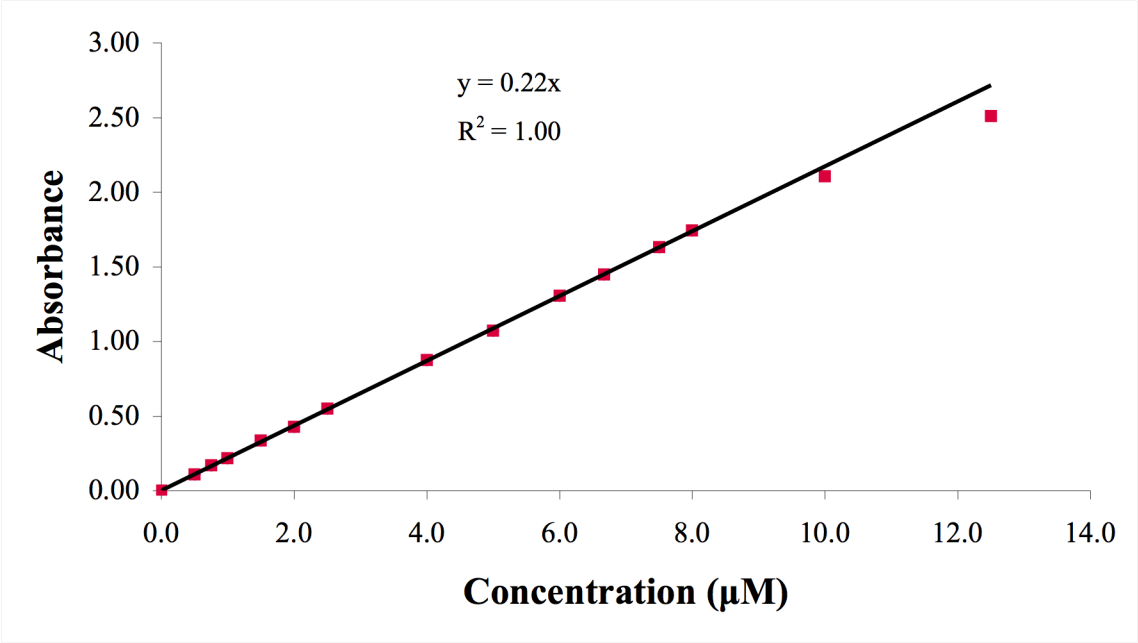

Figure A-3: Silicate calibration curve as described in 3.3.2. [Silicate] = 0-250 µM, absorption at 810 nm using a 1-cm cell.

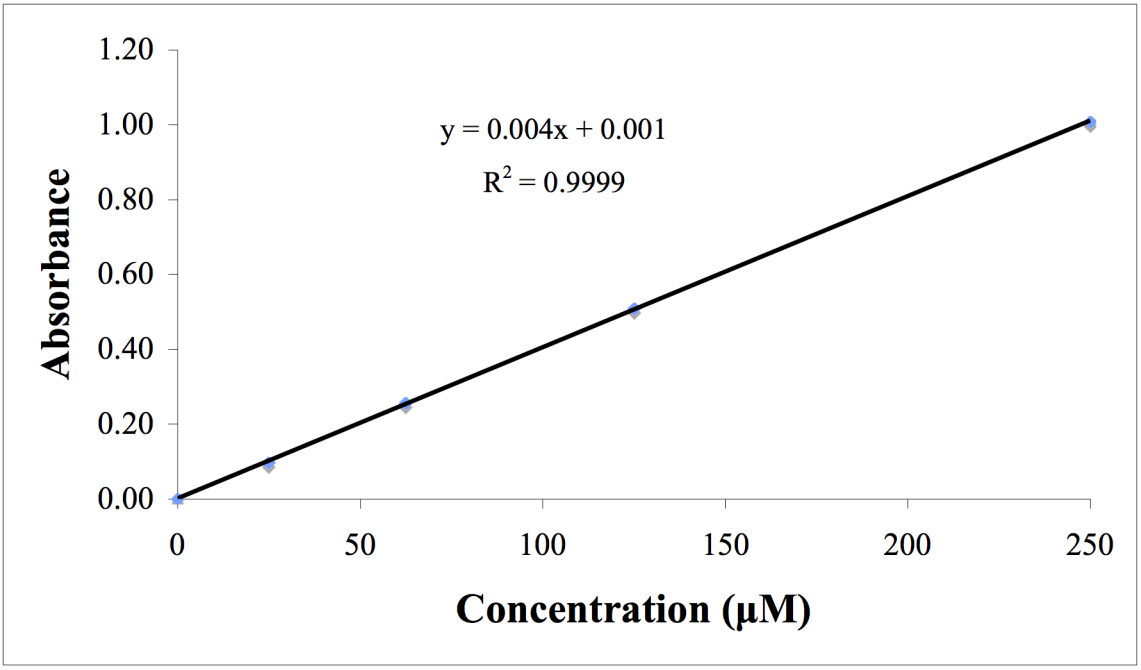

Figure A-4: Arsenate calibration curve as described in 3.3.1. [As(V)] = 0-2.0 µM, flameless AAS.

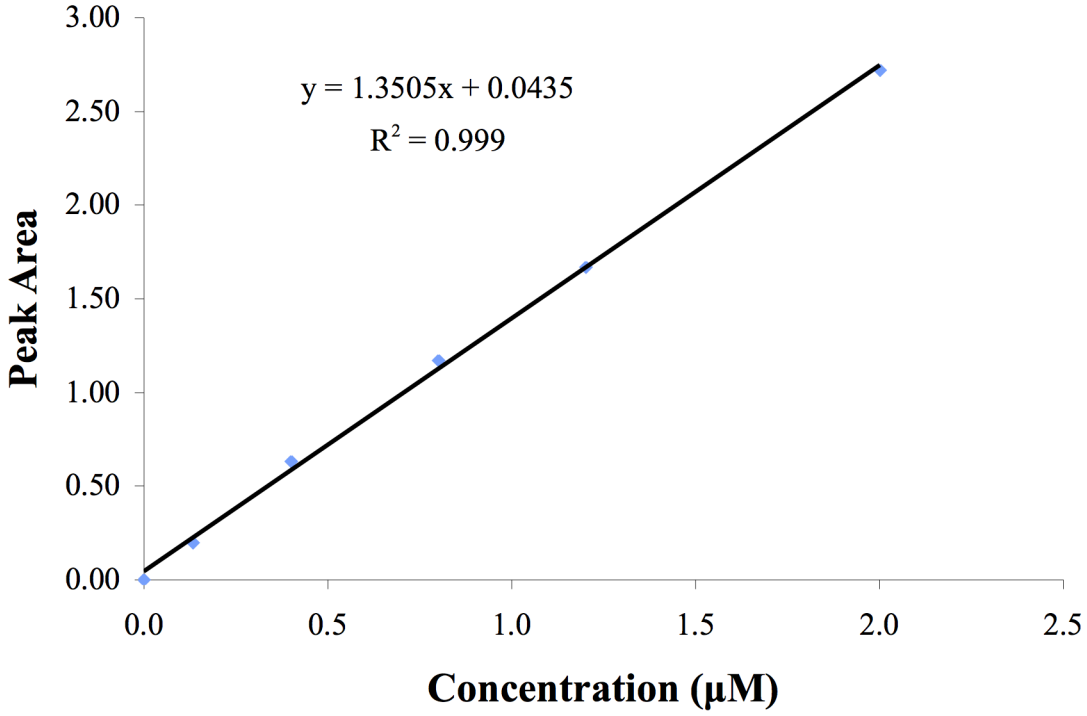

APPENDIX 3: Kinetics of phosphate adsorption

Kinetics data from phosphate adsorption onto HMO from seawater at 23(±3)°C over 8 hours (control experiments) (Fig. 7). [HMO]:solution ratio = 0.15 g/L, Batch # 2. On top: $[SRP]_{initial}$ = 12.4 μM. At the bottom: $[SRP]_{initial}$ = 12.2 μM.

Time (h)	$[SRP]_{solution}$	$[SRP]_{adsorbed}$	$\%[SRP]_{adsorbed}$	% RSD
0	12.4	0.0	0	0.9
0.042	10.3	2.1	17	0.7
0.083	10.2	2.2	18	0.2
0.167	10.1	2.3	18	0.5
0.25	10.1	2.3	18	0.2
0.5	9.8	2.6	21	0.6
1	9.7	2.7	22	0.4
2	9.5	2.9	24	0.2
4	9.3	3.1	25	0.3
6	9.2	3.2	26	0.3
8	9.1	3.3	26	0.2

Time (h)	$[SRP]_{solution}$	$[SRP]_{adsorbed}$	$\%[SRP]_{adsorbed}$	% RSD
0	12.2	0.0	0	0.1
0.042	9.9	2.2	18	0.3
0.083	9.9	2.3	19	0.2
0.167	9.8	2.4	19	0.4
0.25	9.7	2.4	20	0.4
0.5	9.5	2.6	22	0.2
1	9.5	2.7	22	0.3
2	9.3	2.9	23	0.4
4	9.3	2.9	24	0.1
6	9.2	2.9	24	0.3
8	9.2	2.9	24	0.3

Kinetics data from phosphate adsorption onto HMO from seawater at 23(±3)°C over 8 hours (control experiments) (Fig. 7). [HMO]:solution ratio = 0.15 g/L, Batch # 5. On top: $[SRP]_{initial}$ = 12.0 μM. At the bottom: $[SRP]_{initial}$ = 11.7 μM.

Time (h)	$[SRP]_{solution}$	$[SRP]_{adsorbed}$	$\%[SRP]_{adsorbed}$	% RSD
0	12.0	0.0	0	0.3
0.042	10.8	1.2	10	0.2
0.083	10.7	1.3	11	1.1
0.167	10.9	1.1	9	0.1
0.25	10.3	1.7	14	0.4
0.5	9.9	2.1	18	0.3
1	10.0	2.0	17	0.0
2	9.3	2.7	22	0.2
4	9.1	2.9	24	0.1
6	9.3	2.7	22	0.3
8	8.8	3.2	27	0.5

Time (h)	$[SRP]_{solution}$	$[SRP]_{adsorbed}$	$\%[SRP]_{adsorbed}$	% RSD
0	11.7	0.0	0	0.2
0.042	10.5	1.1	10	0.3
0.083	10.7	0.9	8	0.1
0.167	10.1	1.5	13	0.2
0.25	10.2	1.5	13	0.1
0.5	10.1	1.6	14	0.4
1	9.5	2.1	18	0.3
2	9.5	2.2	19	0.4
4	8.9	2.8	24	0.5
6	9.1	2.6	22	0.3
8	8.7	3.0	26	0.2

Kinetics data from phosphate adsorption onto HMO from seawater at 23(±3)°C over 48 hours (Fig. 8). $[SRP]_{initial}$ = 6.4 μM, [HMO]:solution ratio = 0.15 g/L, Batch # 5.

Time (h)	$[SRP]_{solution}$	$[SRP]_{adsorbed}$	$\%[SRP]_{adsorbed}$	% RSD
0	6.4	0.0	0	0.2
0.042	5.9	0.4	7	0.2
0.083	5.9	0.5	7	0.3
0.167	5.7	0.7	11	0.2
0.25	5.6	0.8	13	0.1
0.5	5.5	0.9	15	0.1
1	5.2	1.2	19	0.2
2	5.1	1.3	21	0.1
4	4.9	1.5	23	0.2
6	4.9	1.4	23	0.3
8	4.8	1.6	25	0.3
10	4.8	1.6	25	0.1
24	4.6	1.8	28	0.2
30	4.5	1.9	30	0.4
48	4.4	2.0	31	0.1

Data from the phosphate adsorption isotherm experiment at 23(±3)°C (Fig. 9). $[SRP]_{initial}$ = 2-46 μM, [HMO]:solution ratio = 0.15 g/L, Batches # 4, 6 and 7.

$[SRP]_{initial\ solution}$ (μM)	$[SRP]_{adsorbed}$ (μM)	$[SRP]_{adsorbed}$ (μmol)	Batch #	Mass of adsorbent (g)	Volume surface (m^2)
1.9	0.8	0.5	6	0.07	19.2
2.8	1.0	0.6	4	0.05	14.1
9.6	3.5	1.9	7	0.09	24.1
11.9	3.1	1.7	4	0.05	14.1
15.5	4.3	2.4	4	0.05	14.1
22.3	4.8	2.7	4	0.05	14.1
26.9	5.5	3.1	4	0.05	14.1
30.7	10.2	5.7	7	0.09	24.1
46.2	11.8	6.5	6	0.07	19.2

Percent phosphate adsorption onto HMO from seawater at 23(±3)°C (Fig. 12). $[SRP]_{initial}$ = 2-46 μM, [HMO]:solution ratio = 0.15 g/L (Batch # 4, 6 and 7).

$[SRP]_{initial\ solution}$ (μM)	% adsorption
1.9	44
2.8	36
9.6	32
11.9	32
15.5	26
22.3	28
26.9	17
30.7	20
46.2	25

APPENDIX 4: Kinetics of arsenate adsorption

Kinetics data from arsenate adsorption onto HMO from seawater at 23(±3)°C over 48 hours. $[As(V)]_{initial}$ = 0.6 μM, [HMO]:solution ratio = 0.15 g/L (Batch # 5).

Time (h)	$[As(V)]_{solution}$	$[As(V)]_{adsorbed}$	$\%[As(V)]_{adsorbed}$	% RSD
0	0.59	0.00	0	3
0.042	0.52	0.08	13	2
0.083	0.50	0.09	16	0
0.167	0.48	0.12	20	5
0.25	0.46	0.14	23	3
0.5	0.39	0.20	34	2
1	0.31	0.28	47	4
2	0.22	0.37	62	4
4	0.17	0.43	72	1
6	0.15	0.44	74	4
8	0.13	0.46	78	10
10	0.13	0.46	78	1
24	0.13	0.46	78	8
30	0.12	0.47	79	10
48	0.12	0.47	79	10

Data from the arsenate adsorption isotherm experiment at 23(±3)°C (Fig. 14). $[As(V)]_{initial}$ = 0.6-6 μM, [HMO]:solution ratio = 0.15 g/L, Batches # 5 and 6.

$[As(V)]_{solution}$ (μM)	$[As(V)]_{adsorbed}$ (μM)	$[As(V)]_{adsorbed}$ (μmol)	Batch #	Mass of adsorbent (g)	Volume surface (m^2)
0.6	0.5	0.3	5	0.11	30.7
1.0	0.7	0.4	5	0.11	30.7
1.8	1.3	0.7	5	0.11	30.7
2.7	2.0	1.1	5	0.11	30.7
3.5	2.6	1.4	5	0.11	30.7
4.7	3.6	2.0	5	0.11	30.7
6.0	4.5	2.5	6	0.09	24.1

Percent arsenate adsorption onto HMO from seawater at 23(±3)°C (Fig. 17). $[As(V)]_{initial}$ = 0.6-6 μM, [HMO]:solution ratio = 0.15 g/L (Batch # 5 and 6).

$[As(V)]_{initial\ solution}$ (μM)	% adsorption
0.6	79
1.0	69
1.8	73
2.7	77
3.5	74
4.7	77
6.0	74

APPENDIX 5: Kinetics of simultaneous competitive adsorption

Kinetics data for phosphate during simultaneous competitive adsorption (Fig. 18). [HMO]:solution ratio = 0.15 g/L, Batch # 5 and 6. [As(V)]:[SRP] ratios: 1:2.5 (2.0 μM and 5.0 μM), 1:10 (0.5 μM and 5 μM) , 1:100 (0.5 μM and 50 μM).

	1:2.5			1:10			1:100		
Time (h)	$[SRP]_{sol.}$	% Ads	% RSD	$[SRP]_{sol.}$	% Ads	% RSD	$[SRP]_{sol.}$	% Ads	% RSD
0	5.0	0	0.8	5.2	0	0.1	47	0	0.1
0.042	4.0	19	0.2	4.4	14	0.3	42	11	0.3
0.083	4.0	20	0.2	4.4	15	0.2	42	10	0.1
0.167	4.7	6	0.3	4.6	11	0.3	40	16	0.1
0.25	4.8	3	0.2	4.3	16	0.2	40	16	0.2
0.5	3.9	22	0.3	4.2	19	0.4	39	18	0.1
1	3.4	32	0.7	4.4	16	0.4	39	18	0.2
2	3.5	29	0.6	3.6	30	0.2	38	20	0.1
4	3.5	30	0.3	3.4	34	0.1	38	20	0.3
6	3.4	31	1.0	3.3	36	0.4	38	19	0.1
8	4.3	13	0.3	3.6	30	0.3	38	20	0.3
10	3.3	35	0.3	3.5	33	0.2	38	21	0.2
24	3.2	36	0.2	3.3	36	0.5	37	21	0.2
30	2.7	45	1.3	3.3	37	0.1	37	21	0.1
48	2.7	45	0.5	3.1	40	0.1	38	20	0.4

Kinetics data for arsenate during simultaneous competitive adsorption (Fig. 18). [HMO]:solution ratio = 0.15 g/L. [As(V)]:[SRP] ratios: 1:2.5 (2.0 μM and 5.0 μM), 1:10 (0.5 μM and 5 μM) , 1:100 (0.5 μM and 50 μM).

		1:2.5			1:10			1:100	
Time (h)	$[As(V)]_{sol.}$	% Ads	% RSD	$[As(V)]_{sol.}$	% Ads	% RSD	$[As(V)]_{sol.}$	% Ads	% RSD
0	2.3	0	1.1	0.45	0	1.4	0.49	0	1.28
0.042	1.7	21	1.0	0.38	15	1.5	0.41	16	2.31
0.083	1.5	30	1.3	0.37	17	4.7	0.42	14	1.54
0.167	1.4	35	1.3	0.35	21	4.7	0.40	18	4.35
0.25	1.3	39	2.6	0.32	28	1.4	0.38	21	2.96
0.5	1.1	50	1.1	0.28	36	2.0	0.34	29	2.07
1	0.8	64	0.3	0.22	51	1.8	0.30	39	2.89
2	0.6	74	3.0	0.16	64	2.9	0.25	49	4.97
4	0.5	79	0.1	0.12	72	2.1	0.20	60	3.96
6	0.4	81	3.6	0.11	76	10.0	0.18	62	3.46
8	0.4	81	2.4	0.10	79	9.4	0.20	60	3.46
10	0.4	82	1.1	0.10	78	1.7	0.18	63	6.38
24	0.4	82	1.5	0.09	80	6.6	0.20	58	3.48
30	0.4	83	0.9	0.09	80	5.7	0.19	60	4.18
48	0.4	82	2.9	0.08	82	5.2	0.19	61	4.82

APPENDIX 6: Kinetics of sequential competitive adsorption

Data from the sequential competitive adsorption experiment where 10 μM phosphate was left to equilibrate with 0.15 g/L [HMO] in seawater for 48 hours prior to the addition of 1 μM of arsenate. HMO Batch # 7, Fig. 22.

Time (h)	$[SRP]_{solution}$	% Ads	% RSD	$[As(V)]_{solution}$	% Ads	% RSD
0	6.2	31	0.2	0.9	0	5.6
0.042	6.2	31	0.1	0.8	17	1.2
0.083	6.1	32	0.1	0.6	30	0.7
0.167	6.0	33	0.1	0.5	42	1.2
0.25	6.0	33	0.2	0.5	47	0.5
0.5	6.3	30	0.3	0.4	54	1.3
1	6.1	32	0.2	0.4	59	1.7
2	6.0	34	0.3	0.4	62	0.7
4	6.1	33	0.1	0.3	65	3.1
6	5.9	35	0.1	0.3	66	4.7
8	6.0	33	0.4	0.3	67	0.7
10	6.2	31	0.4	0.3	67	0.5
24	6.2	31	0.1	0.3	69	0.7
30	6.3	30	0.2	0.3	69	1.8
48	6.2	32	0.1	0.3	70	1.4

Data from the sequential competitive adsorption experiment where 1 μM arsenate was left to equilibrate with 0.15 g/L [HMO] in seawater for 48 hours prior to the addition of 10 μM of phosphate. HMO Batch # 7, Fig. 23.

Time (h)	$[As(V)]_{solution}$	% Ads	% RSD	$[SRP]_{solution}$	% Ads	% RSD
0	0.23	80	4.9	9.6	0	0.2
0.042	0.24	80	1.4	8.8	9	0.2
0.083	0.23	80	3.6	8.6	10	0.1
0.167	0.24	80	2.1	8.4	13	0.3
0.25	0.24	80	0.9	8.0	17	0.1
0.5	0.24	80	2.0	7.8	18	0.4
1	0.24	80	0.1	7.9	18	0.2
2	0.25	79	2.3	7.6	21	0.5
4	0.25	79	1.3	7.3	24	0.3
6	0.25	79	2.6	7.2	25	0.1
8	0.26	78	2.3	7.2	25	0.1
10	0.25	78	4.3	7.2	25	0.6
24	0.27	77	1.7	7.1	26	0.3
30	0.28	77	2.8	7.2	26	0.1
48	0.29	75	2.1	7.1	26	0.4

APPENDIX 7: Desorption of phosphate and arsenate from HMO

Desorption of phosphate and arsenate from HMO in seawater with 2.1 μM [SRP] and 14 nM [As(V)]. $[SRP]_{initial}$ = 31 μM, $[SRP]_{adsorbed}$ = 10 μM, $[SRP]_{desorbed}$ = 5 μM, $[As(V)]_{initial}$ = 6 μM, $[As(V)]_{adsorbed}$ = 4 μM, $[As(V)]_{desorbed}$ = 1 μM. Batch # 7, Fig. 24.

Time (h)	$[SRP]_{solution}$ (μM)	$[As(V)]_{solution}$ (μM)
0	2.0	0.01
0.042	2.2	0.07
0.083	2.4	0.10
0.167	2.9	0.16
0.25	3.2	0.23
0.5	4.0	0.42
1	4.5	0.65
2	5.5	0.76
4	6.1	0.89
6	6.4	0.95
8	6.5	0.97
10	6.8	1.01
24	7.1	1.12
30	7.1	1.14
48	7.2	1.16